Dissertation

zur Erlangung des Doktorgrades
der Fakultät für Chemie und Pharmazie
der Ludwig-Maximilians-Universität München

PEG-Shielded and EGF Receptor Targeted DNA Polyplexes: Cellular Mechanisms

vorgelegt von
Katharina Freiin von Gersdorff
aus Frankfurt/Main

2006

Erklärung

Diese Dissertation wurde im Sinne von § 13 Abs. 3 bzw. 4 der Promotionsordnung vom 29. Januar 1998 von Herrn Prof. Dr. Ernst Wagner betreut.

Ehrenwörtliche Versicherung

Diese Dissertation wurde selbständig, ohne unerlaubte Hilfe erarbeitet.

München,

Dissertation eingereicht am 16. März 2006

1. Gutachter: Herr Prof. Dr. Ernst Wagner

2. Gutachter: Herr PD Dr. Carsten Culmsee

Mündliche Prüfung am 27. April 2006

Table of contents

1 INTRODUCTION 6

1.1 Gene therapy 6
1.2 Viral and nonviral vectors for gene delivery 7
1.2.1 Viral vectors 7
1.2.2 Nonviral vectors 7
1.3 Gene delivery with PEI polyplexes 8
1.3.1 Tissue targeting of PEI polyplexes 10
1.3.2 Intracellular processing of PEI polyplexes 11
1.4 EGFR-targeting for cell-specific gene delivery 16
1.5 Objectives of this thesis 20

2 MATERIALS AND METHODS 21

2.1 Chemicals and reagents 21
2.1.1 Chemicals and reagents 21
2.1.2 Polyethylenimine and polyethylene glycol conjugates 22
2.1.3 Plasmid DNA 25
2.2 Cell culture 26
2.3 Covalent labeling of plasmid DNA 26
2.4 Polyplex formation 27
2.5 Measurement of particle size and zeta potential 28
2.6 Metabolic activity 28
2.7 Western blot 28
2.8 Cell synchronization 29
2.9 Luciferase reporter gene expression 30
2.9.1 Luciferase reporter gene expression 30
2.9.2 Luciferase reporter gene expression after cell synchronization 30
2.9.3 Luciferase reporter gene expression in the presence of endocytosis inhibitors 31
2.9.4 Luciferase reporter gene expression of HUH-7 EGFP-Luc cells 31
2.10 EGFP reporter gene expression 31
2.10.1 EGFP reporter gene expression 31
2.10.2 EGFP reporter gene expression after cell synchronization 32
2.11 Flow cytometry 32
2.11.1 Correlation of cell association, EGFP expression and cell cycle phase 32

2.11.2 Analysis of cell surface EGFR levels after transfection 33
2.11.3 Analysis of cellular polyplex association 33
2.11.4 Analysis of cellular polyplex uptake 34
2.11.5 Analysis of cellular polyplex uptake in the presence of uptake inhibitors 35
2.12 Epifluorescence microscopy 35
2.12.1 Analysis of cellular polyplex association 35
2.12.2 Cellular uptake of transferrin and cholera toxin B 35
2.13 Analysis of colocalization of polyplexes with transferrin or CTB by confocal laser scanning microscopy 36
2.14 Generation of stably transfected single cell clones 37
2.14.1 Plasmid DNA amplification and preparation 37
2.14.2 Generation of stably expressing EGFP-Actin cells, EGFP-Tubulin cells and EGFP-Luciferase cells 37
2.15 Statistical analysis 37

3 RESULTS 38

3.1 EGFR-targeting enhances transfection efficiency of PEGylated PEI polyplexes 38
3.1.1 EGFR-targeted and PEG-shielded polyplexes maintain their biophysical properties upon freeze-thawing 38
3.1.2 EGFR-targeting increases transgene expression mediated by PEGylated PEI polyplexes 39
3.1.3 mEGF can substitute huEGF in the synthesis of EGFR-targeted PEI polyplexes 41
3.1.4 EGFR-targeting increases the number of cells transfected by PEGylated PEI polyplexes 43
3.2 EGFR-targeting improves cellular uptake of PEGylated PEI polyplexes 45
3.2.1 EGFR-targeting improves total cellular association of PEGylated PEI polyplexes 45
3.2.2 EGFR-targeted complexes cluster upon cell binding 49
3.2.3 Internalization of EGFR-targeted complexes proceeds very fast 50
3.2.4 Reporter gene expression of EGFR-targeted polyplexes can be detected already 4 h posttransfection 53
3.3 EGFR-targeted complexes specifically bind to the EGFR 54
3.3.1 EGFR-targeted transfection reduces the level of free surface EGFR 54
3.3.2 EGFR-targeted polyplexes trigger EGFR activation 55
3.4 EGFR-targeted gene delivery is cell cycle dependent 57
3.4.1 EGFR-targeted polyplexes transfect postmitotic cells inefficiently 57

3.4.2 Mitosis has a major impact on EGFR-targeted gene delivery 60
3.4.3 Mitosis amplifies efficiency of EGFR-targeted gene delivery 62
3.5 Clathrin- and lipid raft-dependent endocytosis contribute to gene transfer by PEI polyplexes 66
3.5.1 EGFR-targeting does not affect the route of cellular polyplex uptake 66
3.5.2 Particle size affects cellular uptake pathways of PEI polyplexes 68
3.5.3 Clathrin-dependent endocytosis predominantly mediates gene delivery in HUH-7 cells 70
3.5.4 Inhibitors specifically interfere with endocytosis pathways 72
3.5.5 Pathways mediating successful gene delivery vary between cell types 74
3.5.6 Pathways mediating successful gene delivery depend on the polyplex formulation applied 76
3.6 Characterization of dynamic interactions of polyplexes with the cytoskeleton 78

4 DISCUSSION 79

4.1 Transfection efficiency of EGFR-targeted polyplexes 80
4.2 Cellular uptake kinetics of EGFR-targeted polyplexes 82
4.3 Dynamic interactions of polyplexes with the cell 85
4.4 EGFR activation by EGFR-targeted polyplexes 89
4.5 Cell cycle dependency of EGFR-targeted gene delivery 91
4.6 Mode of cellular polyplex uptake 95
4.7 Pathways mediating successful transfection 97

5 SUMMARY 102

6 APPENDIX 104

6.1 Abbreviations 104
6.2 Publications 108
6.2.1 Original papers 108
6.2.2 Book chapters 108
6.2.3 Oral presentations 109
6.2.4 Poster presentations 109

7 REFERENCES 110

8 ACKNOWLEDGMENTS 124

9 CURRICULUM VITAE 125

1 Introduction

1.1 Gene therapy

The basis for gene therapy is to change the expression of selected genes in an attempt to treat, cure or prevent disease. For this purpose, nucleic acids have to be delivered into target cells to turn on or restore gene function (“gain of function”) or to suppress specific gene functions (“loss of function”). Gene replacement strategies typically aim at transduction of double-stranded DNA into the cell nucleus, whereas gene modulating approaches involve the transfer of either antisense oligonucleotides (AS-ON) (1), ribozymes (2) or small interfering RNA (siRNA) (3) into the desired cell or tissue.

Although gene therapy has not yet been established as standard treatment, it has already been applied in more than one thousand clinical trials, most of them (65 %) in the field of cancer therapy. The most common strategies employed there were immunotherapy and enzyme/prodrug approaches. Other gene therapy trials addressed monogenic diseases (Hemophilia A and B, sickle cell disease, cystic fibrosis, severe combined immunodeficiency syndrome (SCID)) and DNA vaccination (4). However, the biggest hurdle that still limits therapeutic applications of genes is the merge of efficient delivery and therapeutic safety concerns. Hence, gene therapy holds tremendous promise for a broad spectrum of clinical applications, provided that appropriate gene vector systems are available.

Two general approaches have been used for gene delivery: those involving viral vector systems and those utilizing lipid- or polymer-based DNA complexes (nonviral vector systems).

1.2 Viral and nonviral vectors for gene delivery

1.2.1 Viral vectors

Viruses have a natural ability to infect host cells, and hence they offer an excellent means of introducing foreign DNA sequences into cells for gene therapy (5). It has been shown that binding of a single virus particle can be sufficient to infect the host cell (6). This is the reason why more than 70 % of current clinical trials for gene therapy employ viral vectors.

A number of different viruses have been adapted as vectors for gene therapy, mainly retroviruses and adenoviruses. Since viral particles differ in their mode of infection and reproduction, their biological characteristics strongly influence their applicability as gene delivery vehicles. Good progress has been made to modify viruses by removing certain viral genes associated with pathogenic function and altering viral tropism. Furthermore, viruses have been rendered replication-defective in order to prevent viral dissemination and reinfection.

In general, viral vectors are highly effective in gene transfer, the main weakness, however, is safety (7). Application of retroviral vectors, for example, can cause insertional oncogenesis resulting from random retroviral integration (8). Furthermore, any virus used as a vehicle for the delivery of genetic material can incite an intense inflammatory or immune response following administration. Since rather high doses of virus are commonly used for efficient therapy, adverse effects can lead to a catastrophic outcome. In 1999, a patient died following infusion of a high dose of adenoviral vector (9;10). This was the first death that has been directly attributed to the effects of the gene therapy.

1.2.2 Nonviral vectors

Nonviral gene delivery has several advantages over viral vector systems, the most important being their low immunogenicity which allows repeated applications. This is due to the fact that nonviral vectors present much less immunogenic proteins or peptides compared to viral vectors (11). Furthermore, they offer easy synthesis and production at low cost as well as high flexibility regarding the size of the genetic material that may be delivered. Because nonviral systems do not show this inherent

selectivity of cell surface binding and internalization (tropism) characteristic of viruses, they can typically be used in a more universal fashion. Furthermore, production by chemical synthesis allows various modifications and easy manipulation so that nonviral vectors can be engineered for cell-specific and enhanced DNA delivery. However, the major drawback of nonviral vector systems is that they are generally many orders of magnitude less efficient than viral vectors, which is currently only partly compensated by the application of high amounts of DNA.

For systemic administration, nucleic acids have to be protected from enzymatic digestion. Therefore, complex-based gene delivery vehicles have been developed. They are based on polymers or lipids, which bind DNA to form polymer/DNA complexes or lipid/DNA complexes called polyplexes or lipoplexes, respectively. Polycationic carriers include natural DNA binding molecules like histones or protamines, chemically synthesized polyaminoacids, e. g. polylysine, or other polycationic polymers (12). More recently, polyethylenimine (PEI), a synthetic polymer with a high cationic charge density, has been demonstrated to be a highly efficient and versatile vehicle for the delivery of DNA and RNA both *in vitro* and *in vivo* (13).

1.3 Gene delivery with PEI polyplexes

In 1995, it was first reported on the ability of PEI to successfully deliver genes and oligonucleotides both *in vitro* and *in vivo* (14). PEI polymers can be synthesized with a linear or a branched topology and are available in a wide range of molecular weights.

PEI is the organic molecule with the highest charge density potential, since every third atom is an amino nitrogen that can be protonated. Ionic interaction between the positively charged amino groups of PEI and the negatively charged phosphates of nucleic acids leads to complexation and subsequent formation of small particles called polyplexes. These compact particles can then enter the cells via natural processes like endocytosis.

By condensing the DNA, PEI provides protection against physical and biochemical degradation of the nucleic acids not only in the extracellular space but also inside the

cell. For efficient complexation, a large excess of PEI is needed yielding polyplexes with a net positive surface charge and leaving a considerable amount of PEI free in solution. Although PEI polyplexes mediate efficient gene delivery *in vitro*, they are typically found to exhibit strong cellular and systemic toxicity *in vivo* (15). Analysis of purified PEI polyplexes showed that free PEI is the major cause of toxicity of PEI polyplexes (16). Nevertheless, free PEI remains an essential factor for intracellular gene delivery as it appears to enhance transfection efficiency (16).

Biophysical properties and cell biological behavior of these nanometric particles depend on several factors, mainly the ratio of PEI to DNA used for complex formation (calculated on the basis of PEI nitrogen and DNA phosphate and expressed as N/P ratio) and the salt concentration during complex formation. At low salt concentrations and/or N/P ratios above 6, small particles are formed, whereas aggregation is observed in the presence of salt at lower N/P ratios (17;18). *In vitro*, transfection efficiency is enhanced when large aggregated particles or polyplexes with high N/P ratios are used. Increased cellular association (17) and improved intracellular delivery were found to account for this effect (17;19).

Since the capability of viruses to efficiently deliver nucleic acids into the cell can be attributed to their manifold strategies for breaking down various cellular barriers, scientists have put much effort in emulating these features (20;21). The amino groups of PEI polymers offer easy chemical modification and hence the possibility to incorporate in a modular fashion several virus-mimetic components to provide efficient cellular delivery characteristics. Several types of molecules have already been linked to PEI, including proteins, peptides, sugar molecules and hydrophilic polymers. They have been used in particular to reduce unspecific interactions, to mediate cell-specific gene delivery and to improve endosomal release.

Introduction of foreign genes into cells is not natural, and hence cells have biological barriers that protect them against invasion by foreign genes. Therefore, identifying and overcoming each hurdle along the DNA entry pathway can improve DNA delivery and hence overall transfection efficiency. Despite encouraging progress made in this field, these barriers still represent a considerable challenge for nonviral vector systems.

1.3.1 Tissue targeting of PEI polyplexes

The first step in gene delivery entails the approach of the vector to the target cell from the outside environment. Specificity for the target tissue is a key issue in gene therapy and requires multiple modifications of the PEI/DNA polyplex.

Unmodified positively charged PEI polyplexes do not display the capability to distinguish between target and non-target tissue but rather stick to any cell membrane they reach. Therefore, systemic administration of PEI polyplexes into the tail vein of a test animal is always associated with high gene expression in the lung (22) and considerable systemic toxicity (23).

To prevent non-specific trapping and to reduce toxicity, PEI polymers have been grafted with polyethylene glycol (PEG), a hydrophilic polymer, which shields the positive surface charge but maintains the solubility of the particles. PEGylation has been shown to prevent erythrocyte aggregation, reduce cytotoxicity and significantly prolong circulation time (24). However, owing to decreased cellular binding of PEGylated polyplexes gene delivery turned out to be less efficient (25;26). Moreover, differences in the mode of internalization and intracellular routing or entrapment in the endosomal compartment might account for this effect.

Some selectivity for tumor tissue can be achieved by administration of small polyplexes displaying a neutral surface charge. Thus, passive accumulation of PEGylated PEI polyplexes in distant tumors has been observed because of the incomplete vasculature within the tumor. This mechanism, called “enhanced permeability and retention effect” (EPR), enables the influx of polyplexes from the blood into the tumor via leaky or incomplete blood vessels (27).

To introduce cell specificity and to restore the transfection efficiency of shielded polyplexes, receptor-mediated endocytic pathways have been exploited for nonviral gene delivery. For this purpose, targeting molecules have been attached to PEI polyplexes to direct them to only those cells that express the corresponding receptor. A number of ligands targeting receptors that confer specificity for a cell type (e. g. asialoglycoprotein receptor for hepatocytes) or selectivity for a target cell subpopulation (e. g. tumor cells overexpressing epidermal growth factor receptor)

have been used to increase efficiency (28;29). These include proteins, peptides, carbohydrates, vitamins or antibodies against cell surface receptors (Table 1).

RECEPTOR	LIGAND	TARGET CELLS	REFERENCES
Asialoglycoprotein receptor	Galactose	hepatocytes	(30-32)
Mannose receptor	Mannose	dendritic cells	(33)
Folic acid receptor	Folate	various	(34)
Transferrin receptor	Transferrin	different tumor cell lines	(35)
EGF receptor	EGF	different tumor cell lines	(36-38)
CD-3	Anti-CD-3	T cell-derived leukaemia cells, activated PBMC´s	(39;40)

Table 1: Receptor-mediated targeting of PEI polyplexes to specific cell populations.

To date, transferrin-mediated uptake of gene transfer vehicles is among the best-studied targeting systems. Covalent linkage of transferrin to PEI produced an up to several-hundred-fold increase in transfection efficiency depending on the cell type targeted (35).

Another targeting ligand that has been employed for PEI-mediated gene delivery is the epidermal growth factor (EGF) since the epidermal growth factor receptor (EGFR) is up-regulated in many human tumors (see 1.4).

1.3.2 Intracellular processing of PEI polyplexes

Upon binding to the target cell, polyplexes are internalized in order to deliver their cargo. For successful gene delivery, several intracellular barriers then have to be faced. These include cellular uptake, endosomal release and trafficking towards the nucleus where the transgene can be transcribed. Figure 1 illustrates cellular uptake and intracellular trafficking of PEI polyplexes carrying multiple functional domains to overcome these obstacles.

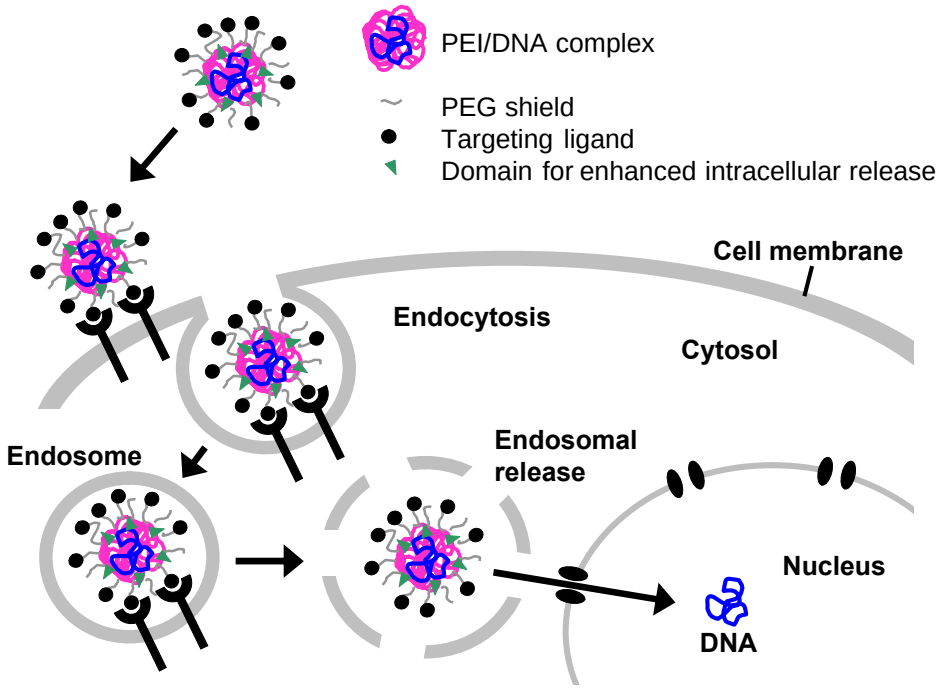

Figure 1: Schematic of cellular uptake and intracellular trafficking of shielded and targeted PEI polyplexes. After binding to receptors on the plasma membrane, PEG-shielded and receptor-targeted PEI polyplexes are mainly taken up into cells by receptor-mediated endocytosis. For efficient gene delivery, polyplexes need to escape from the endosome and traffic towards the nucleus, enter the nucleus and expose the DNA to the cell's transcription machinery. Novel components for overcoming these hurdles are being incorporated into synthetic vectors in order to enhance gene transfer efficiency.

1.3.2.1 Endocytosis pathways mediating cellular uptake of PEI polyplexes

Despite various studies investigating the mechanisms of uptake and intracellular trafficking (41-46), current understanding of the processes involved in cellular uptake of PEI/DNA polyplexes is still limited.

In general, the types of endocytosis can be divided into clathrin-dependent and clathrin-independent pathways (Figure 2). Clathrin-dependent endocytosis is initiated by the formation of clathrin-coated pits yielding clathrin-coated vesicles and leads to the formation of early and late endosomes which ultimately fuse with lysosomes (47). Clathrin-independent endocytosis occurs via caveolin-dependent and caveolin-independent endocytic pathways (also classified as raft-dependent endocytosis), macropinocytosis or phagocytosis. Caveolae are smooth invaginations of the plasma membrane associated with caveolin-1 (48) and enriched in cholesterol and sphingolipids. They can be considered as a specialized form of lipid rafts. Internalization occurs via a cholesterol-sensitive pathway forming caveolar vesicles.

These then fuse with caveosomes which have been found to show a neutral pH (49). Macropinocytosis is an actin-driven process forming large vesicles by the closure of ruffling membrane domains (50). Phagocytosis is restricted to specialized cells including macrophages that function to clear large pathogens or cell debris from the circulation.

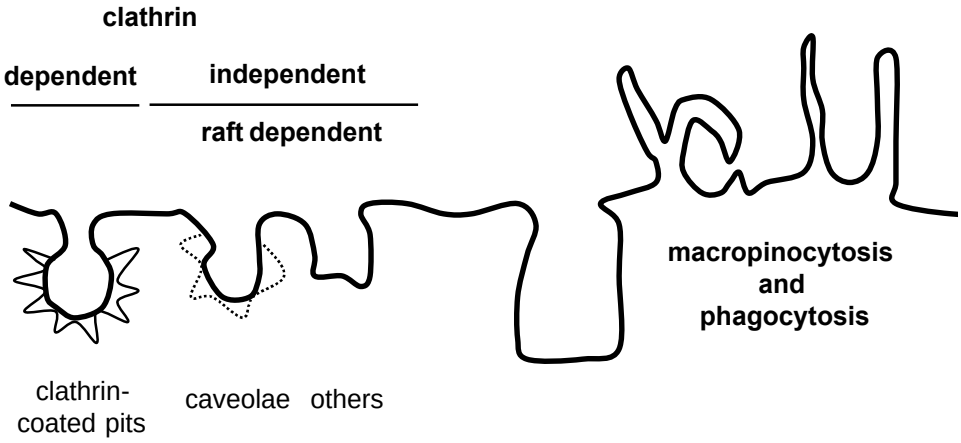

Figure 2: Modes of internalization. Endocytosis can be divided into clathrin-dependent and clathrin-independent pathways, the latter including caveolin-dependent and caveolin-independent endocytosis (raft-dependent), macropinocytosis and phagocytosis. Clathrin-dependent endocytosis starts with clathrin-coated pit formation and leads to the formation of endosomes. Caveolae are cholesterol-rich invaginations of the plasma membrane containing caveolin-1. They are internalized via a cholesterol-sensitive pathway forming caveosomes. Macropinocytosis is an actin-driven process forming large vesicles by the closure of ruffling membrane domains.

To shed light on the mode of internalization of nonviral vectors, inhibitors specific to the various endocytosis pathways have been applied in several studies (41-43;46;51;52). Chlorpromazine – which has been shown to disturb intracellular clathrin processing (53) – was used to inhibit clathrin-dependent endocytosis. Filipin III has been employed to block caveolae/raft-mediated endocytosis since it complexes membrane cholesterol and thus interferes with cholesterol-sensitive processes (54).

In order to elucidate which types of endocytosis are involved in the cellular uptake of PEI polyplexes, recent studies reported on the close relation between particle size and internalization pathway, however with inconsistent results. Rejman et al. (41) proposed that particles < 200 nm are taken up via the clathrin-dependent mechanism whereas larger particles (200-500 nm) enter the cells through caveolin-1-rich vesicles. Other authors (51) claimed that large complexes (> 200 nm) are internalized by macropinocytosis, medium-sized particles by clathrin-coated pits and small

complexes (≤ 100 nm) via caveolae. This correlation between particle size and uptake pathway is indeed plausible since some of these pathways are confined in the size of their vesicles – e. g. clathrin-coated and caveolae-derived vesicles (47;49). Large PEI polyplexes were also proposed to exploit non-endocytic pathways for cellular entry since it was found that the high charge density of PEI polyplexes is capable of inducing local membrane damage especially when large aggregates interact with the plasma membrane (55). Nevertheless, all these hypotheses might fail when decoding the uptake pathways of modified PEI polyplexes.

Much research is being conducted to identify the cellular structures involved in the cellular uptake of PEI polyplexes. For complexes bearing a net positive surface charge (unshielded PEI polyplexes), heparansulphate proteoglycans (HSPGs) – negatively charged transmembrane proteins ubiquitously expressed on adherent cells – were proposed to play a role as potential receptors mediating cellular polyplex uptake (45;56;57). Recently, a more detailed model was hypothesized (43) suggesting that syndecans might be involved as receptors for initial particle binding. These HSPGs were postulated to subsequently trigger actin filament-mediated engulfment (“phagocytosis”) of the polyplex. However, direct evidence for an interaction of polyplexes with cell surface structures and the actin filament network was still lacking.

Eukaryotic cells utilize the different endocytic pathways to internalize a variety of substances and to accomplish different tasks. It is therefore conceivable that the mode of internalization of PEI polyplexes affects their intracellular processing and thus transfection efficiency as such. Rejman and coworkers recently addressed this issue on the relative contribution of each pathway to gene transfer efficiency and proposed that only the caveolae/raft-mediated pathway leads to efficient transfection of branched PEI/DNA polyplexes (42). However, further evidence will be necessary to unambiguously clarify the role of each pathway and its determinants in PEI-mediated gene delivery.

1.3.2.2 Endosomal release of PEI polyplexes

Internalized gene transfer complexes are mostly found in intracellular vesicles such as endosomes. Due to the action of vesicular ATP-dependent proton pumps, endosomal compartments undergo continuous acidification from the initial cell surface pH (pH ~ 7), ultimately to that found in lysosomes (pH ~ 4.5). Subsequent release of PEI polyplexes into the cytoplasm represents a major bottleneck for gene delivery (58;59) since DNA must exit the vesicles before it is degraded in the lysosomes. The high transfection efficiencies observed with PEI have been attributed to its strong buffering capacity within the physiological pH range. This can be explained by the so-called proton sponge effect: protonation of PEI´s ionizable amino groups leads to chloride ion accumulation and subsequent osmotic endosome swelling by influx of water which eventually causes rupture and enhanced escape of the polyplex. Direct measurements of acidification, chloride accumulation, and endosomal swelling support this hypothesis (19;44;60-62). However, release of PEI polyplexes can be significantly hampered when using low molecular weight PEI (63) or either small or purified PEI complexes at low DNA concentrations (16;17). To overcome endosomal entrapment of polyplexes, inactivated adenovirus particles (64) or membrane active peptides like melittin (65) have been incorporated into polyplexes and significantly enhanced gene delivery.

For efficient nuclear import, the polyplexes have to travel towards the cell nucleus. Since the cytoplasm contains a filamentous cytoskeleton network embedded in a concentrated mix of soluble proteins and organelles, passive diffusion of large molecules like DNA and polyplexes is highly inefficient (66). Little is known about the transport processes which allow the polyplexes to enter the cell and reach the nucleus. In order to unravel the dynamics of the processes involved, newly developed single particle tracking techniques are being employed (6). First results of such experiments indicate that once inside the cell, polyplexes are actively transported to the perinuclear region (67). Based on the effect of microtubule disrupting drugs on the intracellular transport of polyplexes, it was hypothesized that the cellular microtubule network plays a pivotal role in the transfection process (67), although it could not yet be elucidated whether this transport is mediated within vesicles. Nevertheless, convincing evidence on the basis of dynamic data

characterizing the movement of polyplexes inside the cell has not yet been presented.

1.3.2.3 Nuclear import of PEI polyplexes

The nuclear membrane presents a major barrier to the entry of free and polyplex-associated DNA from the cytoplasm (68). In several studies, less than 0.1 % of plasmid DNA which had been injected into the cytoplasm was found to be transcribed (69). In general, there are two paths to nuclear entry: one through the “nuclear pore complex” (NPC) and one via nuclear disassembly that occurs during cell division. Entry through the NPC may be passive or active. Passive diffusion through the NPC is determined mainly by the size of the molecule: DNA of up to 300 bp and DNA nanoparticles up to a diameter of 25 nm were found to traverse the NPC (70), since their small size permitted nuclear uptake across the 25 nm nuclear membrane pore. In polyplex-mediated gene delivery, the major path of nuclear entry seems to be via nuclear disassembly during mitosis since dividing cells yield much higher transfection efficiencies than postmitotic cells. For lipoplex- and polyplex-based transfections, highest reporter gene expression levels have been recorded for cells in the G_2/M phase with a 30- to 500-fold increase as compared to G_1 cells (71). Interestingly, polymer-mediated transfection using linear PEI was far less dependent on cell cycle compared to branched PEI (72). In order to enhance nuclear uptake, signal-mediated active transport mechanisms have been explored for trafficking vectors to the nucleus. Covalent coupling of a single nuclear localization signal (NLS) peptide to a CMV-Luciferase gene led to an up to 1000-fold enhancement in transfection efficiency presumably attributed to improved nuclear translocation by the nuclear import machinery (73).

1.4 EGFR-targeting for cell-specific gene delivery

Epidermal growth factor (EGF) is a globular protein of 6.2 kDa consisting of 53 amino acids that binds specifically and with high affinity (74) to the EGFR.

The EGF receptor (EGFR, also known as HER1 or ErbB1) represents one of the four members of the ErbB receptor family of receptor tyrosine kinases. The ubiquitous 170 kDa membrane-spanning glycoprotein is composed of an N-terminal

extracellular ligand binding domain, a hydrophobic transmembrane region and a cytoplasmic domain which contains the tyrosine kinase (75).

EGFR activity controls proliferation, differentiation and cell survival of a wide range of cell types. EGFRs can be detected both within and outside lipid rafts (76). This is apparently an important regulatory mechanism since sequestration of the receptors in non-caveolar lipid rafts inhibits ligand binding (77). However upon binding EGF, EGFRs can migrate out of the raft membrane and undergo clathrin-dependent endocytosis (76).

On the molecular level, EGF binding induces the dimerization of EGFRs (78) and the trans-autophosphorylation of tyrosine residues in the cytoplasmic domain of EGFRs which leads to subsequent internalization of the activated EGFR complex via clathrin-dependent endocytosis (Figure 3) (79). After internalization, receptors can be sorted to recycling endosomes from which they travel back to the cell surface. Alternatively, they can be directed to lysosomes where they are degraded (80). The phosphorylated tyrosines serve as docking sites for a number of adaptor molecules that can initiate a plethora of signaling pathways, resulting in cell proliferation, protection from apoptosis or transformation (81). Cytoplasmic signal transducers that can be activated by the EGFR include, for example, MAPKs, Akt, the stress-activated protein kinases (SAPKs) and JNK (81;82). In the nucleus, these signaling pathways can initiate distinct transcriptional programs involving enhanced activity of the proto-oncogenes c-jun and elk-1 (81). It has been shown that EGFRs localized both in the plasma membrane and in the endosomal membrane can recruit effector proteins and trigger such signaling pathways (83-85).

Recently, it was reported that EGFRs were exclusively internalized through the clathrin pathway only when stimulated with low doses of EGF. At higher (physiological) concentrations of ligand, however, EGFRs become ubiquitinated and are partially endocytosed through a lipid raft-dependent route (Figure 3) (86;87). This pathway does not contribute to EGFR signaling, but is preferentially associated with receptor degradation (86;87).

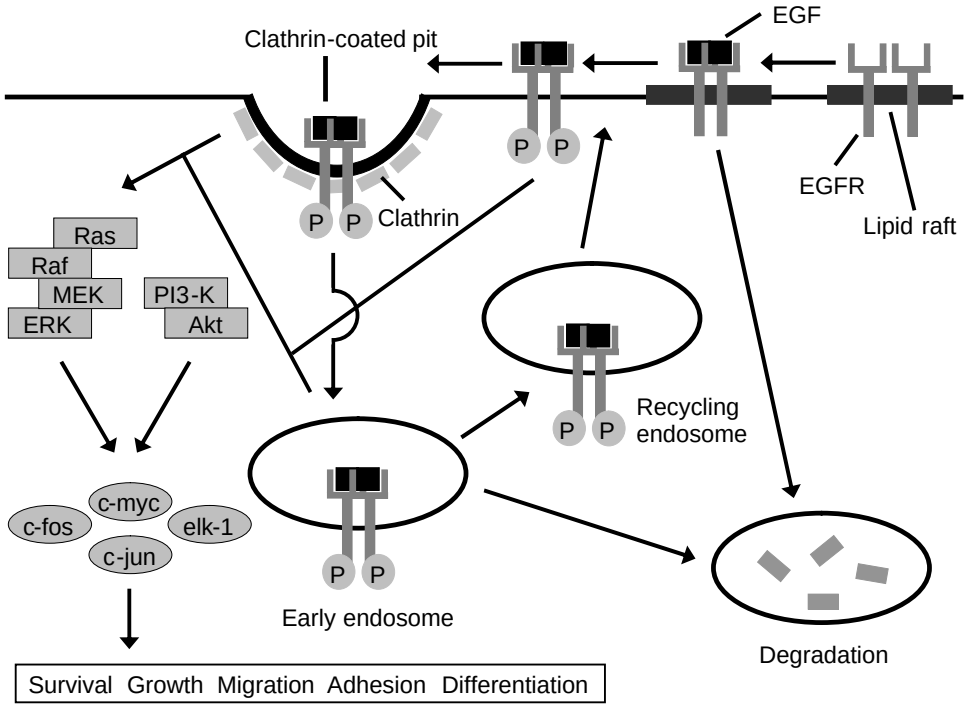

Figure 3: Epidermal growth factor receptor trafficking and signaling. EGF binding induces the dimerization of EGFR and autophosphorylation in the cytoplasmic domain. Assembly of clathrin proteins leads to the formation of clathrin-coated pits and subsequent internalization of the activated EGFR complex. After internalization into early endosomes, EGFRs can be sorted to the recycling endosome, from which they are transported back to the cell surface. Alternatively, EGFRs can be directed to late endosomes/lysosomes to be degraded. Activated EGFRs further initiate several downstream signaling pathways triggering cell proliferation etc. At high doses of EGF, internalization can also occur via lipid rafts leading to EGFR degradation. This route does not contribute to EGFR signaling.

Over the past years, the EGFR and its ligands have repeatedly been observed in the nucleus of different cell lines and tissues including many human cancers (88-91). It has been shown that binding of the cognate ligand is required for nuclear localization and accordingly, the complete ligand–receptor complex was reported to be present in the nucleus (92). The route(s) by which the EGFR or fragments of it move into the nucleus have not been clearly elucidated yet. Although existing data do not discern the function of this only recently discovered process, understanding of the phenomenon might open up new possibilities to target nonviral vectors towards the cell nucleus.

The EGFR is a tempting target for gene delivery since it is overexpressed in a wide variety of human tumors, including cancers of lung, liver, breast, and also in hepatocellular carcinoma (HCC). For example, HCC cells express EGFR levels of approximately 3×10^5 receptors per cell (93). Moreover, the EGFR shows high

affinity to its ligand EGF: 10 % of the receptors exhibit a dissociation constant (K_d) of 3 x 10^{-10} M and 90 % a K_d of 2 x 10^{-9} M (94). Because of these favorable characteristics, the EGFR has been used as a target for cell attachment of polyplexes. In particular, polylysine conjugates of anti-EGFR antibodies (95;96), fusion proteins containing the EGFR ligand TGF alpha (97) and polycation conjugates of EGF (36;37;98;99) or EGF-derived peptides (100-102) have already been applied for EGFR-specific gene delivery. On the cellular level, such EGF-containing polyplexes showed significantly increased cellular uptake (103) and enhanced transfection efficiency compared to polyplexes without EGF.

Both unshielded and PEGylated EGFR-targeted polyplexes have proven successful in improving gene delivery into EGFR-expressing cells (36). For systemic administration however, shielding is inevitable to render the polyplexes less susceptible to interactions with non-target tissue. Three different strategies were pursued for the formation of PEGylated EGFR-targeted PEI polyplexes (36): (i) post-PEGylation of EGF-PEI/DNA polyplexes, (ii) PEGylation of PEI/DNA polyplexes and subsequent covalent attachment of the ligand EGF, (iii) complexation of DNA with a mixture of PEI, PEG-PEI and EGF-PEG-PEI conjugates in a one-step-process. Although the 6 kDa EGF ligand is rather small compared to the 20 kDa PEG shield, all three formulations were able to mediate EGFR-specific gene transfer (36).

Recently, cryoconservable PEG-shielded and EGFR-targeted polyplexes were engineered for tumor-directed gene delivery (37). They were formed by complexing DNA with a mixture of linear PEI (LPEI, 22 kDa), PEG(20kDa)-PEI22 and a conjugate where mEGF is linked to branched PEI (BPEI, 25 kDa) via a heterobifunctional 3.4 kDa PEG spacer (strategy iii, see above). *In vitro*, these EGFR-targeted polyplexes significantly enhanced gene transfer efficiency into human EGFR-overexpressing HCC cells compared to non-targeted PEG-shielded polyplexes. They were also able to target subcutaneous tumors after tail vein injection into HCC xenograft bearing mice (37). Notably, no acute toxicity was observed in any of the animals. These findings suggest that this strategy might be considered a promising approach for the treatment of patients with HCC. However, until now the process of EGFR-specific gene delivery has not been characterized in detail.

1.5 Objectives of this thesis

A detailed understanding how the nonviral vectors interact with cellular components is a key aspect towards improving their design. Therefore, the aim of the present work was to shed light on the cellular mechanisms of EGFR-targeted gene delivery. Regarding these processes, it was focussed on the following issues:

Cellular uptake of EGFR-targeted polyplexes

Receptor-mediated uptake processes are known to be very fast. If specific binding between complex-bound EGF and the EGFR indeed occurs, it can be assumed that uptake of EGF(+) polyplexes proceeds much faster than that of non-targeted complexes.

EGFR activation by EGFR-targeted polyplexes

Since EGFR activity controls proliferation and cell survival, the potential ability of EGF(+) complexes to trigger EGFR activation of the target tumor cells might be of relevance for therapeutic applications.

Cell cycle dependency of EGFR-targeted gene delivery

The EGFR and its ligands have repeatedly been observed in the nucleus of different cell lines. If this route would also be available for EGFRs bound to EGF(+) polyplexes, EGFR-targeted vectors might have the capability of transfecting postmitotic cells.

Internalization mode of EGFR-targeted polyplexes

Little is known about the uptake processes of PEI polyplexes, their relative contribution to efficient gene transfer and the factors influencing their significance. Although much research has been conducted to elucidate the mechanisms of EGFR internalization, the mechanisms involved in cellular entry and intracellular processing of EGFR-targeted polyplexes have not been addressed so far.

2 Materials and methods

2.1 Chemicals and reagents

2.1.1 Chemicals and reagents

Thymidine, nocodazole, EDTA, chlorpromazine, filipin III, DAPI, MTT and Hoechst 33342 were purchased from Sigma-Aldrich (Munich, Germany). PI, YOYO-1, Alexa Fluor® 647 transferrin and Alexa Fluor® 488 cholera toxin subunit B (CTB) were supplied by Molecular Probes (Leiden, Netherlands). Cell culture plates were purchased from TPP (Trasadingen, Switzerland). The gel filtration columns Sephadex G-10 HR10/30 and Sephadex G-25 superfine were obtained from Amersham Biosciences (Germany). The cation-exchange column Macro-prep High S 10/10 was purchased from BioRad (Munich, Germany).

Recombinant murine epidermal growth factor (mEGF, MW = 6000) and human epidermal growth factor (huEGF, MW = 6200) were obtained from Pepro Tech EC Ltd. (London, Great Britain). The amounts of mEGF and huEGF were determined by measuring the absorbance at 280 nm (1 mg mEGF = A_{280}/3.1; 1 mg huEGF = A_{280}/3).

Succinimidyl 3-(2-pyridyldithio)propionate (SPDP) was purchased from Sigma-Aldrich. The amount of dithiopyridine linker conjugated to mEGF was determined after reduction of an aliquot by dithiothreitol (DTT) followed by measurement at 340 nm (104).

α-Maleimide-ω-N-hydroxysuccinimide ester-polyethylene glycol (NHS-PEG-MAL, MW = 3400) was obtained from Nektar Therapeutics (Birmingham, AL, USA). The amount of reactive maleimide linker in the conjugates was determined by measuring the absorbance before and after addition of dithiothreitol (DTT) at 300 nm.

The amount of mercapto-groups in mEGF-SH was determined by the Ellmans assay (105).

The concentration of BPEI was measured by the trinitrobenzenesulfonic acid (TNBS) assay (106).

2.1.2 Polyethylenimine and polyethylene glycol conjugates

Branched PEI with an average molecular weight of 25 kDa (BPEI) and linear PEI with an average molecular weight of 22 kDa (LPEI) were obtained from Sigma-Aldrich (Munich, Germany) and Euromedex (Exgen 500, Euromedex, Souffelweyersheim, France), respectively. They were dissolved in water, neutralized with HCl and gelfiltrated on a Sephadex G-25 superfine column using 20 mM HEPES, 0.25 M NaCl, pH 7.4. For complex preparation, PEI was used as a 1 mg/ml working solution.

2.1.2.1 Synthesis of PEG-PEI22

PEG-PEI22 conjugate was synthesized and purified as previously described by Kursa et al. (107). Two different conjugates with molar ratios PEG (20 kDa)/LPEI of 0.9/1 and 1.7/1 were used.

2.1.2.2 Synthesis of mEGF-PEG-PEI25

Murine EGF-(2-pyridyldithio)propionate

A solution of 5 mg mEGF (lyophilized in 10 mM Tris buffer, pH 8.5) was reconstituted in 2.5 ml of water and was dialyzed (dialysis tubing Spectra/Por 6, MWCO = 1000, Serva, Heidelberg, Germany) overnight against 2 l of 20 mM HEPES pH 7.1, degassed with argon. 3.36 mg (0.56 µmol) of mEGF in 3.5 ml was obtained and mixed with 5 µmol of SPDP prepared in 1.5 ml 100 % ethanol. After 3 h at room temperature, purification was performed by gel filtration on a G-10; HR10/30 column with 20 mM HEPES pH 7.1, 20 % ethanol. The flow rate was 0.5 ml/min. The conjugate was detected at 300 nm and eluted between 18 and 26 min. 4 ml of conjugate consisting of 0.56 µmol of mEGF (3.36 mg) modified with 0.77 µmol of dithiopyridine was obtained.

Murine EGF-SH

mEGF-PDP (0.56 µmol in 4 ml 20 mM HEPES pH7.1, 20 % ethanol) was mixed with 50 equivalents of DTT in 0.1 ml water and kept under argon. After 5 min at room temperature, the reaction mixture was loaded on a gel-filtration column (Sephadex G-10; HR10/30) and eluted with 20 mM HEPES pH 7.1, 20 % ethanol. The flow rate was 0.5 ml/min. Detection at 280 nm showed that the product eluted between 17 and

28 min. 5.5 ml of conjugate consisting of 0.28 µmol of mEGF and 0.51 µmol of mercapto groups was obtained (molar ratio of 1/1.82).

PEI25-PEG-MAL

BPEI (1.6 µmol, hydrochloride salt, after gel filtration with Sephadex G-25 superfine) was dissolved in 1.3 ml of 0.25 M NaCl and the pH was adjusted to 4.4. It was mixed with 6.4 µmol NHS-PEG-MAL in 0.4 ml water for 1 h at room temperature. The reaction mixture was adjusted to a final salt concentration of 1 M NaCl, loaded on a cation-exchange column (Macro-prep High S; 10/10) and fractioned with a salt gradient from 1 to 3 M NaCl in 20 mM sodium acetate buffer pH 4.5, over 10 min. The flow rate was 0.5 ml/min. Detection at 240 and 300 nm showed that the PEI conjugate eluted at 3 M NaCl. The amount of reactive maleimide-groups was determined to be 0.94 µmol by MAL assay. The molar ratio of BPEI/MAL was 1/1.6.

Synthesis of mEGF-PEG-PEI25 (I)

mEGF-SH in 5.5 ml of 20 mM HEPES pH 7.1, 20 % ethanol equivalent to 0.28 µmol of mEGF and 0.51 µmol of mercapto-groups was mixed under argon with PEI25-PEG-MAL equivalent to 0.51 µmol maleimide. The pH of the reaction mixture was 6 and the salt concentration was 0.3 M NaCl. After 26 h at room temperature, the salt concentration of the reaction mixture was adjusted to 0.5 M NaCl with 3 M NaCl, loaded on a cation-exchange column (Macro-prep High S; 10/10) and fractioned with a salt gradient from 0.5 to 3 M NaCl in 20 mM HEPES pH 7.1, over 60 min. The flow rate was 0.5 ml/min. Detection at 280 nm showed that the conjugate eluted between 2.4 and 3 M NaCl. The resulting 10 ml of the conjugate was dialyzed (dialysis tubing Spectra/Por 1, MWCO 6000 - 8000, Serva) overnight at 4 °C against 2 l HEPES-buffered saline (HBS: 150 mM NaCl, 20 mM HEPES) pH 7.3, degassed with argon. The amount of mEGF in the conjugate was determined to be 0.65 mg by measurement at 280 nm. The amount of BPEI in the conjugate was determined to be 136 nmol by the TNBS assay. The molar ratio of mEGF/BPEI in the conjugate was 0.8/1.

Synthesis of mEGF-PEG-PEI25 (II)

mEGF-SH (0.52 µmol) in 6 ml of 20 mM HEPES pH 7.1, 20 % ethanol was mixed under argon with 0.52 µmol NHS-PEG-MAL (1.77 mg) in 0.1 ml water. After 10 min at room temperature, 0.21 µmol of gelfiltrated BPEI in 0.5 ml of 0.25 M NaCl was added under argon. After 20 h at room temperature, the salt concentration of the reaction mixture was adjusted to 0.6 M NaCl with 3 M NaCl, loaded on a cation-exchange column (Macro-prep High S; 10/10) and fractioned with a salt gradient from 0.6 to 3 M NaCl in 20 mM HEPES pH 7.1, over 60 min. The flow rate was 0.5 ml/min. Detection at 280 nm showed that the product eluted at approximately 2.4 to 3 M NaCl. The resulting 5 ml of conjugate was dialyzed (dialysis tubing Spectra/Por 1, MWCO 6000 - 8000, Serva) overnight at 4 °C against 0.5 x HBS (75 mM NaCl, 10 mM HEPES, pH 7.3), degassed with argon, and concentrated by speed vac. 2.5 ml of the conjugate in HBS consisting of 0.95 mg (158 nmol) of mEGF modified through PEG bridges with 2.4 mg (96 nmol) of BPEI with a molar ratio of 1.6/1 was obtained.

2.1.2.3 Synthesis of huEGF-PEG-PEI25

Human EGF-(2-pyridyldithio)propionate

huEGF (2 mg, 323 nmol) was reconstituted in 0.5 ml water, degassed with argon. The amount of huEGF was determined at 280 nm. The solution was added to 0.5 ml of 200 mM sodium acetate buffer pH 6.0, 60 % ethanol while mixing vigorously. This solution was mixed with 10 equivalents of SPDP in 0.5 ml of 100 % ethanol under argon. The slightly acidic pH of the reaction mixture (pH 6) was necessary to selectively modify the N-terminal amino group of huEGF. After 4 h at room temperature, the functionalized peptide was purified by gel-filtration on a Sephadex G-10 column, HR10/30, and eluted using 20 mM HEPES pH 7.1, 30 % ethanol. The molar ratio of huEGF/dithopyridine was determined as described above. The purified conjugate contained about 1.3 PDP groups per huEGF peptide.

Human EGF-SH

huEGF-PDP (0.24 µmol in 3.5 ml of 20 mM HEPES pH 7.1, 30 % ethanol) was mixed with 50 equivalents of DTT in 0.1 ml water under argon. After 5 min at room

temperature, the reaction mixture was loaded onto a gel-filtration column (Sephadex G-10; HR10/30) and eluted using 20 mM HEPES pH 7.1, 30 % ethanol to remove low molecular weight products. The amount of huEGF (0.52 µmol) was determined at 280 nm. The amount of mercapto-groups in the product was determined by the Ellmans assay .The molar ratio of huEGF/SH was 1/1.3.

huEGF-PEG-PEI25

huEGF-SH (0.18 µmol in 4.5 ml of 20 mM HEPES pH 7.1, 30 % ethanol) was mixed under argon with 0.18 µmol NHS-PEG-MAL linker in 0.1 ml water. After 10 min at room temperature, 71 nmol of gelfiltrated BPEI in 0.5 ml of 0.25M NaCl was added to the reaction mixture under argon. After 20 h at room temperature, the salt concentration of the reaction mixture was adjusted to 0.6 M NaCl with 3 M NaCl, loaded onto a cation-exchange column (Macro-prep High S; 10/10) and fractioned with a salt gradient from 0.6 to 3 M NaCl in 20 mM HEPES pH 7.1, over 60 min. The flow rate was 0.5 ml/min. Detection at 280 nm showed that the product (8 ml) was eluted at approximately 2.4 to 3 M NaCl. The conjugate was dialyzed (dialysis tubing Spectra/Por 1, MWCO 6000 - 8000, Serva) overnight at 4 °C against 0.5 x HBS, degassed with argon and concentrated by speed vac. The amount of BPEI in the conjugate was determined by the TNBS assay. 2 ml of conjugate in HBS consisting of 0.26 mg (42 nmol) of huEGF modified through PEG bridges with 1 mg (40 nmol) of BPEI with a molar ratio of about 1/1 was obtained.

2.1.3 Plasmid DNA

Plasmid pCMVLuc (Photinus pyralis luciferase under control of a cytomegalovirus (CMV) enhancer/promoter) described in (108) was produced endotoxin-free by Elim Biopharmaceuticals (San Francisco, CA, USA), Aldevron (Fargo, ND, USA) or PlasmidFactory (PlasmidFactory GmbH & Co. KG, Bielefeld, Germany) or was purified with the EndoFree Plasmid Kit from Qiagen GmbH (Hilden, Germany).

Plasmid pEGFP-N1 (encoding Enhanced Green Fluorescent Protein (EGFP) under control of a CMV promoter) was purchased from Clontech Laboratories (Heidelberg, Germany) or Elim Biopharmaceuticals.

The plasmids pEGFP-Actin, pEGFP-Tubulin and pEGFP-Luc (encoding fusion proteins of Enhanced Green Fluorescent Protein (EGFP) and human cytoplasmic β-actin, human α-tubulin or luciferase, respectively, under control of a CMV promoter) were purchased from Clontech Laboratories. All vectors contain a neomycin resistance cassette (Neor), which allows stably transfected eukaryotic cells to be selected using G418. pEGFP-Actin, pEGFP-Tubulin and pEGFP-Luc plasmids have a size of 5.8, 6.0 and 6.4 kb, respectively.

2.2 Cell culture

Cell culture media, antibiotics, fetal bovine serum (FBS), G418 (geneticin) and trypsin/EDTA solution were purchased from Invitrogen GmbH (Karlsruhe, Germany). All cultured cells were grown at 37 °C in 5 % CO_2 humidified atmosphere.

HUH-7 hepatocellular carcinoma cells (JCRB 0403; Tokyo, Japan) were cultured in DMEM/F12 (1/1) with Glutamax I medium supplemented with 10 % FBS.

The mouse renal carcinoma cell lines Renca-EGFR (Renca cells stably cotransfected with the plasmids pLTR-EGFR and pSV2neo) and Renca-LacZ (Renca cells stably transfected with a construct encoding *E. coli* β-galactosidase) were cultured in RPMI-1640 with Glutamax I medium supplemented with 10 % FBS and 0.5 mg/ml G418. Both cell lines had been kindly provided by Winfried Wels, Georg-Speyer-Haus, Frankfurt am Main, Germany.

HeLa human cervical carcinoma cells (ATCC CCL-2) were cultured in DMEM supplemented with 10 % FBS.

2.3 Covalent labeling of plasmid DNA

Plasmid pCMVLuc was covalently labeled with the fluorophores Cy3 or Cy5 using the Label IT kits (MIRUS, Madison, WI) according to the manufacturer´s instructions.

20 µg of DNA were diluted with 1 x Buffer A to a final volume of 195 µl. After addition of 5 µl reconstituted Label IT reagent, the reaction mixture was incubated for 3 h at 37 °C. To precipitate labeled DNA, 550 µl of ice-cold 100 % ethanol and 22 µl of 3 M sodium acetate were added. The solution was then mixed and placed at - 20 °C overnight. Subsequent centrifugation at 16,000•g for 60 min (4 °C) allowed removal

of unreacted label in the supernatant. The pellet was gently washed with ice-cold 70 % ethanol, centrifuged again and all traces of ethanol were removed. Labeled DNA was allowed to dry for 5 min and finally resuspended in sterile HBG.

Cy3 (ε_{550nm} = 150,000 l•mol^{-1}•cm^{-1}) and Cy5 (ε_{650nm} = 250,000 l•mol^{-1}•cm^{-1}) content were measured by absorption at 550 nm and 650 nm, respectively. DNA was quantified by measuring the absorbance at 260 nm with the ratio of 260 nm/280 nm serving as an index for DNA purity (≥1.8; ≤1.9). On average, one dye molecule was bound per 50 bp to 100 bp, approximately.

2.4 Polyplex formation

In general, polyplexes were generated by condensing plasmid DNA encoding luciferase or EGFP with PEI or PEI conjugates at a molar ratio of PEI nitrogen to DNA phosphate (N/P) of 6, if not indicated otherwise. For this reason, plasmid DNA and PEI or PEI conjugates were each diluted in the buffer indicated and rapidly mixed by pipetting up and down 5 to 8 times. Polyplexes were allowed to stand for at least 20 min at room temperature before use.

Unshielded DNA/PEI polyplexes were prepared freshly at a final DNA concentration of 20 µg/ml by flash-mixing of plasmid DNA with PEI in HEPES-buffered glucose (HBG, 5 % (w/w) glucose, 20 mM HEPES, pH 7.1), HEPES-buffered saline (HBS, 150 mM NaCl, 20 mM HEPES, pH 7.1), HBS ½ (2.5 % (w/w) glucose, 75 mM NaCl, 20 mM HEPES, pH 7.1) or OptiMEM at the indicated N/P ratio.

EGFR-targeted polyplexes (mEGF(+) complexes) were prepared by first diluting and mixing EGF-PEG-PEI25 and PEG-PEI22 conjugates with free LPEI at a molar ratio of EGF/PEG/PEI of 13 %/22 %/100 % in HBG. For the EGF-free polyplexes (EGF(-) complexes), the PEG-PEI22 conjugate was mixed with free LPEI at a molar ratio of PEG/PEI of 22 %/100 % in HBG. The PEI conjugate buffer solution was then mixed with plasmid DNA diluted in HBG at an N/P ratio of 6 and a final DNA concentration of 200 µg/ml. Complexes were incubated for 30 min at room temperature, snap-frozen in liquid nitrogen, subsequently stored at - 80 °C and, before use, allowed to stand for 30 min at room temperature after thawing.

2.5 Measurement of particle size and zeta potential

Median particle size of polyplexes was determined by laser-light scattering using a Malvern Zetasizer 3000HS (Malvern Instruments, Worcestershire, UK). Complexes were generated and subsequently diluted to 10 µg/ml prior to measurement as previously described (16).

For estimation of the surface charge, transfection complexes were diluted in 10 mM NaCl to give a final DNA concentration of 2 µg/ml and the zeta potential was measured as previously described (109).

2.6 Metabolic activity

Cells were seeded in 24 well plates at a density of 5 x 10^4 (HUH-7) or 3 x 10^4 (HeLa) cells per well 24 h prior to the experiment. Cells were treated with different concentrations of chlorpromazine or filipin III in fresh serum-free medium for 3 h at 37 °C. After further incubation for 22 h in the presence of 1 ml FBS-supplemented medium per well (without inhibitors) metabolic activity was determined using an MTT/thiazolyl blue assay: the medium was reduced to 500 µl per well and 25 µl of a 5 mg/ml solution of MTT in PBS was added to each well. After incubation for 1-2 h at 37 °C, the medium was removed, 250 µl DMSO was added and the plate was incubated for 30 min at 37 °C under constant shaking. Absorbance was measured at 590 nm (reference wavelength 630 nm) using a microplate reader (Spectrafluor Plus, Tecan Austria GmbH, Grödig, Austria) and cell viability was expressed as percentage relative to untreated control cells.

2.7 Western blot

For western blot analysis, cells were seeded in 12 well plates at a density of 8 x 10^4 cells per well 24 h prior to the experiment. Polyplexes containing 6 µg of DNA (pCMVLuc) and free mEGF at a concentration equivalent to the amount of mEGF incorporated into the mEGF(+) complexes (20 pmol) were added to the cells in 1 ml fresh culture medium. After the indicated time, cells were washed once with ice-cold PBS and collected in 250 µl of homogenizing buffer (50 mM Tris/HCl, pH 7.4, 250 mM mannitol, 1 mM EDTA, 1 mM EGTA, 1 mM dithiothreitol, 1 % (v/v) TritonX-

100, protease inhibitor cocktail tablets (Roche), and phosphatase inhibitors mixtures I and II (Sigma)) . Lysed cells were then centrifuged at 15,000•g for 15 min at 4 °C, and the protein content in the supernatant was determined using the Pierce BCA kit (Perbio Science, Bonn, Germany). For immunoblot analysis, 40 µg of solubilized protein were separated by electrophoresis in a polyacrylamide gel and transferred to a polyvinylidene fluoride (PVDF) sheet. The PVDF membrane was incubated for 1 h in 5 % non-fat milk at room temperature and immunoreacted overnight at 4 °C with monoclonal anti-phospho-Akt (New England Biolabs, Beverly, MA, USA), polyclonal anti-Akt (New England Biolabs), monoclonal anti-extracellular-signal-regulated kinase (Erk) 1,2 (New England Biolabs), polyclonal anti-phospho-Erk 1,2 (New England Biolabs) or monoclonal anti-phospho-EGFR (New England Biolabs) antibodies (0.1 mg/ml, 1:1000). The membrane was then processed using horseradish peroxidase-conjugated secondary anti-rabbit antibodies (VectorLabs, Burlingame, CA, USA) (1:2000) followed by a chemiluminescence detection method (ECL, Amersham, Arlington Heights, IL, USA). Electrophoresis and immunoblotting were performed in cooperation with Stefan Landshamer.

2.8 Cell synchronization

Cells were synchronized at G_1 phase by a standard thymidine blocking procedure (110). Strategy (i): Cells were cultured in complete medium containing 20 mM thymidine for 16 h. After medium change, cells were further cultured in the presence of 25 mM thymidine to keep the number of mitotic cells low (“continuous thymidine block”). Strategy (ii): Cells were cultured in complete medium containing 5 mM thymidine for 16 h. After medium change, cells were further cultured in the absence of thymidine to allow cell cycle progression of synchronized cells (“thymidine release”).

For analysis of cell cycle phases at different time points, cells were fixed as follows: Approximately 10^5 cells including cell supernatants were harvested, centrifuged and resuspended in 0.2 ml PBS. The cell suspension was then added dropwise to 2 ml of ice-cold 80 % ethanol and kept at - 20 °C (at least overnight). Cells were stained by incubation with 50 µg/ml PI, 0.005 % Triton X-100 and 10 µg/ml RNase A (Qiagen) for 60 min at 37 °C and analyzed using a Cyan™ MLE flow cytometer (Dako,

Copenhagen, Denmark). PI fluorescence was excited at 488 nm and emission was detected using a 613/20 nm bandpass filter. Data acquisition and analysis were performed in linear mode. To discriminate between viable and dead cells and to exclude doublets, cells were appropriately gated by forward/side scatter and pulse width.

Data analysis was carried out using Summit (Summit v3.3, Dako) and `WinMDI´ (http://facs.scripps.edu/software.html). Cell cycle distribution was analyzed using `Cylchred´ software (http://www.cardiff.ac.uk/index.html).

2.9 Luciferase reporter gene expression

2.9.1 Luciferase reporter gene expression

Cells were seeded in 96 well plates at a density of 10^4 cells per well 24 h prior to transfection. Transfection complexes with indicated amounts of DNA (pCMVLuc) were added to the cells in 100 µl fresh culture medium. Medium was replaced 4 h after transfection and gene expression was measured after further 20 h. Detection of luciferase activity was carried out as described recently (65). Transfection efficiency was expressed as relative light units (RLU) per seeded cells.

2.9.2 Luciferase reporter gene expression after cell synchronization

Cells were seeded in 24 well plates at a density of 4×10^4 cells per well 24 h prior to thymidine treatment. Cells were cultured in complete medium containing 20 mM thymidine for 16 h followed by a medium change with 25 mM thymidine (“continuous thymidine block”). Subsequently, transfection complexes were added to the cells. Medium was replaced 4 h after transfection and gene expression was measured after further incubation for 14 h. Detection of luciferase activity was carried out as described in 2.9.1.

Cells were seeded in 24 well plates at a density of 2.5×10^4 cells per well 24 h prior to thymidine treatment. Cells were cultured in complete medium containing 5 mM thymidine for 16 h. After medium change, cells were further cultured in the absence of thymidine to allow cell cycle progression of synchronized cells (“thymidine release”). 4 h after thymidine removal, transfection complexes were added to the

cells. Medium was replaced 4 h after transfection and gene expression was measured at the indicated time points. Detection of luciferase activity was carried out as described in 2.9.1.

2.9.3 Luciferase reporter gene expression in the presence of endocytosis inhibitors

Cells were seeded in 24 well plates at a density of 5 x 10^4 (HUH-7) or 3 x 10^4 (HeLa) cells per well 24 h prior to the experiment. Cells were preincubated with chlorpromazine or filipin III in fresh serum-free medium for 1 h. Subsequently, transfection complexes were added and incubation was continued for 2 h before replacing with FBS-supplemented medium without inhibitor. After further incubation for 22 h, luciferase activity was determined as described in 2.9.1. Where indicated, luciferase activity was normalized for protein content (Pierce BCA protein assay, Pierce, Rockford, Illinois) using BSA as a standard.

2.9.4 Luciferase reporter gene expression of HUH-7 EGFP-Luc cells

HUH-7 cells stably expressing EGFP-Luc (see 2.14) were seeded in 24 well plates at a density of 5 x 10^4 cells per well 24 h prior to the experiment.

Cells were treated with different concentrations of chlorpromazine or filipin III in fresh serum-free medium for 3 h at 37 °C. After further incubation for 22 h in the presence of FBS-supplemented medium (without inhibitors), luciferase activity was determined as described in 2.9.1.

Cells were cultured in complete medium containing 20 mM thymidine for 16 h followed by a medium change with 25 mM thymidine (“continuous thymidine block”). Gene expression was measured after further incubation for 22 h. Detection of luciferase activity was carried out as described in 2.9.1.

2.10 EGFP reporter gene expression

2.10.1 EGFP reporter gene expression

Cells were seeded in 12 well plates at a density of 8 x 10^4 cells per well 24 h prior to transfection. Transfection complexes with indicated amounts of DNA (pEGFP-N1) were added to the cells in 1 ml fresh culture medium. Medium was replaced 4 h after

transfection. Cells were harvested 48 h posttransfection by treatment with trypsin/EDTA solution and kept on ice until analysis. The percentage of transfected cells was determined using a Cyan™ MLE flow cytometer (Dako). EGFP fluorescence was excited at 488 nm and emission was detected using a 530/40 nm bandpass filter and a 575/25 nm bandpass filter to analyze EGFP-positive cells by diagonal gating (17). To discriminate between viable and dead cells and to exclude doublets, cells were appropriately gated by forward/side scatter and pulse width, and 2 x 10^4 gated events per sample were collected.

2.10.2 EGFP reporter gene expression after cell synchronization

Cells were seeded in 12 well plates at a density of 8 x 10^4 cells per well 24 h prior to thymidine treatment. Cells were cultured in complete medium containing 20 mM thymidine for 16 h followed by a medium change with 25 mM thymidine ("continuous thymidine block"). Subsequently, transfection complexes were added to the cells. Medium was replaced 4 h after transfection and cells including cell supernatants were harvested after further incubation for 18 h by treatment with trypsin/EDTA solution. The percentage of transfected cells was determined as described in 2.10.1.

Cells were seeded in 12 well plates at a density of 5 x 10^4 cells per well 24 h prior to thymidine treatment. Cells were cultured in complete medium containing 5 mM thymidine for 16 h. After medium change, cells were further cultured in the absence of thymidine to allow cell cycle progression of synchronized cells ("thymidine release"). 4 h after thymidine removal, transfection complexes were added to the cells. Medium was replaced 4 h after transfection and cells including cell supernatants were harvested after the indicated time points by treatment with trypsin/EDTA solution. The percentage of transfected cells was determined as described in 2.10.1.

2.11 Flow cytometry

2.11.1 Correlation of cell association, EGFP expression and cell cycle phase

Cells were seeded in 6 well plates at a density of 2 x 10^5 cells per well 24 h prior to transfection. Polyplexes containing Cy5-labeled DNA (20 % Cy5-DNA) were added to

the cells at a DNA concentration of 10 µg/ml and cells were harvested after 6 h incubation at 37 °C by treatment with trypsin/EDTA solution. Cells were washed with PBS and stained with 5 µg/ml Hoechst 33342 for 30 min at 37 °C. Cells were then assayed using a Cyan™ MLE flow cytometer (Dako) equipped with a water-cooled Enterprise II laser (model 621, Coherent) delivering light at 364 nm and 488 nm and a laser diode with emission at 635 nm. Hoechst 33342 was excited at 364 nm and emission was detected at 450/50 nm. The fluorophore Cy5 was excited at 635 nm and emission was detected at 665/20 nm. Flow cytometric analysis was performed as described in 2.10.1.

2.11.2 Analysis of cell surface EGFR levels after transfection

Cells were seeded in 12 well plates at a density of 8 x 10^4 cells per well 24 h prior to transfection. Polyplexes were added to the cells at a DNA concentration of 3 µg/ml in 1 ml of fresh culture medium. After 2 h, cells were detached using 5 mM EDTA in PBS. Cells were washed with PBS, resuspended in 0.1 % BSA and incubated with mouse anti-huEGFR antibody (1:500) (clone H11, M3563, Dako, Hamburg, Germany) for 1 h at 4 °C. Control cells were incubated accordingly with IgG_1 mouse antibody (1:100) (X0931, Dako, Germany). After washing with 0.1 % BSA, samples were stained with goat anti-mouse IgG_1 antibody linked to Alexa Fluor® 350 (1:200) (Molecular Probes) for 1 h at 4 °C. Shortly before acquisition, YOYO-1 was added at a final concentration of 1 µM. EGFR levels were determined by flow cytometry. Alexa Fluor® 350 was excited at 364 nm and emission was detected at 450/50 nm. To discriminate between viable and dead cells, cells incorporating high levels of YOYO-1 and showing a reduction in forward scatter as a measure for cell size were excluded from further analysis. To exclude doublets, cells were appropriately gated by forward scatter/pulse width. 2 x 10^4 gated events per sample were collected.

2.11.3 Analysis of cellular polyplex association

Cells were seeded in 12 well plates at a density of 8 x 10^4 cells per well 24 h prior to transfection. Polyplexes containing Cy5-labeled DNA (20 % Cy5-DNA) were added to the cells in 1 ml of fresh culture medium. Cells were harvested after 30 min, 2 h or 4 h incubation at 37 °C by treatment with trypsin/EDTA solution and kept on ice until analysis. Cell association of polyplexes was assayed by flow cytometry. The

fluorophore Cy5 was excited at 635 nm and emission was detected at 665/20 nm. To discriminate between viable and dead cells and to exclude doublets, cells were appropriately gated by forward/side scatter and pulse width, and 2 x 10^4 gated events per sample were collected. Median channel values +/- SD of triplicates (representing the median intensity of cell-associated DNA) were determined and presented as relative fluorescence units (RFU) with the highest value defined as 100 %.

2.11.4 Analysis of cellular polyplex uptake

To assay the kinetics of cellular internalization, a procedure described by Ogris et al. (111) was adopted and slightly modified. Cells were seeded in 12 well plates - coated with collagen G (Biochrom AG, Berlin, Germany) - at a density of 8 x 10^4 cells per well 24 h prior to transfection. Polyplexes containing Cy5-labeled DNA (20 % Cy5-DNA) were added to the cells in fresh culture medium. Cells were harvested after 30 min, 2 h or 4 h incubation at 37 °C by treatment with 105 Units per ml collagenase A solution (Biochrom). To remove extracellularly-bound PEI and EGF(-) complexes, cells were first treated with 100 I.E. heparin for 30 min at 37 °C (in the presence of 75 mM sodium azide to inhibit endocytosis) and then harvested by treatment with trypsin/EDTA solution. To remove extracellularly-bound mEGF(+) complexes, cells were treated with HEPES buffer (20 mM HEPES, pH 7.1) containing 150 mM sodium azide, 1000 I.E./ml heparin, 0.5 % (w/v) trypsin and 2.5 mM EDTA for 30 min at 37 °C. Cells were then harvested and centrifuged. To assure that all extracellularly-bound polyplexes were removed, cells were stained on ice with YOYO-1 at a final concentration of 1 µM. To allow correlation of Cy5 and YOYO-1 fluorescence signals, control transfections were carried out for 1 h at 4 °C when endocytosis is inhibited (with additional 40 mM sodium azide during incubation at 37 °C while harvesting). Cellular polyplex uptake was assayed by flow cytometry. The fluorophores YOYO-1 and Cy5 were excited at 488 nm and 635 nm, respectively, and emission was detected at 530/40 nm and 665/20 nm, respectively. To discriminate between viable and dead cells, cells incorporating high levels of YOYO-1 and showing a reduction in forward scatter as a measure for cell size were excluded from further analysis. To exclude doublets, cells were appropriately gated by forward scatter/pulse width. 2 x 10^4 gated events per sample were collected.

2.11.5 Analysis of cellular polyplex uptake in the presence of uptake inhibitors

Cells were seeded as described in 2.11.2. They were preincubated with chlorpromazine or filipin III in fresh serum-free medium for 1 h. Subsequently, polyplexes containing Cy5-labeled DNA (20 % Cy5-DNA) were added to the cells. After 2 h, extracellularly-bound complexes were removed and cells were analyzed as described in 2.11.3.

Flow cytometric data were analyzed using Summit (Summit v3.3, Dako) and `WinMDI´ software (http://facs.scripps.edu/software.html).

2.12 Epifluorescence microscopy

2.12.1 Analysis of cellular polyplex association

Cells were seeded on medco glass slides (10 well, Medco, Munich, Germany) coated with collagen G (Biochrom) at a density of 3 x 10^3 cells per well 24 h prior to transfection. Cells were transfected with Cy3-labeled DNA complexes (4 % Cy3-DNA) at a concentration of 250 ng DNA per well. After 2 h incubation at 37 °C, the slides were washed twice with PBS, fixed with 4 % paraformaldehyde, permeabilized with 0.1 % Triton X-100 and the nuclei were stained with DAPI. Afterwards, samples were mounted with vectashield mounting medium (Vector Laboratories, Burlingame, CA, USA) and covered with a coverslip. Samples were visualized on an Axiovert 200 fluorescence microscope (Carl Zeiss, Jena, Germany) equipped with a Zeiss Axiocam camera. Light was collected through a 63 x 1.4 NA oil immersion objective (Zeiss). Cy3 fluorescence was excited using a 546/12 nm bandpass filter and emission was detected using a 575-640 nm bandpass filter (Zeiss Filter Set 20). DAPI fluorescence was excited using a G 365 nm filter and emission was detected using a 420 nm longpass (Zeiss Filter Set 02). Digital image recording and image analysis were performed with the Axiovision 3.1 software (Zeiss).

2.12.2 Cellular uptake of transferrin and cholera toxin B

Cells were seeded in Lab-Tek 8 Chambered Coverglasses (Nalge Nunc International, Naperville, IL, USA) at a density of 2 x 10^4 cells per chamber 24 h prior to the experiment. Cells were treated with chlorpromazine or filipin III in fresh serum-

free medium for 1 h at 37 °C. Subsequently, Alexa Fluor® 647 transferrin or Alexa Fluor® 488 CTB were added at a concentration of 10 µg/ml or 5 nM, respectively. After 30 min at 37 °C, medium was replaced. Living cells were visualized as described in 2.12.1. Alexa Fluor® 647 fluorescence was excited using a 620/60 nm bandpass filter and emission was detected using a 700/75 nm bandpass filter (Chroma Technology Corp.). Alexa Fluor® 488 fluorescence was excited using a 450-490 nm bandpass filter and emission was detected using a 515-565 nm bandpass filter (Zeiss Filter Set 10).

2.13 Analysis of colocalization of polyplexes with transferrin or CTB by confocal laser scanning microscopy

Cells were seeded in Lab-Tek 8 Chambered Coverglasses (Nalge Nunc) at a density of 2 x 10^4 cells per chamber 24 h prior to transfection. Alexa Fluor® 647 transferrin (10 µg/ml) and Cy3-labeled polyplexes (20 % Cy3-DNA) or Alexa Fluor® 488 CTB (5 nM) and Cy5-labeled polyplexes (20 % Cy5-DNA) were added to the cells to allow simultaneous internalization. Live cell imaging was performed 1-4 h after transfection using a confocal laser scanning microscope (LSM 510, Zeiss) equipped with an argon and two helium/neon lasers delivering light at 488, 543 and 633 nm, respectively. Light was collected through a 100 x 1.4 NA oil immersion objective (Zeiss). Cy3 fluorescence was excited with the 543 nm line; emission was collected using a 565-615 nm bandpass filter. Excitation of Cy5 and Alexa Fluor® 647 fluorescence was achieved by using the 633 nm line with the resulting fluorescent wavelengths observed with a 650 nm longpass filter. Alexa Fluor® 488 was excited with the 488 nm line and emission was collected using a 500-550 nm bandpass filter. No signal overspill between the individual fluorescence channels was observed. An optical section thickness of 0.8 µm was chosen.

Digital image recording and image analysis were performed with the LSM 5 software (version 3.0, Zeiss).

2.14 Generation of stably transfected single cell clones

2.14.1 Plasmid DNA amplification and preparation

For amplification of plasmid DNA, competent cells of bacterial strain E. coli DH5α (Invitrogen) were transformed with the plasmid DNA, the transformation mix was plated onto a selection agar plate (kanamycin, 30 µg/ml) and incubated at 37 °C overnight. A single bacterial colony was picked, inoculated into 1 ml of LB medium containing kanamycin and incubated at 37 °C with vigorous shaking for 8 h. This culture was then inoculated into 250 ml of LB medium containing the appropriate antibiotic. After incubation at 37 °C overnight with shaking, the bacterial culture was harvested by centrifugation and the plasmid DNA was isolated using the EndoFree Plasmid Maxi Kit (Qiagen) according to the manufacturer´s instructions. The DNA was resuspended in 150 µl of sterile destilled water and quantified by absorption at 260 nm.

2.14.2 Generation of stably expressing EGFP-Actin cells, EGFP-Tubulin cells and EGFP-Luciferase cells

For the generation of stably expressing EGFP-Actin cells, EGFP-Tubulin cells or EGFP-Luciferase cells, vectors were linearized wih the restriction enzymes ApaL I, MlU I or Dra III, respectively. HUH-7 cells were transfected using LPEI polyplexes generated in HBS ½ with an N/P ratio of 6. Cells were incubated in fresh medium for 48-72 h and then selected with 200 µg/ml (EGFP-Actin/-Tubulin) or 100 µg/ml (EGFP-Luciferase) G418. After several days, surviving cells were seeded at low densities into 6 well plates in order to obtain separate colonies. When the cells had grown up, single cell clones were isolated and expanded. The generated clones were analyzed for the percentage of EGFP-positive (EGFP-Actin, EGFP-Tubulin or EGFP-Luciferase stably transfected) cells by flow cytometry. Single cell clones characterized by a single population with all cells positive for EGFP were chosen and expanded.

2.15 Statistical analysis

Where indicated, one-way analysis of variance (ANOVA) with subsequent Duncan test was performed.

3 Results

3.1 EGFR-targeting enhances transfection efficiency of PEGylated PEI polyplexes

To elucidate the cellular mechanisms of EGFR-targeted gene delivery, transfection characteristics of PEG-shielded EGF-containing PEI polyplexes (EGF(+) complexes) were compared to those of PEG-shielded EGF-free polyplexes (EGF(-) complexes) in EGFR-expressing cell lines.

3.1.1 EGFR-targeted and PEG-shielded polyplexes maintain their biophysical properties upon freeze-thawing

For the formation of mEGF(+) polyplexes, LPEI, PEG-PEI25 and mEGF-PEG-PEI25 conjugates were diluted in HEPES-buffered glucose (HBG) and then mixed with plasmid DNA at a ratio of PEI nitrogen to DNA phosphate (N/P ratio) of 6. This gave rise to small-sized particles displaying a nearly neutral surface charge owing to the shielding coat of 20 kDa PEG. The EGF ligand attached to the distal end of a 3.4 kDa PEG chain was supposed to show good accessibility to its receptor. These polyplexes were compared to EGF-free particles containing the same amount of PEG shield (EGF(-) complexes). Targeted and non-targeted complexes did not differ in particle size (approximately 140 nm in diameter) and zeta potential (approximately + 2.5 mV) (Table 2).

PEGylated PEI polyplexes generated in HBG have been shown to maintain their biophysical properties upon freeze-thawing (107). This was found to be important for the retention of transfection rates (17). Therefore, after incubation for 30 min at room temperature, polyplexes were snap-frozen in liquid nitrogen and stored at - 80 °C. After thawing, biophysical properties of both formulations were comparable to those of the corresponding fresh complex (Table 2).

particle size (nm)		
polyplex	before freezing	after thawing
EGF(-)	119 (+/- 11)	116 (+/- 11)
mEGF(+)	146 (+/- 8)	156 (+/- 14)
zeta potential (mV)		
polyplex	before freezing	after thawing
EGF(-)	2.3 (+/- 0.2)	2.3 (+/- 0.1)
mEGF(+)	2.7 (+/- 0.6)	2.6 (+/- 0.8)

Table 2: Biophysical properties of EGF(-) and mEGF(+) polyplexes before and after the freezing/thawing procedure.

3.1.2 EGFR-targeting increases transgene expression mediated by PEGylated PEI polyplexes

To evaluate the capacity of EGFR-targeted polyplexes to improve gene transfer into EGFR-expressing cells, transfection efficiency was assayed and compared to that of EGF(-) complexes. Therefore, luciferase activity was analyzed in two different tumor cell lines (HUH-7 and Renca-EGFR) after transfection with increasing amounts of DNA.

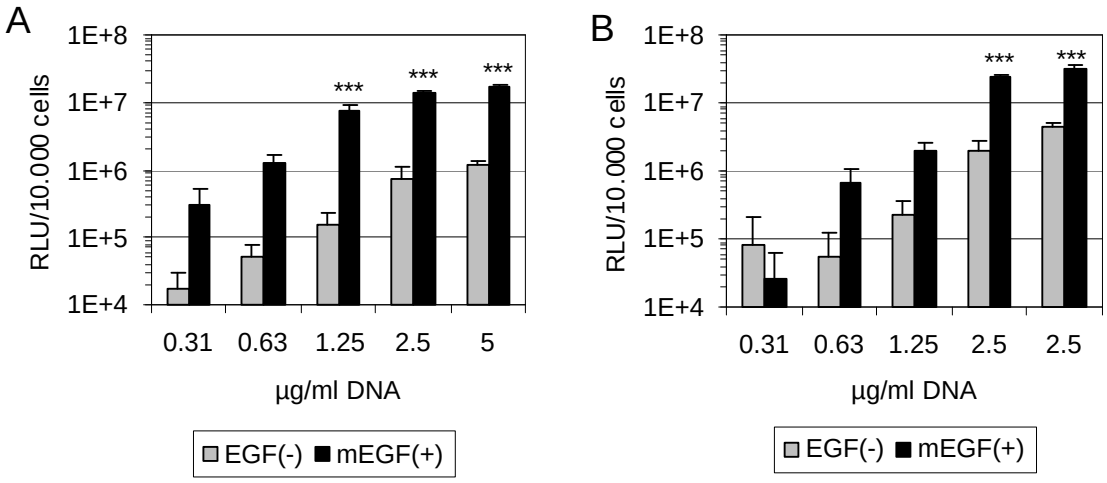

*Figure 4: Reporter gene expression (luciferase activity) after transfection with EGF(-) and mEGF(+) polyplexes. HUH-7 (A) and Renca-EGFR (B) cells were transfected with increasing amounts of DNA. Luciferase activity was assayed 24 h after transfection and is presented as mean values + SD of triplicates. ***p < 0.001; **p < 0.01; *p < 0.05, compared to EGF(-) complexes at the same DNA concentration (ANOVA, Duncan).*

In HUH-7, a human hepatocellular carcinoma cell line overexpressing the EGFR, mEGF(+) complexes mediated a strong increase in luciferase activity at all DNA concentrations tested (Figure 4A). They were found to be up to 50-fold more efficient than EGF(-) complexes. In Renca-EGFR, a cell line stably expressing a plasmid

encoding EGFR, luciferase activity was enhanced up to 12-fold at DNA concentrations above 500 ng/ml, whereas at very low concentrations no targeting effect could be detected (Figure 4B).

To evaluate whether the EGFR was involved in EGFR-mediated gene transfer, a competition assay was performed. Transfection was carried out in the presence of a 1000-fold molar excess of free mEGF. The same amount of BSA was added to control cells.

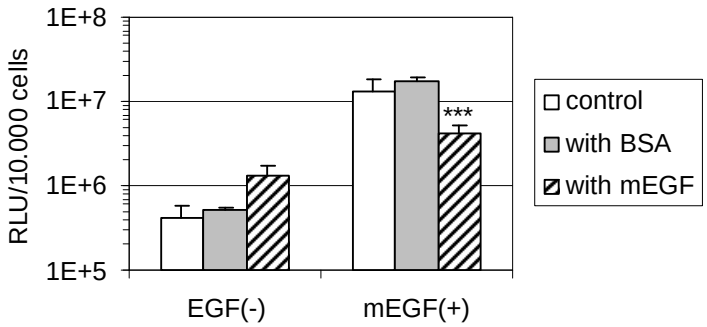

*Figure 5: Reporter gene expression (luciferase activity) with competitive inhibition of EGFR-mediated gene transfer. HUH-7 cells were transfected with EGF(-) and mEGF(+) polyplexes at a DNA concentration of 2.5 µg/ml. Cells were coincubated with a 1000-fold molar excess of free competing ligand (mEGF). Control cells were transfected in the presence of BSA. Luciferase activity was assayed 24 h after transfection and is presented as mean values + SD of triplicates. ***p < 0.001; **p < 0.01; *p < 0.05, compared to cells with BSA treatment (ANOVA, Duncan).*

Competition of free EGF with EGF-containing polyplexes resulted in a decrease in transfection efficiency down to the levels of EGF(-) complexes (Figure 5). In contrast, addition of BSA – a protein which does not interact with the EGFR – did not reduce EGFR-mediated gene transfer. Notably, luciferase activity of EGF(-) complexes increased when free EGF was added. This might be due to the fact that EGF is capable of triggering mitotic signaling leading to a higher percentage of dividing cells. This favors nuclear entry during nuclear disassembly. However, despite the high concentration of free EGF, luciferase activity did not reach the levels mediated by mEGF(+) complexes, indicating that EGFR activation, if at all involved, is not the major reason for enhanced transfection efficiency of targeted polyplexes.

3.1.3 mEGF can substitute huEGF in the synthesis of EGFR-targeted PEI polyplexes

EGF proteins are evolutionary closely conserved. For example, human and murine EGF have 37 amino acids in common. Since murine EGF (mEGF, $K_d = 10^{-6}$ - 10^{-10} M (112)) displays a binding activity towards the human EGFR similar to human EGF (huEGF, $K_d = 10^{-9}$ - 10^{-10} M (94)), it can be used to substitute huEGF in the synthesis of gene delivery carriers. For this purpose, mEGF is even favored over huEGF because it contains only one amino group at the N-terminus whereas huEGF contains two lysines in the peptide chain (Lys 28 and Lys 48) bearing further reactive amino groups which hampers specific chemical coupling via amino functions (113;114).

Experiments described above (3.1.1 and 3.1.2) were performed with poyplexes carrying murine EGF as the ligand for EGFR-specific gene delivery. In order to validate this model, a huEGF-PEG-PEI25 conjugate was evaluated for transfection efficiency where huEGF was selectively coupled to PEG via its N-terminal amino group. N-terminal site-specific PEGylation was achieved by modification of huEGF at a slightly acidic pH to enable selective deprotonation of the α-amino group (114).

huEGF(+) polyplexes were generated with amounts of EGF and PEG equivalent to that of mEGF(+) polyplexes and analyzed in terms of luciferase reporter gene expression in HUH-7 cells.

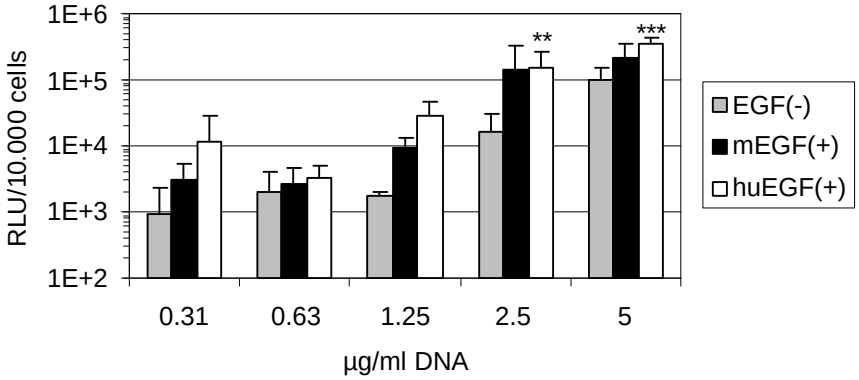

*Figure 6: Reporter gene expression (luciferase activity) after transfection with EGF(-), mEGF(+) and huEGF(+) polyplexes. HUH-7 cells were transfected with increasing amounts of DNA. Luciferase activity was assayed 24 h after transfection and is presented as mean values + SD of triplicates. Transfection data of huEGF(+) polyplexes were analyzed for statistical significance. ***p < 0.001; **p < 0.01; *p < 0.05, compared to EGF(-) complexes at the same DNA concentration (ANOVA, Duncan).*

It was found that gene transfer efficiency of huEGF(+) polyplexes was only slightly higher than that of the corresponding mEGF(+) complexes (Figure 6). This indicates that mEGF is able to substitute huEGF in the design of EGFR-targeted gene delivery vehicles.

In order to assess receptor specificity of EGFR-targeted gene transfer, free huEGF at a 1000-fold molar excess was added to the culture medium during transfection. Control cells were transfected in the presence of BSA at a protein concentration equivalent to the amount of free huEGF.

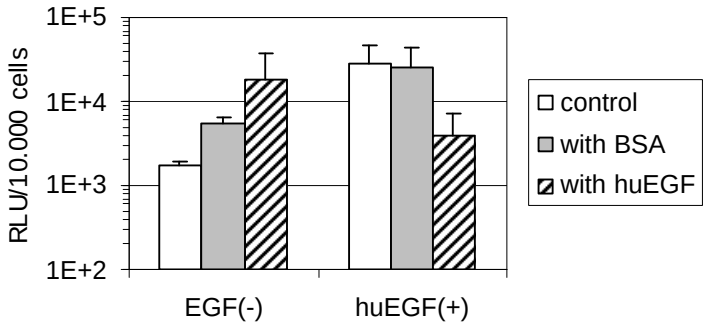

*Figure 7: Reporter gene expression (luciferase activity) with competitive inhibition of EGFR-mediated gene transfer. HUH-7 cells were transfected with EGF(-) and huEGF(+) polyplexes at a DNA concentration of 1.25 µg/ml. Cells were coincubated with a 1000-fold molar excess of free competing ligand (huEGF). Control cells were transfected in the presence of BSA. Luciferase activity was assayed 24 h after transfection and is presented as mean values + SD of triplicates. ***p < 0.001; **p < 0.01; *p < 0.05, compared to cells with BSA treatment (ANOVA, Duncan).*

A pattern similar to that with mEGF(+) complexes (Figure 5) was observed: transfection efficiency of huEGF(+) polyplexes was reduced in the presence of free competing ligand, however not significantly. In contrast, exogeneous EGF enhanced gene transfer by EGF(-) complexes (Figure 7), probably due to the mitogenic activity of the free growth factor. Surprisingly, non-targeted transfection in the presence of free huEGF yielded higher efficiencies than EGFR-targeted gene delivery under the same conditions. This suggested that in this experiment, further important factors played a role which, however, could not be identified.

3.1.4 EGFR-targeting increases the number of cells transfected by PEGylated PEI polyplexes

In order to test whether enhanced gene transfer efficiency by EGFR-targeted polyplexes was associated with an increase in the number of transfected cells, the percentage of transfected cells was analyzed. HUH-7 and Renca-EGFR cells were transfected using Enhanced Green Fluorescent Protein (EGFP)-encoding DNA complexes and EGFP expression was determined 48 h posttransfection. In line with the results obtained in the luciferase assay (Figure 4), EGF-containing polyplexes showed a strong increase in transfection efficiency. With EGF(-) complexes, the percentage of transfected cells was very low (0.4 %) in HUH-7 and moderate (11 %) in Renca-EGFR. With mEGF(+) complexes, however, up to 13 % (HUH-7) and 20 % (Renca-EGFR) expressed EGFP. This corresponds to a 29-fold and 2-fold increase, respectively (Figure 8).

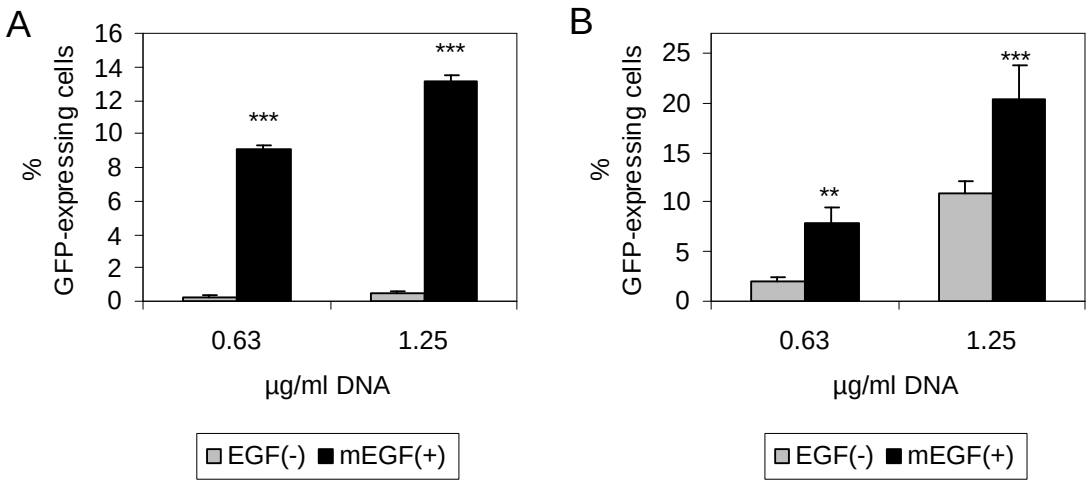

*Figure 8: Reporter gene expression (EGFP expression) after transfection with EGF(-) and mEGF(+) polyplexes. HUH-7 (A) and Renca-EGFR (B) cells were transfected with the indicated amounts of DNA. The percentage of EGFP-positive cells was analyzed by flow cytometry 48 h after transfection and is presented as mean values + SD of triplicates. ***p < 0.001; **p < 0.01; *p < 0.05, compared to EGF(-) polyplexes at the same DNA concentration (ANOVA, Duncan).*

To test whether this increase in transfection efficiency was mediated by a specific interaction between the EGFR and its ligand, transfection was carried out in the presence of a 1000-fold molar excess of free competing ligand or BSA as irrelevant control.

Figure 9 illustrates that gene transfer efficiency of EGF(-) complexes in the presence of free mEGF did not change, whereas EGFR-mediated transfection was reduced to

nearly the levels found for the receptor-independent transfection when free mEGF was added. Notably, transfection efficiency of EGF(-) complexes was not enhanced in the presence of free mEGF, as it had been observed in the luciferase assay (Figure 5, Figure 7).

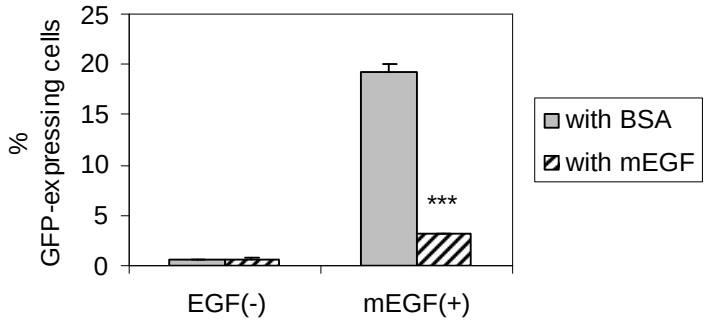

*Figure 9: Reporter gene expression (EGFP expression) with competitive inhibition of EGFR-mediated gene transfer. HUH-7 cells were transfected with EGF(-) and mEGF(+) polyplexes at a DNA concentration of 0.63 µg/ml. Cells were coincubated with a 1000-fold molar excess of free competing ligand (mEGF). Control cells were transfected in the presence of BSA. The percentage of EGFP-positive cells was analyzed by flow cytometry 48 h after transfection and is presented as mean values + SD of triplicates. ***p < 0.001; **p < 0.01; *p < 0.05, compared to cells with BSA treatment (ANOVA, Duncan).*

To further confirm that the EGFR was essential for improved transfection efficiency of EGFR-targeted polyplexes, EGFR-free Renca-LacZ cells were transfected with EGF(-) and mEGF(+) complexes.

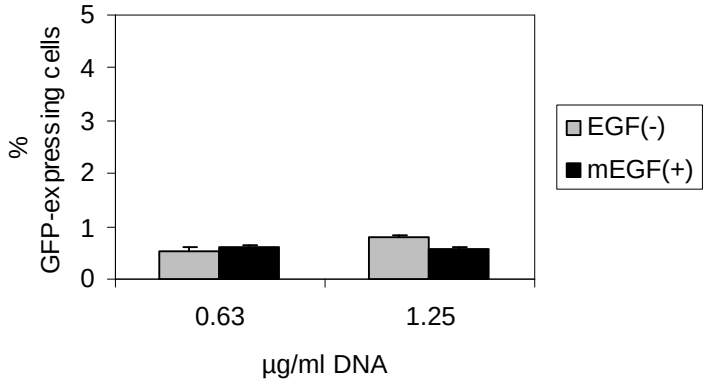

Figure 10: Reporter gene expression (EGFP expression) after transfection with EGF(-) and mEGF(+) polyplexes. Renca-LacZ cells were transfected with the indicated amounts of DNA. The percentage of EGFP-positive cells was analyzed by flow cytometry 48 h after transfection and is presented as mean values + SD of triplicates.

No difference between transfection efficiency of targeted and non-targeted polyplexes could be detected, indicating that EGF(+) complexes do not enhance gene transfer into EGFR-free cells (Figure 10). Accordingly, transfection of Renca-

LacZ cells with mEGF(+) complexes could not be reduced by coincubation with free mEGF (data not shown).

In summary, EGFR-targeted PEI polyplexes (mEGF(+)) mediated enhanced gene transfer into both HUH-7 and Renca-EGFR cells compared to non-targeted, shielded (EGF(-)) complexes. Overall transgene expression as well as the number of transfected cells increased after transfection with complexes containing murine EGF. Transfection efficiency of mEGF(+) polyplexes was comparable to that of huEGF(+) complexes, indicating that human EGF can be substituted by murine EGF in the synthesis of EGFR-targeted gene delivery vectors. Furthermore, receptor specificity of EGFR-targeted transfection was suggested by the observation that addition of free EGF as competing ligand reduced transfection efficiency close to the level of non-targeted transfection. This finding suggests that free mEGF acts by interference with EGFR-mediated cellular polyplex binding and internalization. Therefore, cellular uptake characteristics of mEGF(+) polyplexes were analyzed next.

3.2 EGFR-targeting improves cellular uptake of PEGylated PEI polyplexes

Cellular uptake processes of PEI polyplexes can be divided into two steps: First, the particle attaches to the cell membrane due to receptor-ligand interactions or electrostatic attraction, and second, the particle gets internalized, usually by subsequent formation of small vesicles. Both steps might be enhanced by incorporation of a ligand into the polyplex.

3.2.1 EGFR-targeting improves total cellular association of PEGylated PEI polyplexes

To determine whether enhanced cellular binding contributed to the increased transfection efficiencies of mEGF(+) complexes, cellular association studies were performed using both HUH-7 and Renca-EGFR cells. EGF(-) and mEGF(+) polyplexes were generated with Cy5-labeled DNA to enable analysis of cell-associated particles by flow cytometry.

First, to determine how much complex attached to the exterior cell membrane, the assay was performed by incubation at low temperatures when endocytosis is

inhibited. Cells were incubated with polyplexes on ice and median Cy5 fluorescence was determined 1 h posttransfection. Incubation with EGFR-targeted complexes resulted in a more than six-fold increase in cellular association compared to EGF(-) polyplexes which was only due to enhanced binding of particles to the cell surface, because uptake processes were inhibited (data not shown).

Second, total cellular association was analyzed representing the amount of extracellularly-bound and internalized complexes. Cells were transfected and total cellular association of particles was analyzed after 30 min, 2 h and 4 h at 37 °C. Median values of Cy5 fluorescence were determined and converted into relative fluorescence units (RFU), with the highest value defined as 100 %.

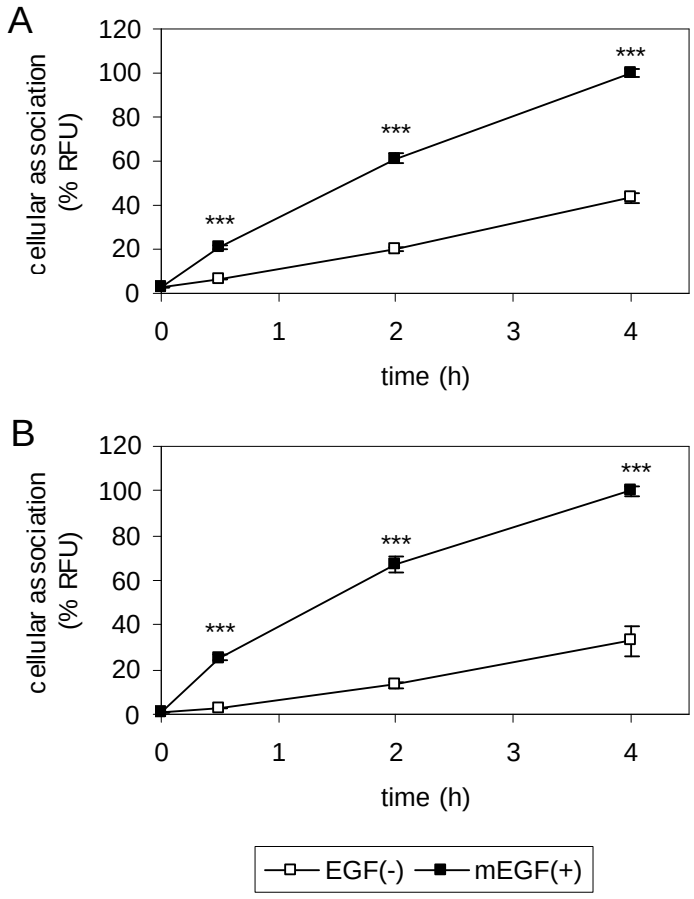

*Figure 11: Total cellular association of EGF(-) and mEGF(+) polyplexes. HUH-7 (A) and Renca-EGFR (B) cells were transfected with complexes containing Cy5-labeled DNA at a DNA concentration of 0.63 µg/ml. Cellular association was analyzed by flow cytometry after 30 min, 2 h and 4 h. Median channel values were determined and presented as relative fluorescence units (RFU), with the highest value defined as 100 %. Mean values +/- SD of triplicates are presented. ***p < 0.001; **p < 0.01; *p < 0.05, compared to EGF(-) polyplexes at the same time point (ANOVA, Duncan).*

Incubation with mEGF(+) complexes resulted in strong cellular association which was 2- to 10-fold higher compared to EGF(-) complexes (Figure 11). The difference in cellular association was already pronounced after only 30 min of incubation, indicating a fast interaction of mEGF(+) polyplexes with the membrane of EGFR-expressing cells.

Therefore, to evaluate involvement of the EGFR in this process, the assay was carried out in the presence of free mEGF as competing ligand (1000-fold molar excess) or BSA as irrelevant control. In contrast to the control cells incubated with BSA, competition of free ligand with EGF-containing polyplexes reduced total cellular association to nearly the same values found with non-targeted complexes (Figure 12). In contrast, receptor-independent cell association of EGF(-) complexes was not affected by free EGF.

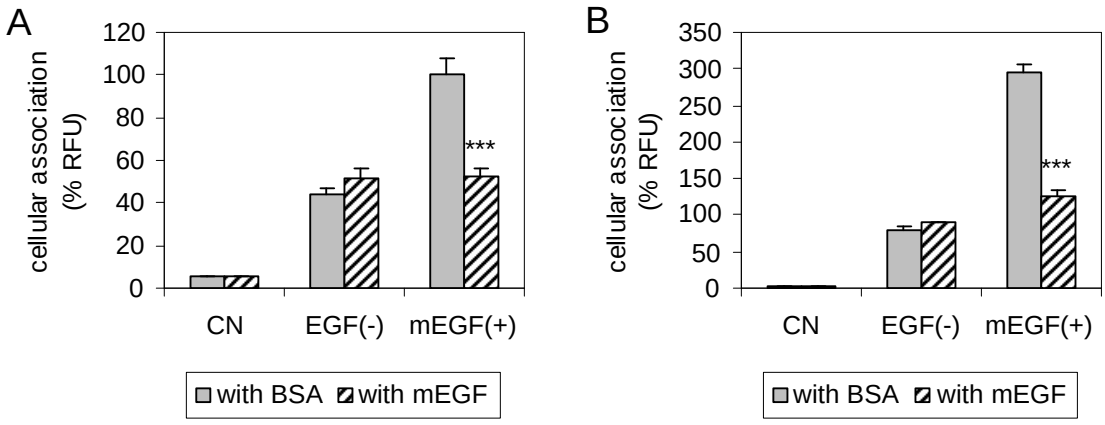

*Figure 12: Total cellular association of EGF(-) and mEGF(+) polyplexes with competitive inhibition of EGFR/ligand interaction. HUH-7 (A) and Renca-EGFR (B) cells were transfected with complexes containing Cy5-labeled DNA at a DNA concentration of 0.63 µg/ml. Cells were coincubated with a 1000-fold molar excess of free competing ligand (mEGF). Control cells were transfected in the presence of BSA. Cellular association was analyzed by flow cytometry after 4 h. Median channel values were determined and presented as relative fluorescence units (RFU), with the highest value defined as 100 %. Mean values + SD of triplicates are presented. ***p < 0.001; **p < 0.01; *p < 0.05, compared to cells with BSA treatment (ANOVA, Duncan).*

To confirm EGFR specificity of cellular mEGF(+) polyplex binding, transfection was performed in EGFR-free Renca-LacZ cells. As expected, no relevant differences in total cellular association between targeted and non-targeted polyplexes could be detected (Figure 13).

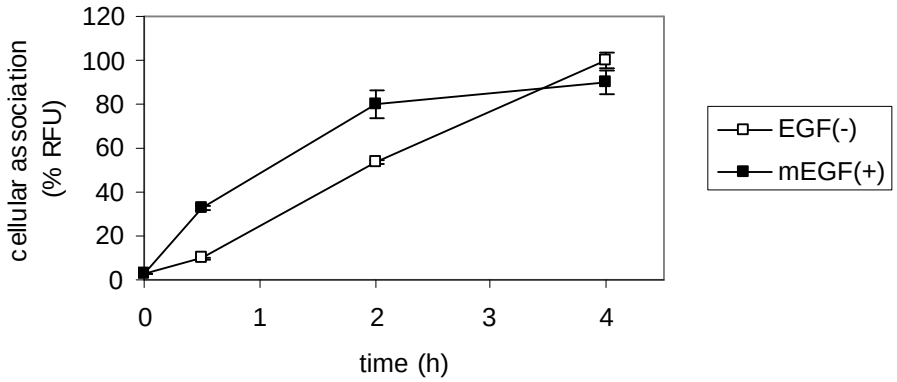

Figure 13: Total cellular association of EGF(-) and mEGF(+) polyplexes. Renca-LacZ cells were transfected with complexes containing Cy5-labeled DNA at a DNA concentration of 1.25 µg/ml. Cellular association was analyzed by flow cytometry after 30 min, 2 h and 4 h. Median channel values were determined and presented as relative fluorescence units (RFU), with the highest value defined as 100 %. Mean values +/- SD of triplicates are presented.

Furthermore, huEGF(+) complexes were compared to EGF(-) and mEGF(+) complexes in terms of total cellular association. huEGF(+) polyplexes attached to HUH-7 cells just as well as mEGF(+) complexes, with fluorescence signals 2.5- to 3.5-fold higher than those of EGF(-) complexes (Figure 14).

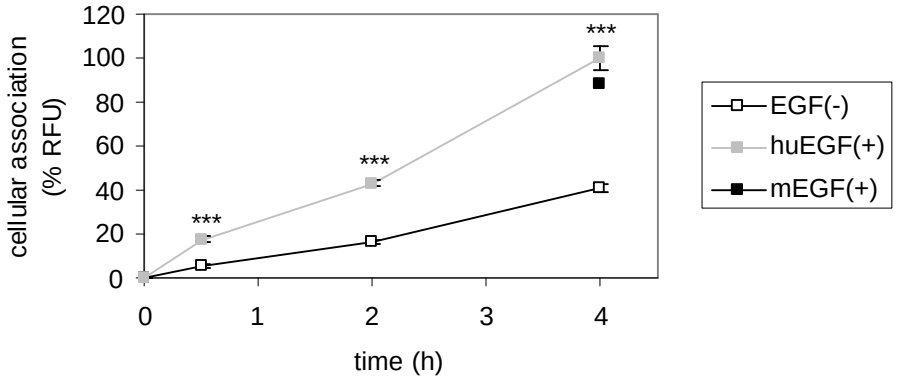

*Figure 14: Total cellular association of EGF(-) and huEGF(+) polyplexes. HUH-7 cells were transfected with complexes containing Cy5-labeled DNA at a DNA concentration of 1.25 µg/ml. Cellular association was analyzed by flow cytometry after 30 min, 2 h and 4 h. Cellular association of mEGF(+) polyplexes at the same DNA concentration served as a standard. Median channel values were determined and presented as relative fluorescence units (RFU), with the highest value defined as 100 %. Mean values +/- SD of triplicates are presented. ***p < 0.001; **p < 0.01; *p < 0.05, compared to EGF(-) polyplexes at the same time point (ANOVA, Duncan).*

3.2.2 EGFR-targeted complexes cluster upon cell binding

To further characterize cellular association of polyplexes, HUH-7 cells were transfected with complexes containing Cy3-labeled DNA and visualized by fluorescence microscopy. Increased cell binding of mEGF(+) polyplexes was associated with clustering of complexes bound to the cells. While EGF(-) polyplexes appeared as a faint punctual pattern on the cells (Figure 15A), mEGF+ polyplexes were observed as large aggregates of micrometer size (Figure 15B).

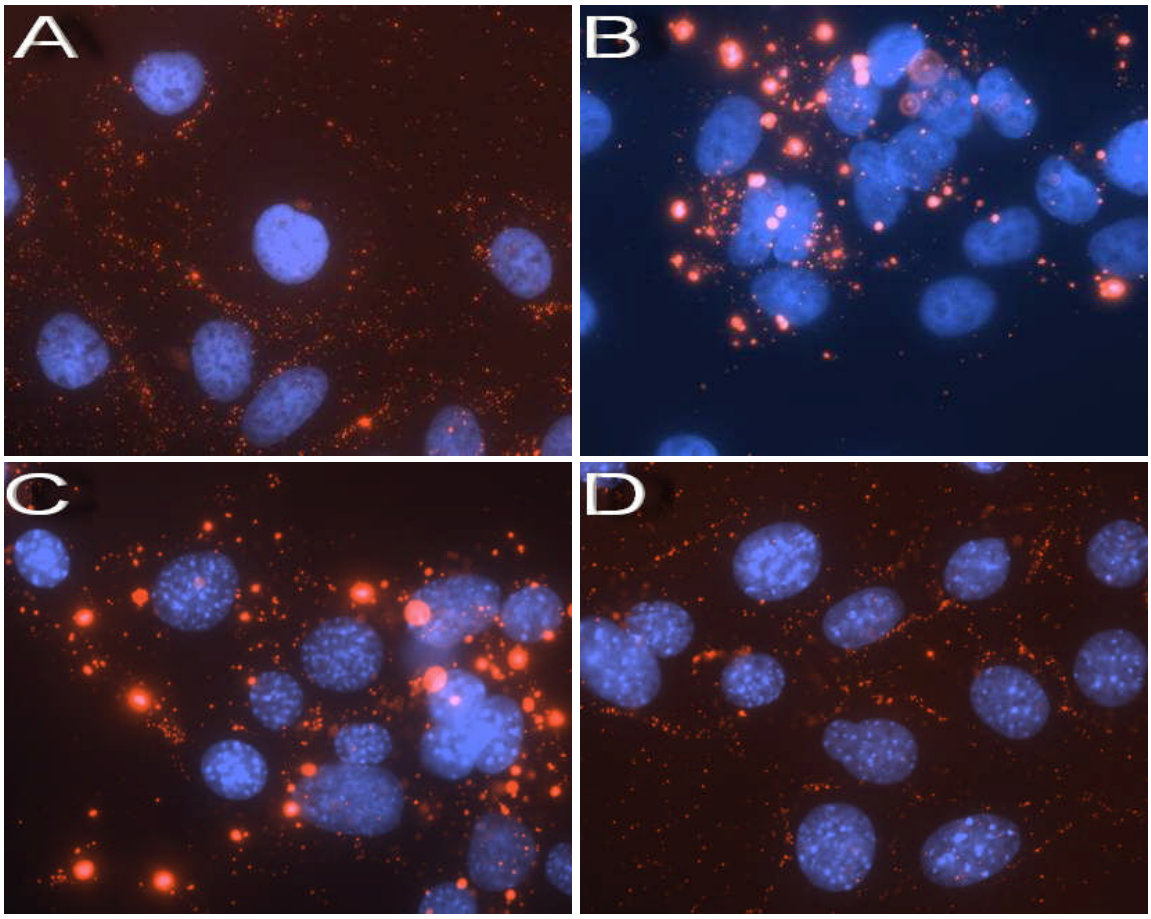

Figure 15: Clustering of mEGF(+) polyplexes upon cell binding. HUH-7 (A, B), Renca-EGFR (C) and RencaLacZ (D) cells were incubated with Cy3-labeled EGF(-) (A) and mEGF(+) (B, C, D) polyplexes. After 2h, cells were washed, fixed and counterstained with DAPI to visualize cell nuclei. Samples were visualized by epifluorescence microscopy. Blue: DAPI-stained nuclei. Red: Cy3-labeled polyplexes.

Since both mEGF(+) and EGF(-) polyplexes had a similar particle size prior to transfection, it was assumed that this effect relied on the interaction of polyplex-bound EGF with the EGFR. Notably, when incubating mEGF(+) polyplexes with (EGFR-positive) Renca-EGFR cells or (EGFR-negative) Renca-LacZ cells, only Renca-EGFR cells mediated clustering of mEGF(+) polyplexes (Figure 15C, D).

3.2.3 Internalization of EGFR-targeted complexes proceeds very fast

Total cellular association data did not provide any information about polyplex internalization. Since receptor-mediated endocytosis is known to be a fast process (115), it was assumed that uptake of receptor-targeted polyplexes proceeds much faster than that of non-targeted complexes. To differentiate between extracellular and intracellular polyplexes, cells were incubated with heparin which is able to remove extracellularly-bound particles. The remaining Cy5 fluorescence then represented only internalized particles. The absence of extracellularly-bound particles was verified by subsequent addition of YOYO-1, a membrane impermeable DNA stain.

The kinetics of internalization of mEGF(+) polyplexes were analyzed using HUH-7 cells and compared to shielded (EGF(-)) and unshielded (LPEI) complexes. LPEI polyplexes were generated in HBG at N/P 6 and had a size similar to that of EGF(-) and mEGF(+) complexes (approximately 100 nm) but displayed a positive surface charge (approximately + 20-30 mV). They were therefore used here to compare their cellular binding/uptake properties to that of neutrally charged EGFR-targeted polyplexes.

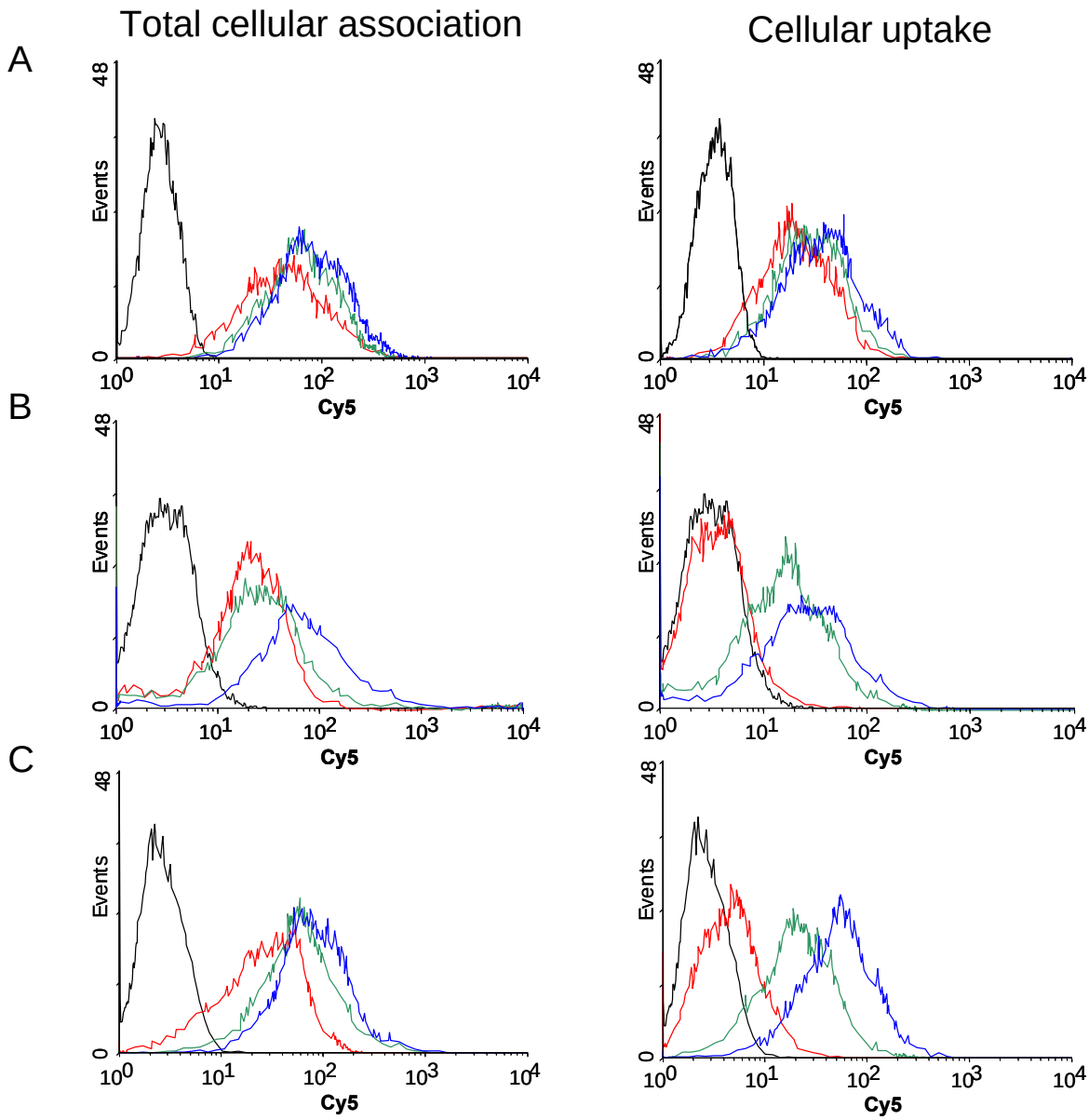

Figure 16: Total cellular association and internalization after transfection with polyplexes. HUH-7 cells were transfected with mEGF(+) (A), EGF(-) (B) and LPEI complexes (HBG, N/P 6) (C) containing Cy5-labeled DNA at a DNA concentration of 3 µg/ml. Internalization and total cellular association were analyzed by flow cytometry after 30 min, 2 h and 4 h. Black: control. Red: 30 min. Green: 2 h. Blue: 4 h.

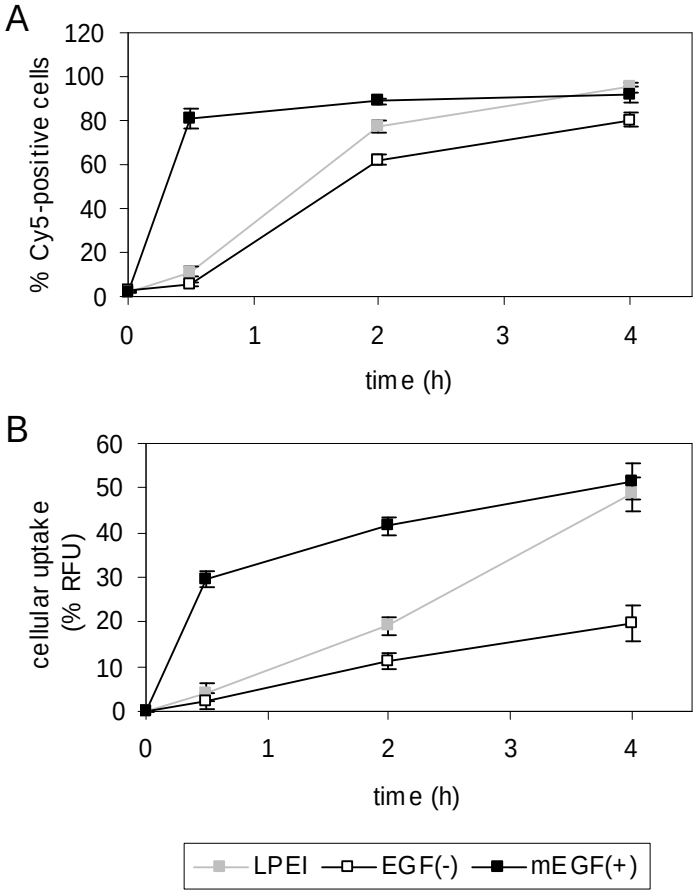

Figure 17: Cellular internalization of LPEI (HBG, N/P 6), EGF(-) and mEGF(+) polyplexes. Data are derived from the results presented in Figure 16. (A) Percentage of cells containing polyplexes. (B) Cellular uptake of polyplexes. Total cellular association of mEGF(+) polyplexes (after 4 h) was defined as 100 %. Mean values +/- SD of duplicates are shown.

Uptake of EGFR-targeted polyplexes was very fast. Already 30 min after transfection, approximately 81 % of the cells had taken up a significant amount of mEGF(+) complexes (Figure 16 A, Figure 17A). After 2 h and 4 h, approximately 89 % and 93 % of the cells had internalized mEGF(+) complexes, respectively. In contrast, binding and uptake of EGF(-) polyplexes was very slow with only approximately 5 % of cells containing complexes 30 min posttransfection. Significant internalization, however, could not be detected until 2 h (approximately 62 % Cy5-positive cells) (Figure 16 B, Figure 17A). LPEI polyplexes – due to their strong positive zeta potential – attached to the cells very fast (Figure 16 C) but uptake was obviously slow: approximately 11 % and 77 % of cells had taken up LPEI polyplexes after 30 min and 2 h, respectively (Figure 16 C, Figure 17A).

A similar pattern was found regarding the mean cellular polyplex uptake (Figure 17B): EGFR-targeted complex internalization was much faster than that of non-targeted polyplexes. However, uptake velocity of mEGF(+) complexes was not constant over the 4 h time period but slowed down already shortly after transfection (approximately 30 min posttransfection). Notably, 4 h posttransfection, the mean cellular uptake level was similar to that of LPEI polyplexes (Figure 17B). In contrast, internalization levels of EGF(-) complexes were low at all time points, with 3- to 13-fold less uptake compared to mEGF(+) polyplexes.

3.2.4 Reporter gene expression of EGFR-targeted polyplexes can be detected already 4 h posttransfection

Fast uptake of mEGF(+) complexes should lead to an early onset of luciferase activity after transfection with luciferase-encoding DNA polyplexes. In order to evaluate this, time course measurements were performed. Cells were transfected and luciferase activity was determined after 4 h, 8 h, 12 h and 24 h.

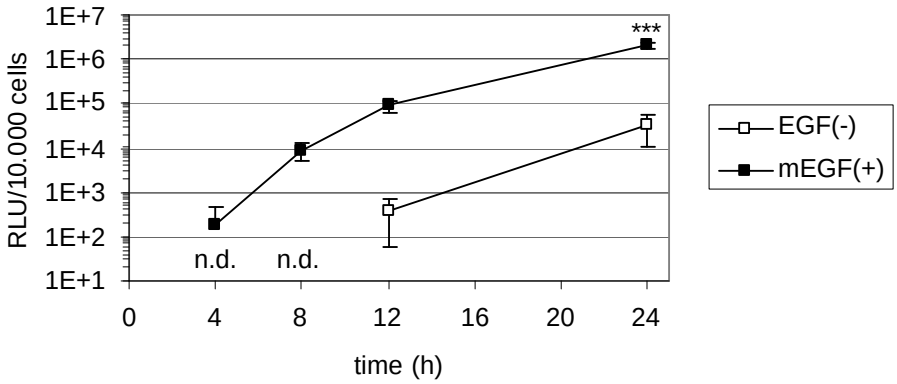

*Figure 18: Reporter gene expression (luciferase activity) at different time points after transfection. HUH-7 cells were transfected with EGF(-) and mEGF(+) polyplexes at a DNA concentration of 1.25 µg/ml and luciferase activity was determined 4 h, 8 h, 12 h and 24 h posttransfection. Transfection efficiencies of EGF(-) polyplexes 4 h and 8 h posttransfection were not detectable (n. d.). Mean values +/- SD of triplicates are shown. ***p < 0.001; **p < 0.01; *p < 0.05, compared to EGF(-) polyplexes at the same time point (ANOVA, Duncan).*

Using mEGF(+) complexes, luciferase expression could already be detected 4 h after transfection, whereas no activity was found with EGF(-) complexes at that time point (Figure 18). The difference in transfection efficiency between the two formulations used was most pronounced during the first 12 h of transfection, when efficiency was enhanced up to 250-fold with mEGF(+) polyplexes compared to EGF(-) polyplexes. This difference became smaller with time, resulting in an approximately 65-fold

enhancement 24 h after transfection. This result was in accordance with the observation that mEGF(+) polyplexes were internalized within a few minutes, whereas EGF(-) complexes needed at least 2 h for significant uptake (Figure 17).

In summary, both cellular binding and uptake were accelerated and enhanced when using EGFR-targeted polyplexes compared to non-targeted complexes (EGF(-)). Cellular association of mEGF(+) complexes was comparable to that of huEGF(+) complexes and could be inhibited by addition of free mEGF as competing ligand. Remarkably, increased cellular binding of the targeted complexes was associated with clustering of the particles bound to the cell. As expected, the fast internalization process of mEGF(+) complexes was accompanied by a very early onset of reporter gene expression which was already detectable 4 h posttransfection.

All these cellular binding and uptake kinetics data suggested that EGFR-targeted polyplexes were internalized by the cells via receptor-mediated endocytosis. Therefore, the putative interaction between EGFR-targeted polyplexes and the receptor was further evaluated.

3.3 EGFR-targeted complexes specifically bind to the EGFR

To further characterize the cellular mechanism of EGFR-targeted gene delivery, direct involvement of the EGFR had to be proven. However, evidence for specific EGFR binding of mEGF(+) complexes is not only a key issue in elucidating the mechanism of EGFR-targeted gene delivery but also of pharmacological value since EGFR activity controls a wide variety of biological responses.

3.3.1 EGFR-targeted transfection reduces the level of free surface EGFR

To confirm binding of mEGF(+) polyplexes to the EGFR, the level of free surface receptors was analyzed after transfection using a competitive antibody against the EGFR. HUH-7 cells were incubated with EGF(-) and mEGF(+) complexes for 2 h before staining free surface EGFR with a primary anti-huEGFR antibody and a secondary antibody labeled with Alexa Fluor® 350. Cellular binding of mEGF(+) complexes clearly decreased receptor levels accessible to the antibody, whereas that of EGF(-) complexes did not (Figure 19).

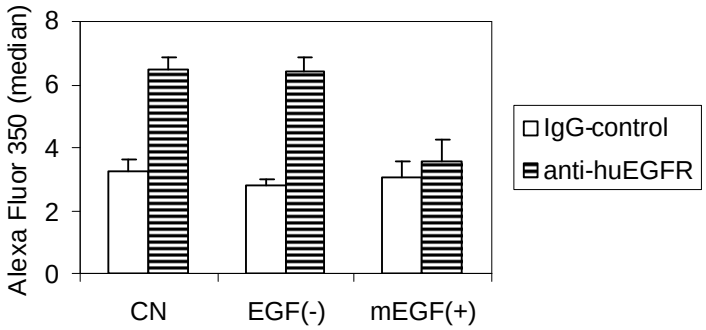

Figure 19: Level of free surface EGFR after transfection with polyplexes. HUH-7 cells were transfected with EGF(-) and mEGF(+) complexes for 2 h at a DNA concentration of 3 µg/ml before staining free surface EGFR with mouse anti-huEGFR antibody and goat anti-mouse IgG_1 antibody labeled with Alexa Fluor® 350. The median fluorescence intensity was determined by flow cytometry. Two independent experiments were performed. Mean values + SD are presented.

3.3.2 EGFR-targeted polyplexes trigger EGFR activation

Receptor activation can serve as a strong indicator for a specific interaction between complex-bound EGF and the EGFR. On the molecular level, ligand binding induces dimerization of EGFRs and autophosphorylation in the cytoplasmic domain of EGFRs (78). EGFR activation then initiates various signaling cascades involving PI3-kinase/Akt and MAPK (Erk-1/2) signaling pathways (81;82;116). These are the most prominent signaling pathways downstream EGFR activation mediating cell survival and proliferation.

To assess whether EGFR binding by mEGF(+) polyplexes triggers these pathways, western blot analysis was performed. Free mEGF equivalent to the amount of mEGF incorporated into the mEGF(+) polyplex was used as a control.

Already 10 min after transfection, EGFRs were activated by EGF-containing polyplexes (Figure 20). Receptors remained phosphorylated for approximately one hour. Accordingly, the downstream signaling transducer Akt was also found to be initiated after 10 min. Notably, phospho-Erk levels were already detectable under control conditions, indicating constitutive Erk activity which was probably attributed to the proliferating status of the tumor cells. mEGF(+) polyplexes then induced a decrease of phospho-Erk levels below the level of untreated control cells.

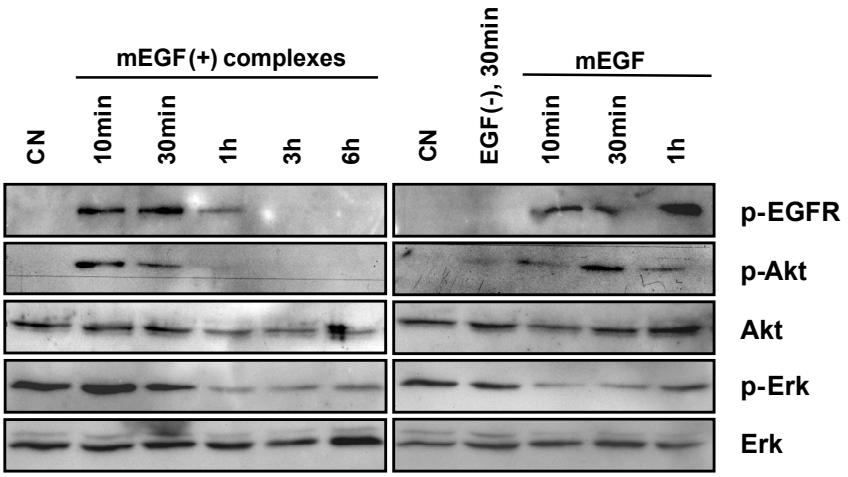

Figure 20: Activation of the EGFR and its downstream signaling transducer Akt by mEGF(+) complexes. HUH-7 cells were treated with mEGF (20 pmol/ml = 120 ng/ml), mEGF(+) complexes or EGF(-) polyplexes (DNA concentration 6 µg/ml). After the indicated time, western blot analysis of phospho-EGFR, phospho-Akt and phospho-Erk-1/2 was performed. To confirm equal protein loading in each lane, the levels of Akt and Erk-1/2 were analyzed. (CN: negative control)

Similar results were obtained with control cells treated with free mEGF alone (Figure 20). Increased levels of phospho-EGFR and phospho-Akt were detected within the first 30 min after addition of the growth factor, whereas phospho-Erk levels decreased. In contrast to mEGF(+) polyplexes, control complexes without EGF (EGF(-)) did not induce EGFR activation and initiation of the downstream signaling transducer Akt (Figure 20, right panel). This proved that the targeting ligand alone was responsible for the EGFR activation observed with EGFR-targeted polyplexes. This was also in line with (114) where it was reported that site-specific coupling of EGF via its N-terminal amino group retained its biological activity.

In summary, incubation of EGFR-expressing cells with mEGF(+) polyplexes reduced the amount of surface EGFR accessible to a competitive anti-huEGFR antibody, indicating that mEGF(+) polyplexes might be able to occupy and/or downregulate membrane EGFRs. Further evidence lies in the observation that EGFR-targeted transfection was accompanied by activation of the receptor and its downstream signaling transducer Akt. Ligand-induced and EGFR-mediated nuclear polyplex accumulation was therefore considered to be another possible reason for enhanced gene delivery with EGFR-targeted polyplexes. This would mean that EGFR-targeted polyplexes are able to transfect postmitotic cells. Consequently, the cell cycle dependency of EGFR-targeted gene delivery was further analyzed.

3.4 EGFR-targeted gene delivery is cell cycle dependent

In the previous section (3.3.2), evidence for a specific interaction between cell surface EGFR and complex-bound EGF was presented. Interestingly, it was recently reported that the EGFR after stimulation with EGF is able to translocate to the nucleus (92). Therefore, the possibility was considered that EGF mediates enhanced nuclear accumulation of the polyplexes. For polyplex-mediated gene delivery, the major path to nuclear entry seems to be via nuclear disassembly during mitosis (71). If, however, EGF had a significant effect on nuclear import, this cell cycle dependency should be less pronounced when using EGFR-targeted polyplexes. As a prerequisite, EGFR expression levels were determined to be stable during cell cycle progression (data not shown).

3.4.1 EGFR-targeted polyplexes transfect postmitotic cells inefficiently

To assess the role of mitosis in the process of EGFR-targeted transfection, gene transfer experiments were carried out in a cell population which had been depleted of mitotic cells.

To reduce the number of dividing cells, cell cycle progression was blocked at the G_1/S boundary by incubation with 20 mM thymidine (for 16 h). Notably, high dose thymidine treatment is known to inhibit the ribonucleotide reductase which leads to blockage of DNA replication at S phase. Thus, the percentage of cells in G_2/M phase decreased from 14 % (Figure 21: black) to 3.5 % (Figure 21: red). Since it was intended to perform the transfection while keeping the number of mitotic cells low, treatment was continued with 25 mM thymidine. As required, cell cycle distribution remained similar with less than 5 % in G_2/M phase after 34 h (Figure 21: blue).

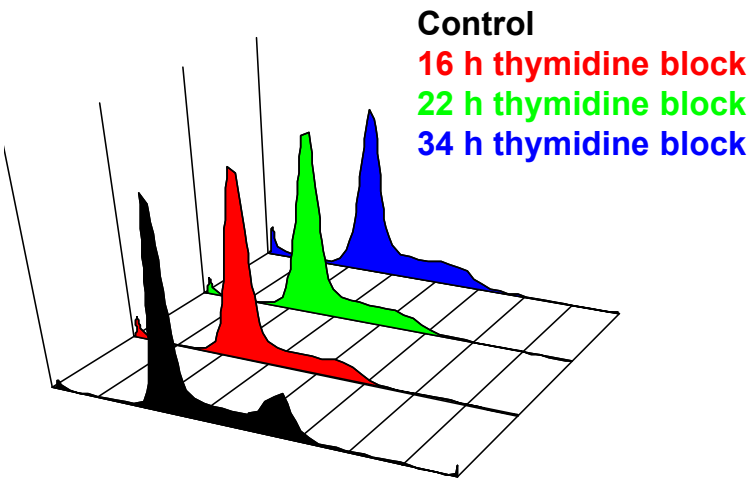

Figure 21: Cell cycle distribution after thymidine block. HUH-7 cells were incubated with 20 mM thymidine for 16 h and further cultured in medium containing 25 mM thymidine. After the indicated time, cells were fixed with ethanol and cell cycle distribution was assayed by flow cytometry using PI.

In order to evaluate the impact of mitosis on the transfection of EGFR-targeted and non-targeted polyplexes, cell cycle progression was blocked as described above. Transfection complexes coding for either luciferase or EGFP were then added at the 16 h time point (Figure 21: red). Since thymidine treatment was continued until analysis (34 h time point, Figure 21: blue), the number of mitotic cells during transfection remained low.

In this gene transfer experiment, mEGF(+) complexes were compared to both shielded EGF(-) and unshielded LPEI polyplexes (HBS ½, N/P 6).

Transfection efficiency of both EGF(-) and mEGF(+) complexes decreased when the number of mitotic cells was reduced by thymidine treatment. Transfection levels of LPEI polyplexes were reduced five- and four-fold regarding luciferase activity and EGFP expression rates, respectively (Figure 22). With EGF(-) complexes, transfection decreased by a factor of six and nine, respectively (Figure 22). And with mEGF(+) complexes, transfection efficiency was reduced four- and eight-fold, respectively (Figure 22). Since transfection rates of EGFR-targeted complexes decreased to an extent similar to that of non-targeted particles, these results suggested that mEGF(+) polyplexes were not capable of transfecting postmitotic cells efficiently. It was therefore assumed that EGF did not efficiently promote nuclear import of PEI polyplexes.

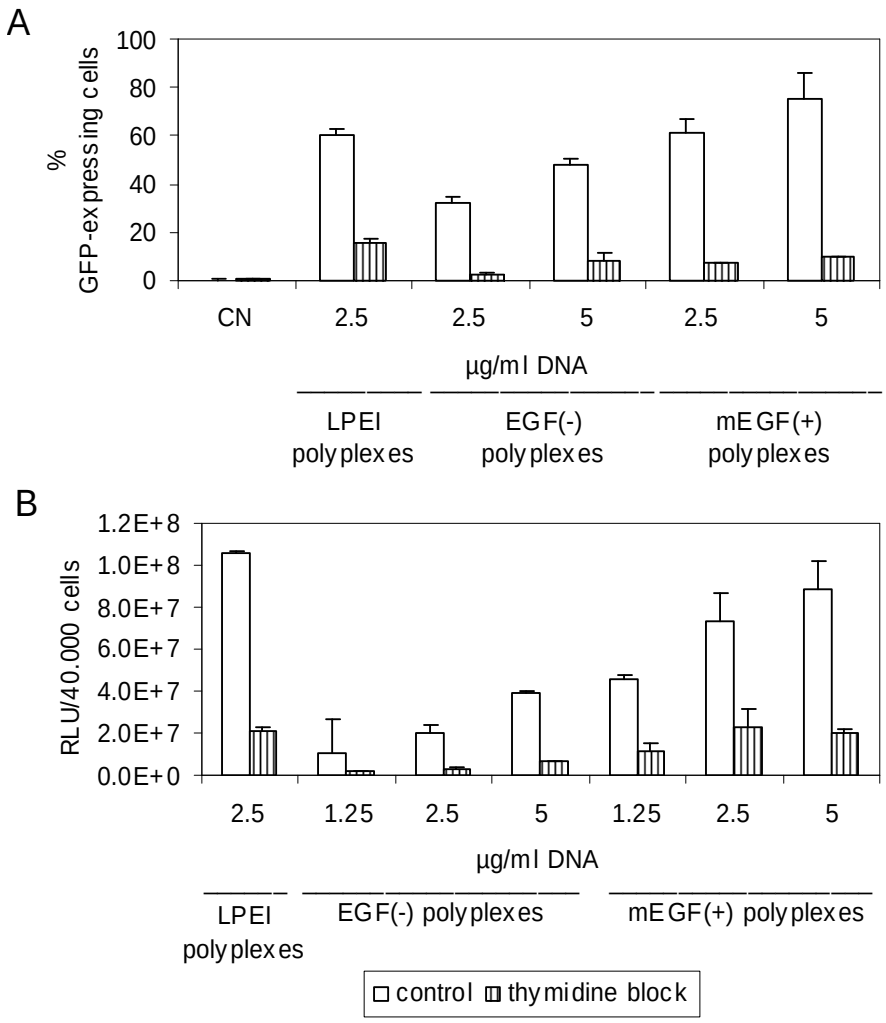

Figure 22: Reporter gene expression after transfection of cells synchronized at the G_1/S boundary: (A) EGFP expression and (B) Luciferase activity. HUH-7 cells were synchronized by a single thymidine block (16 h) and transfected with LPEI (HBS ½, N/P 6), EGF(-) and mEGF(+) complexes in the presence of thymidine (18 h). Control cells did not receive thymidine treatment. Luciferase activity and the percentage of EGFP-expressing cells are presented as mean values + SD of duplicates.

It has to be taken into account, however, that reduced cell cycle progression also decreases the cell number. Furthermore, thymidine might affect transgene expression on the level of protein synthesis. Therefore, as a control, HUH-7 cells stably expressing the luciferase gene were treated for the time of the complete experiment (34 h) with the same amount of thymidine. In these cells, luciferase activity was found to be 62.3 % (+/- 2.3 %) of untreated control cells (data not shown). This result helped to estimate the impact of thymidine treatment on the level of non-transient transgene expression.

3.4.2 Mitosis has a major impact on EGFR-targeted gene delivery

To obtain further evidence for the role of mitosis in EGFR-targeted gene delivery, transfection experiments were performed in synchronized but cycling cells. Hence, it was expected that synchronized cells that pass mitosis simultaneously should show a fast increase in transgene expression – provided that transfection is strongly cell cycle dependent.

First, simultaneous cell cycle progression of synchronized cells was ensured: Cells were synchronized by incubation with 5 mM thymidine for 16 h which was followed by a medium cange to remove the thymidine. Cell cycle progression was then assayed every 4 h.

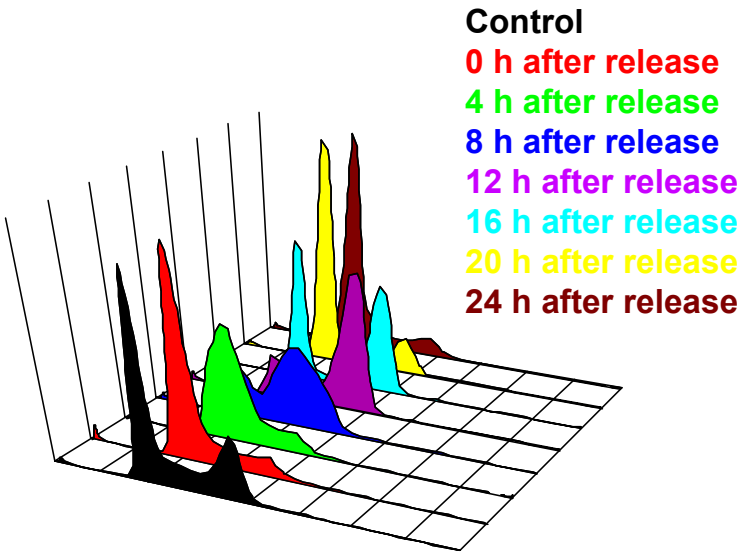

Figure 23: Cell cycle distribution after thymidine release. HUH-7 cells were incubated with 5 mM thymidine for 16 h and further cultured in medium without thymidine. After the indicated time, cells were fixed with ethanol and cell cycle distribution was assayed by flow cytometry using PI.

It revealed that after thymidine release, cells re-entered the cell cycle simultaneously and were found to pass mitosis between 12 h and 20 h later (Figure 23).

In order to evaluate the impact of mitosis on transfection efficiency of EGFR-targeted and non-targeted polyplexes, cells were synchronized as described above. Transfection complexes coding for either luciferase or EGFP were then added 4 h after thymidine removal. Consequently, cells passed mitosis simultaneously 8-16 h posttransfection. It was expected that at this time, transgene expression should show a fast increase – provided that transfection was strongly cell cycle dependent.

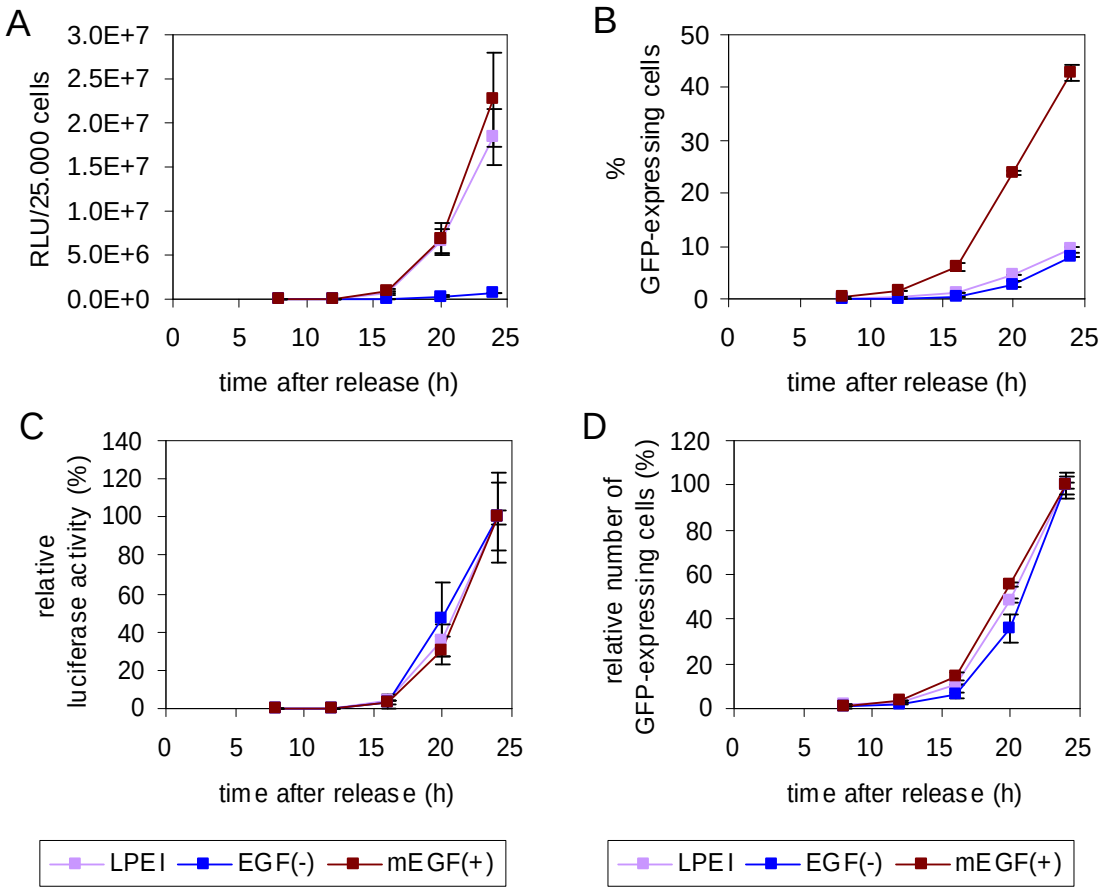

Figure 24: Reporter gene expression after transfection of cells synchronized at the G_1/S boundary. HUH-7 cells were synchronized by a single thymidine block (16 h) and transfected with LPEI (HBS ½, N/P 6), EGF(-) and mEGF(+) complexes in the absence of thymidine (4 h after thymidine release). Control cells did not receive thymidine treatment. Luciferase activity (A, C) and the percentage of EGFP-expressing cells (B, D) are presented as mean values +/- SD of duplicates. In (C, D), reporter gene expression is presented as relative transfection efficiency, with the values at the 24 h time point defined as 100 %.

16 h after release (i. e. 4 h after entering mitosis (see Figure 23)), reporter gene expression was detectable (Figure 24). As illustrated by Figure 24 C and D, progression in transgene expression mediated by targeted polyplexes was similar to that mediated by non-targeted polyplexes. This suggests that nuclear disassembly during mitosis is as important in EGFR-mediated transfection as it is in non-targeted transfection.

3.4.3 Mitosis amplifies efficiency of EGFR-targeted gene delivery

To further elucidate the cell cycle dependency of EGFR-targeted gene delivery, EGFP reporter gene expression, cell cycle distribution and total cellular association were monitored in parallel. Thus, 6 h posttransfection, flow cytometric analysis should reveal correlations between these parameters. Notably, EGFR expression levels had been determined to be stable during cell cycle progression (data not shown). It was further ensured that gene transfer efficiency of labeled polyplexes was not reduced compared to unlabeled particles (data not shown).

The Cyan^{TM} MLE flow cytometer used here was equipped with an enterprise II laser delivering light at 364 nm and 488 nm and a laser diode with emission at 635 nm. These three laser lines were applied to excite Hoechst 33342, EGFP and Cy5, respectively. Sequential excitation of the three dyes minimized the risk of emission crosstalk. Accordingly, no signal overspill between the three channels was observed (data not shown). The use of Hoechst 33342 to quantify nuclear DNA was possible due to the availability of a 364 nm excitation wavelength and enabled measurement of living cells while avoiding fixative-induced artifacts. This was of high relevance since many fixatives destroy plasma membrane integrity and thus cause leaking of the fluorescent protein GFP (117;118).

Figure 25 illustrates the results after transfection with mEGF(+) complexes. Notably, all three polyplex formulations showed similar results regarding these parameter relations, irrespective the differences in EGFP expression and in the level of total cellular polyplex association (Table 3).

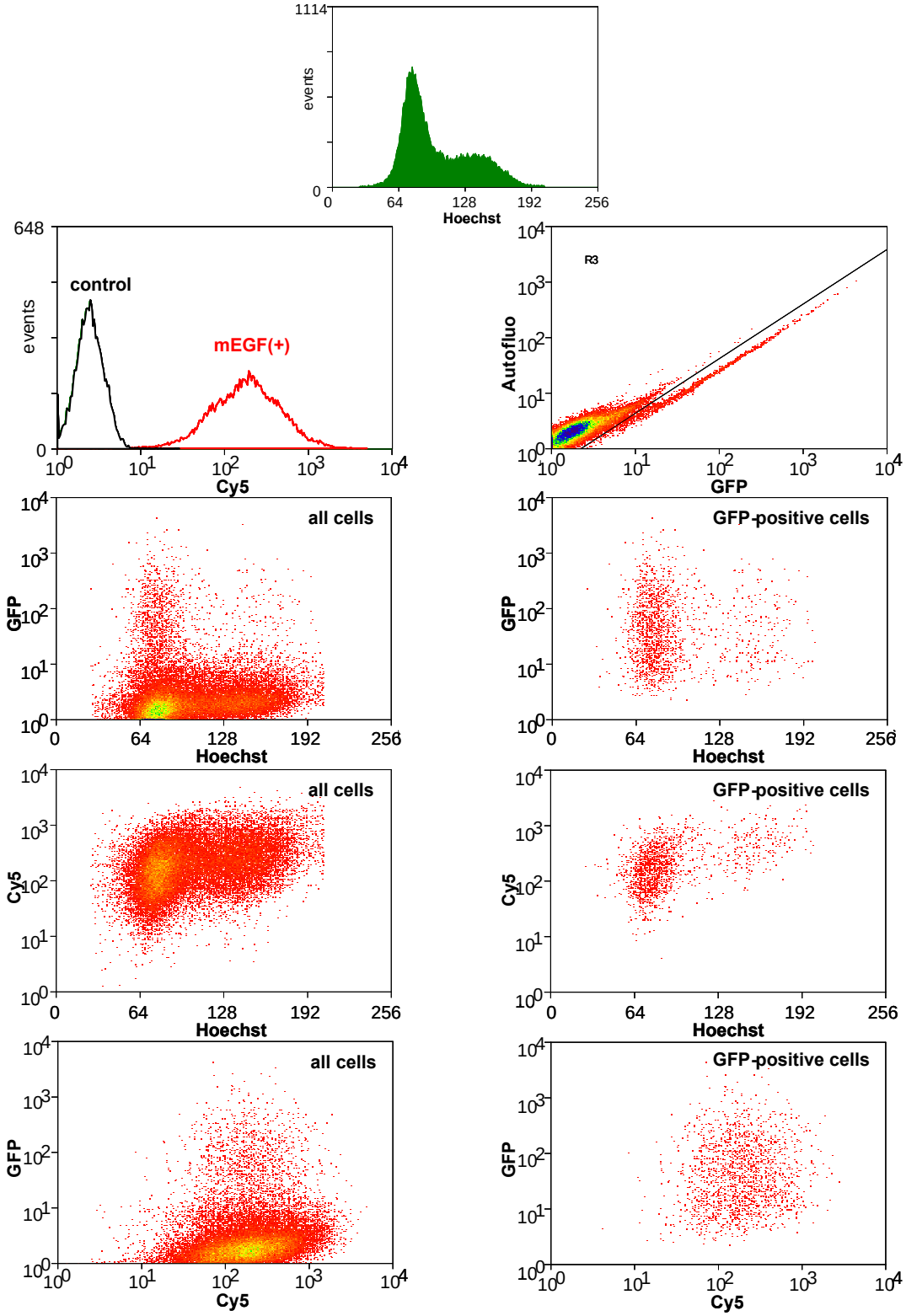

Figure 25: Correlation of EGFP expression, cell cycle phase and cellular polyplex association after transfection with mEGF(+) polyplexes. HUH-7 cells were transfected with Cy5-labeled LPEI (HBS ½, N/P 6), EGF(-) or mEGF(+) polyplexes coding for EGFP at a DNA concentration of 10 µg/ml. 6 h posttransfection, cells were harvested, stained with Hoechst 33342 and analyzed by flow cytometry. Data after transfection with LPEI or EGF(-) polyplexes are not shown. (Autofluo = Fl-2)

	reporter gene expression		cellular association
	% EGFP-positive cells	EGFP (median) of EGFP-positive cells	Cy5 (median)
LPEI	3.1 (+/- 0.3)	26.5 (+/- 2.7)	174.7 (+/- 4.5)
EGF(-)	2.0 (+/- 0.1)	16.6 (+/- 0.0)	113.9 (+/- 14.5)
mEGF(+)	5.2 (+/- 0.4)	35.25 (+/- 1.8)	174.9 (+/- 13.3)

Table 3: Reporter gene expression (EGFP expression) and total cellular association 6 h after transfection. Data are derived from the experiment illustrated by Figure 25. Mean values +/- SD of duplicates are shown.

Admittedly, transgene expression was low in all samples, attributed to the short transfection time of 6 h. A short incubation was, however, essential to draw conclusions concerning the role of mitosis in this experiment. Accordingly, identification of different cell populations allowed correlations between the parameters cell cycle, reporter gene expression and cellular polyplex association.

	reporter gene expression (% GFP-expressing cells)			
	diploid cells	tetraploid cells	diploid/tetraploid	total
LPEI	3.7 (+/- 0.3) %	1.4 (+/- 0.3) %	2,6	3.1 (+/- 0.3) %
EGF(-)	2.6 (+/- 0.2) %	0.7 (+/- 0.1) %	3,6	2.0 (+/- 0.1) %
mEGF(+)	6.8 (+/- 0.5) %	2.1 (+/- 0.5) %	3,2	5.2 (+/- 0.4) %

Table 4: Correlation of transfection efficiency and cell cycle phase. Data are derived from the experiment illustrated by Figure 25. "diploid cells" (or "tetraploid cells") indicates the number of diploid (or tetraploid) EGFP-positive cells related to the total number of diploid (or tetraploid) cells of each sample. "total" is the total number of EGFP-positive cells related to the total number of cells of each sample. "diploid/tetraploid" indicates the factor by which diploid cells were transfected more efficiently than tetraploid cells ("diploid" divided by "tetraploid"). Mean values +/- SD of duplicates are shown.

To evaluate the role of mitosis in EGFR-targeted gene delivery, the number of diploid (or tetraploid) EGFP-positive cells was related to the total number of diploid (or tetraploid) cells of each sample. 6 h posttransfection, the fraction of diploid cells was expected to be enriched in cells which had just passed mitosis. Table 4 shows that – in line with the results presented in 3.6.1 – the fraction of diploid cells contained more EGFP-positive cells than the fraction of tetraploid cells. This was also observed with EGFR-targeted polyplexes: All three formulations mediated an approximately three-fold higher transfection rate in cells which – at the time of data acquisition – contained a double chromosome set compared to cells with a four-fold chromosome set. Some of these EGFP-expressing cells had passed mitosis during the time of

incubation with polyplexes and were therefore more susceptible to nuclear polyplex import.

Since nuclear membrane integrity is not the only variable during cell cycle progression, cellular polyplex binding levels were monitored in parallel. This was considered to be of relevance since endocytic activity, cell size and other parameters may vary during cell cycle progression.

	cellular association (Cy5 median)			
	diploid cells	tetraploid cells	EGFP-positive cells	total
LPEI	143.3 (+/- 0.0)	294.3 (+/- 0)	181.1 (+/- 4.6)	174.7 (+/- 4.5)
EGF(-)	96.7 (+/- 9.8)	162.8 (+/- 12.4)	151.3 (+/- 3.9)	113.9 (+/- 14.5)
mEGF(+)	143.4 (+/- 7.3)	246.0 (+/- 12.5)	174.7 (+/- 4.5)	174.9 (+/- 13.3)

Table 5: Correlation of cellular polyplex association with cell cycle phase and EGFP expression. Data are derived from the experiment illustrated by Figure 25. Mean values +/- SD of duplicates are shown.

It revealed that tetraploid cells were able to bind a higher amount of complexes which might be explained by cell growth during cell cycle progression (Table 5). However, EGFP-expressing cells were not clearly associated with more polyplexes (Table 5), indicating that high cellular association might not be directly correlated to successful transfection.

In summary, EGFR-targeted transfection efficiency in a cell population with a low percentage of mitotic cells decreased to an extent similar to that of non-targeted transfection. On the other hand, passing of synchronized cells through mitosis led to a progression of EGFR-targeted gene transfer efficiency similar to that of non-targeted transfection efficiency. In line with these results, it was found that the fraction of diploid cells contained more transfected cells than the fraction of tetraploid cells. This indicates that EGFR-targeted gene delivery is cell cycle dependent.

3.5 Clathrin- and lipid raft-dependent endocytosis contribute to gene transfer by PEI polyplexes

Having proven direct involvement of the EGFR in EGFR-targeted gene delivery (3.3), it was considered that the receptor might direct the mEGF(+) polyplexes to EGFR-related endocytosis pathways. Since pathways differ in their ability to deliver the transgene, this might be another mechanism for enhanced transfection efficiencies of EGFR-targeted transfection. Internalization of activated EGFRs is known to occur via both caveolae/raft- and clathrin-dependent endocytosis, depending on the EGF concentration present (86;87). However, other routes might also be used by EGFR-targeted polyplexes. To further characterize EGFR-targeted gene delivery, inhibitors specific to the various endocytosis pathways were employed.

3.5.1 EGFR-targeting does not affect the route of cellular polyplex uptake

To determine the routes of internalization of EGFR-targeted polyplexes, colocalization studies with specific endocytosis pathway markers were performed. Hence, cells were incubated with Cy3- or Cy5-labeled polyplexes (LPEI, HBG, N/P 6; EGF(-); mEGF(+)). Coincubation with Alexa Fluor® 647 transferrin or Alexa Fluor® 488 cholera toxin B (CTB) allowed labeling of the clathrin- or the raft-dependent pathway, respectively. Living cells were visualized with a confocal laser scanning microscope (CLSM) and analyzed for colocalization of complexes and markers (Figure 26).

Notably, polyplexes were found in both types of vesicles, stained with either transferrin or CTB. About 30 % of mEGF(+) complexes colocalized with transferring, suggesting that these 30 % had been taken up via clathrin-dependent endocytosis. About 70 % of the complexes colocalized with CTB and had presumably been internalized via raft-mediated endocytosis. The same pattern was found with EGF(-) and LPEI polyplexes, suggesting that neither PEGylation nor incorporation of EGF influenced the mode of internalization of small polyplexes.

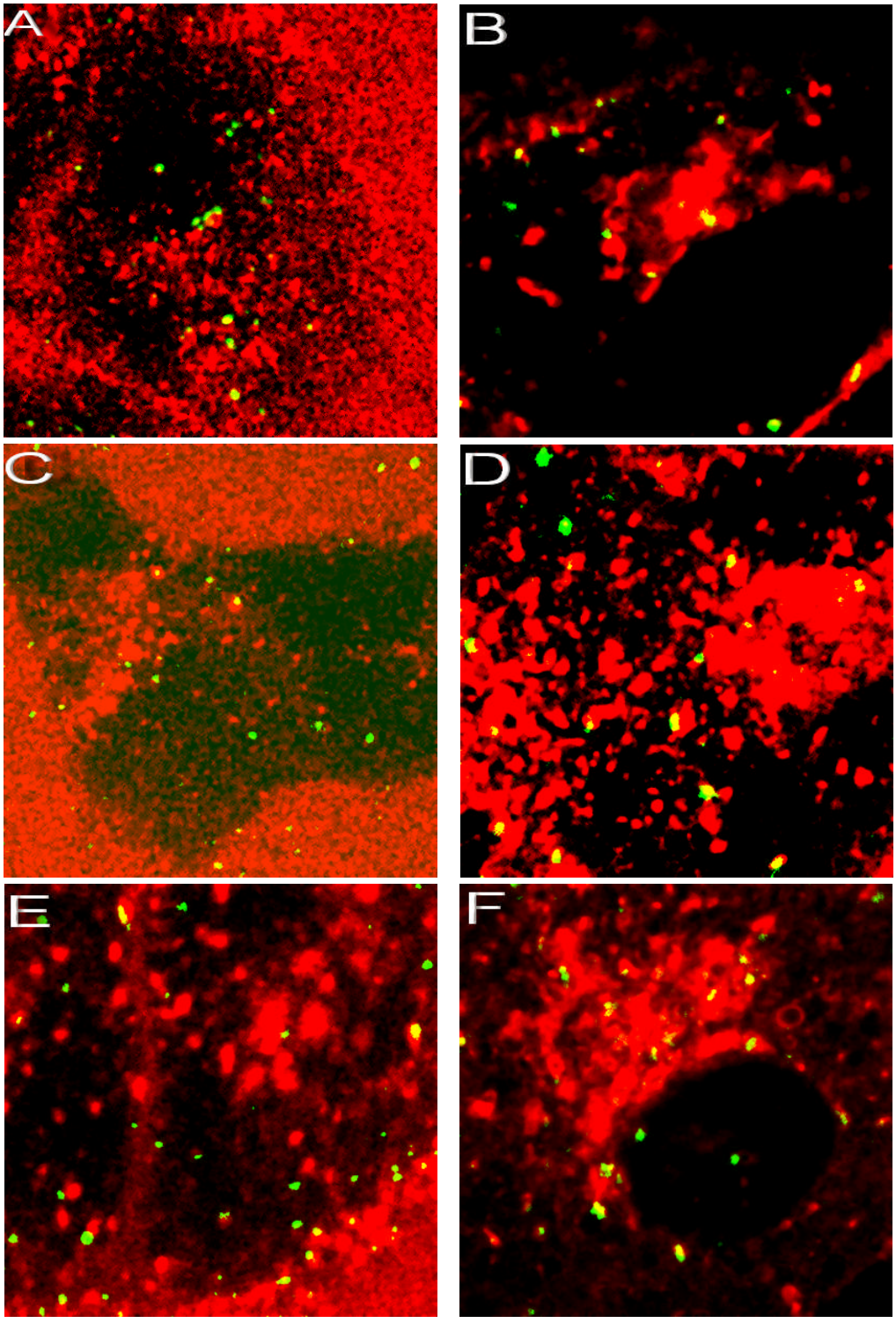

Figure 26: Colocalization of mEGF(+) (A, B), EGF(-) (C, D) and LPEI (HBG, N/P 6) (E, F) polyplexes with the pathway markers transferrin and CTB. Alexa Fluor® 647 transferrin and PEI/Cy3-DNA polyplexes (A, C, E) or Alexa Fluor® 488 CTB and PEI/Cy5-DNA polyplexes (B, D, F) were added to HUH-7 cells to allow simultaneous internalization. Living cells were visualized 1-4 h after transfection using a confocal laser scanning microscope. Red: transferrin/CTB. Green: polyplexes.

3.5.2 Particle size affects cellular uptake pathways of PEI polyplexes

Since all three polyplex formulations were of similar size (LPEI: approximately 100 nm; EGF(-), mEGF(+): approximately 140 nm) (Table 2, Figure 27), it was considered that cellular polyplex processing mainly depends on the particle size. Therefore, cellular uptake of small polyplexes (LPEI, EGF(-), mEGF(+)) and large polyplexes (LPEI, EGF(-)) was analyzed by flow cytometry.

LPEI polyplexes were generated in the presence of salt (OptiMEM = OM) to form large aggregates of approximately 1 µm in diameter (18). EGF(-) and mEGF(+) complexes were formed in HEPES buffer (20 mM HEPES, pH 7.1), snap-frozen in liquid nitrogen and subsequently thawed at room temperature. Since absence of glucose during the freezing/thawing procedure is known to result in polyplex aggregation (119), the initially small polyplexes thus grow in size with diameters of approximately 1-1.5 µm (Figure 27). However, large mEGF(+) polyplexes could not be tested in this experiment because it was not possible to remove them from the cell surface. This was probably due to the strong EGFR binding affinity of these aggregates.

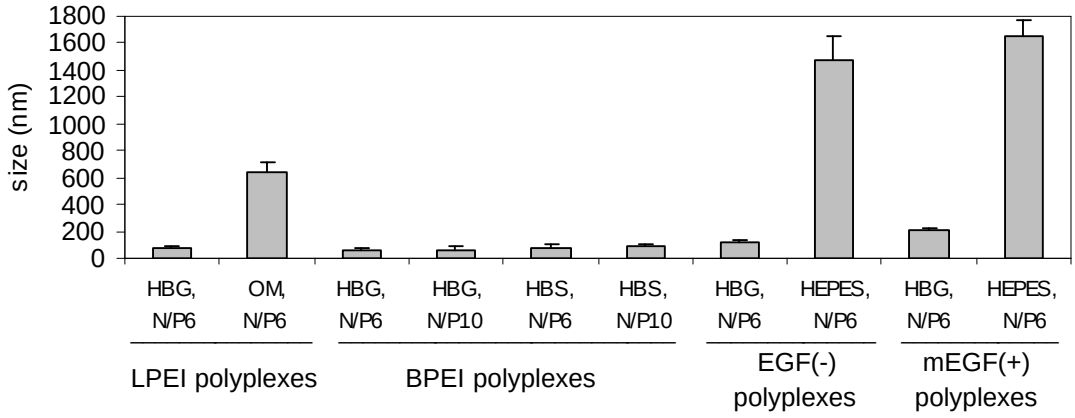

Figure 27: Particle size of various polyplex formulations in the buffer indicated.

To distinguish between the different endocytosis pathways, cells were preincubated with specific uptake inhibitors. Chlorpromazine or filipin were used to interfere with clathrin-mediated or caveolae/lipid raft-dependent endocytosis, respectively. To avoid albumin binding of the inhibitors (120;121), they were administered in serum-free medium.

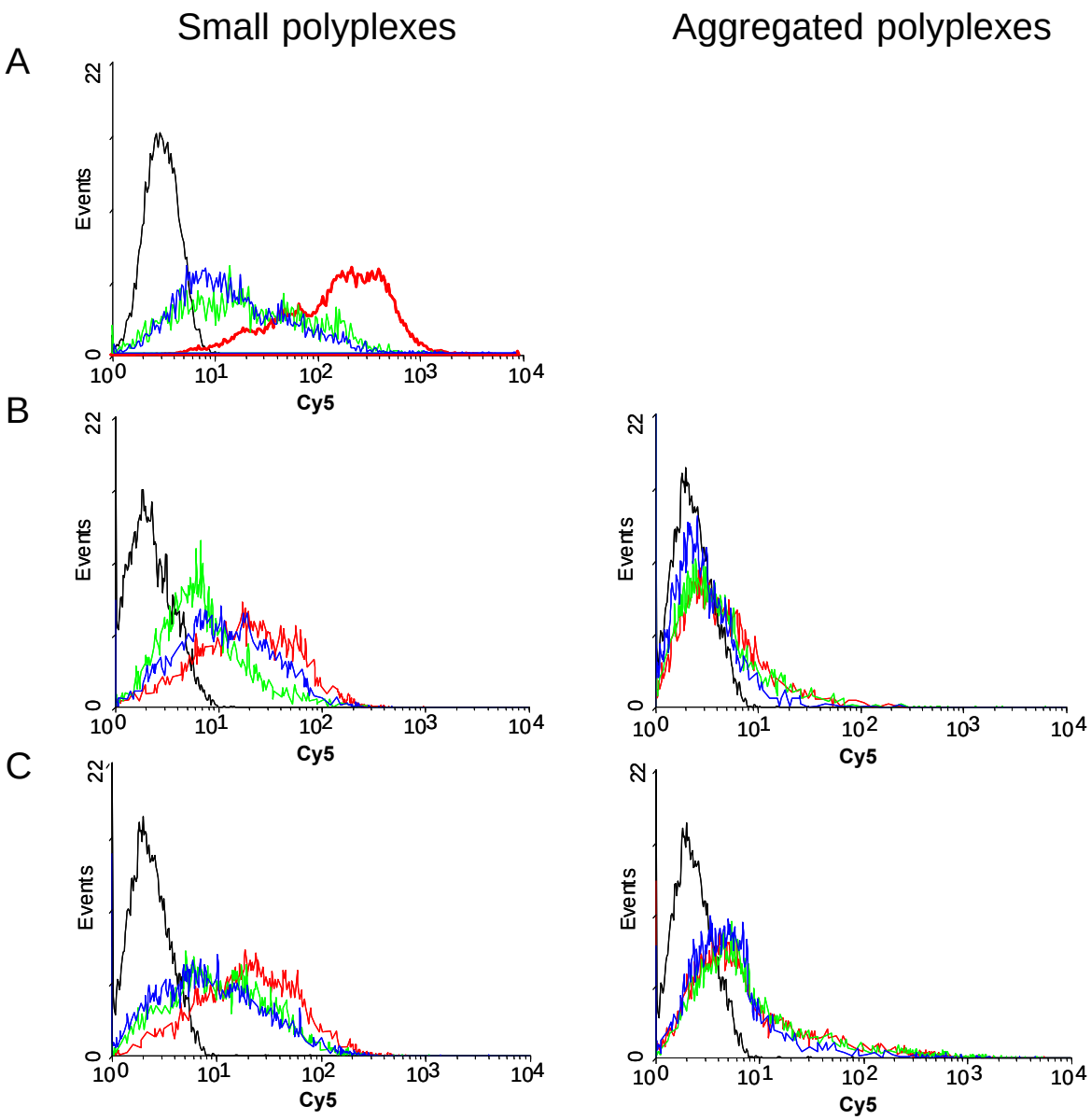

Figure 28: Cellular uptake of mEGF(+) (HBG) (A), EGF(-) (HBG, HEPES) (B) and LPEI (HBG, OptiMEM; N/P 6) (C) polyplexes in the presence of endocytosis inhibitors. HUH-7 cells were preincubated with 10 µg/ml chlorpromazine or 0.5 µg/ml filipin and transfected with Cy5-labeled polyplexes for 2 h. After removal of extracellularly-bound complexes using heparin, the level of internalization was assayed by flow cytometry. Black: control. Red: transfection without inhibitor treatment. Green: chlorpromazine. Blue: filipin.

Neither chlorpromazine nor filipin interfered with cellular uptake of aggregated polyplexes (LPEI, EGF(-)), indicating that large polyplexes entered the cells via a third, clathrin- and raft-independent pathway (Figure 28). In contrast, uptake of small polyplexes (LPEI, EGF(-), mEGF(+)) was reduced by both chlorpromazine and filipin (Figure 28), confirming that both pathways were involved in the uptake of small polyplexes by HUH-7 cells (see Figure 26). It was also interesting to note that again,

neither a change in particle surface potential by PEGylation nor incorporation of a ligand had an impact on the route of cellular polyplex entry (Figure 26, Figure 28).

3.5.3 Clathrin-dependent endocytosis predominantly mediates gene delivery in HUH-7 cells

Having established the effects of endocytosis inhibitors on overall cellular polyplex uptake, it was important to analyze the contribution of each pathway to transfection efficiency since pathways differ in their ability to deliver the transgene. Therefore, HUH-7 cells were preincubated for 1 h with either 10 µg/ml chlorpromazine or 0.5 µg/ml filipin and transfected for 2 h with polyplexes in the presence of the same inhibitor. At these concentrations, cell viability was not affected as shown by MTT assay (see Figure 32).

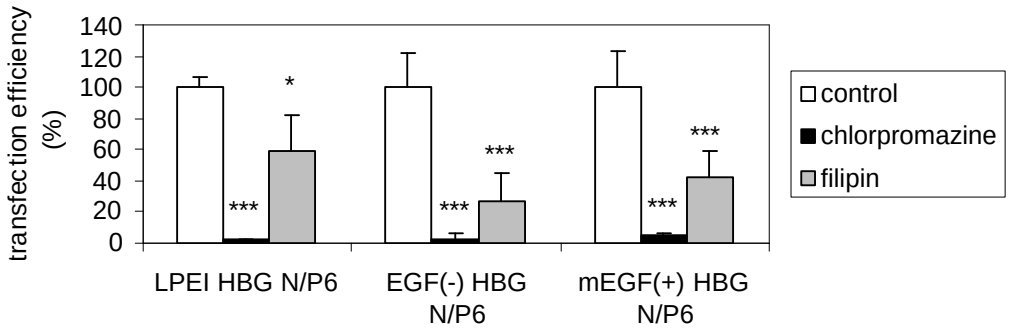

*Figure 29: Transfection efficiency of PEI polyplexes in the presence of endocytosis inhibitors. HUH-7 cells were pretreated with 10 µg/ml chlorpromazine or 0.5 µg/ml filipin, transfected with LPEI, EGF(-) or mEGF(+) polyplexes and luciferase reporter gene expression was determined 24 h after transfection. Data were corrected by protein content and luciferase activity of control cells without inhibitor treatment was set as 100 %. Mean values + SD of at least triplicates are shown. ***p < 0.001; **p < 0.01; *p < 0.05, compared to control cells without inhibitor treatment (ANOVA, Duncan).*

Regardless of the formulation used, treatment with chlorpromazine (inhibitor of clathrin-mediated endocytosis) caused a very pronounced reduction in gene transfer (by 95-98 %), whereas filipin (inhibitor of the lipid raft-dependent pathway) only moderately decreased transfection efficiency (by 42-72 %) (Figure 29). Interestingly, neither PEGylation nor incorporation of mEGF into the polyplex had a detectable effect on the pathways involved in transfection. This result was surprising since the various polyplex formulations were expected to be processed by the cells in different ways. It was also interesting to note that although only one third of small polyplexes were taken up via the clathrin-dependent pathway (Figure 26), these polyplexes predominantly mediated successful gene delivery (Figure 29).

To determine the productive route of aggregated PEI polyplexes, transfection was carried out as described above.

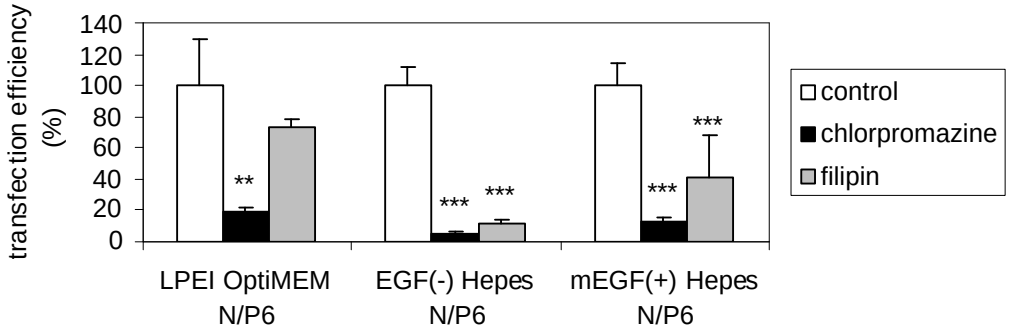

*Figure 30: Transfection efficiency of PEI polyplexes in the presence of endocytosis inhibitors. HUH-7 cells were pretreated with 10 µg/ml chlorpromazine or 0.5 µg/ml filipin, transfected with aggregated LPEI, EGF(-) and mEGF(+) polyplexes and luciferase reporter gene expression was determined 24 h after transfection. Data were corrected by protein content and luciferase activity of control cells without inhibitor treatment was set as 100 %. Mean values + SD of at least triplicates are shown. ***p < 0.001; **p < 0.01; *p < 0.05, compared to control cells without inhibitor treatment (ANOVA, Duncan).*

Similar to the transfection by small polyplexes (Figure 29), gene transfer by aggregated complexes was strongly inhibited by chlorpromazine (by 81-94 %) and only moderately by filipin (by 27-89 %) (Figure 30). This result was surprising since uptake of aggregated polyplexes had been determined to proceed via a clathrin- and raft-independent pathway (Figure 28). This suggested that routes might be involved in the transfection process that do not mediate polyplex uptake itself.

To determine a potential impact of the type of PEI used on the transfection process, various branched PEI (BPEI) polyplex formulations were tested. These complexes were approximately 100 nm in size (Figure 27).

Similar to gene delivery by LPEI polyplexes (Figure 29, Figure 30), transfection by BPEI complexes was strongly inhibited by chlorpromazine (by 95-99 %) and only moderately by filipin (by 44-78 %) (Figure 31).

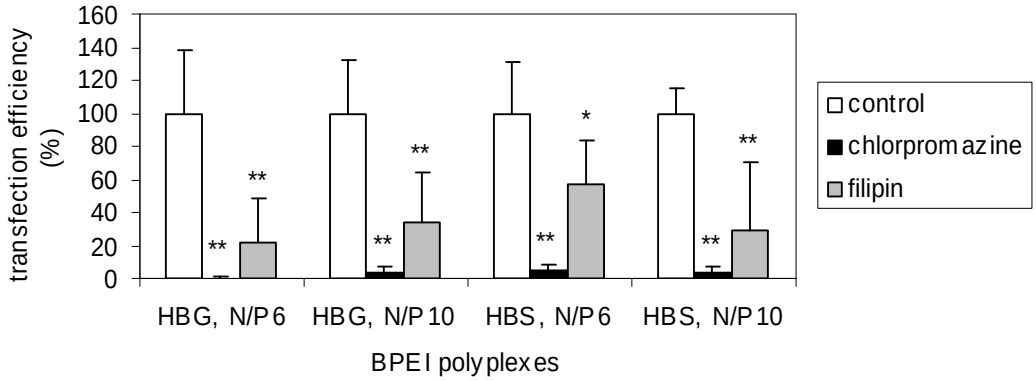

*Figure 31: Transfection efficiency of PEI polyplexes in the presence of endocytosis inhibitors. HUH-7 cells were pretreated with 10 µg/ml chlorpromazine or 0.5 µg/ml filipin, transfected with BPEI polyplexes and luciferase reporter gene expression was determined 24 h after transfection. Data were corrected by protein content and luciferase activity of control cells without inhibitor treatment was set as 100 %. Mean values + SD of triplicates are shown. ***p < 0.001; **p < 0.01; *p < 0.05, compared to control cells without inhibitor treatment (ANOVA, Duncan).*

These data suggested that in HUH-7 cells, clathrin-dependent endocytosis predominantly mediated gene delivery by LPEI and BPEI polyplexes. Neither a change in particle surface potential by PEGylation nor incorporation of a ligand had an impact on the route of efficient transfection.

3.5.4 Inhibitors specifically interfere with endocytosis pathways

To confirm the relevance of clathrin-dependent endocytosis for PEI-mediated transfection in HUH-7 cells, it had to be ruled out that the inhibitors affected transgene expression on the level of protein synthesis. This potential influence on luciferase activity was determined by exposing HUH-7 cells stably expressing the luciferase gene to different concentrations of either chlorpromazine or filipin (Figure 32). Cellular viability measurements (MTT assay) revealed that relative luciferase activity was not reduced below relative viability at any concentration, indicating that both inhibitors did not interfere with transgene expression at subtoxic concentrations. At those concentrations used in the transfection study (Figure 29, Figure 30, Figure 31: 10 µg/ml chlorpromazine and 0.5 µg/ml filipin), neither transgene expression nor viability were reduced.

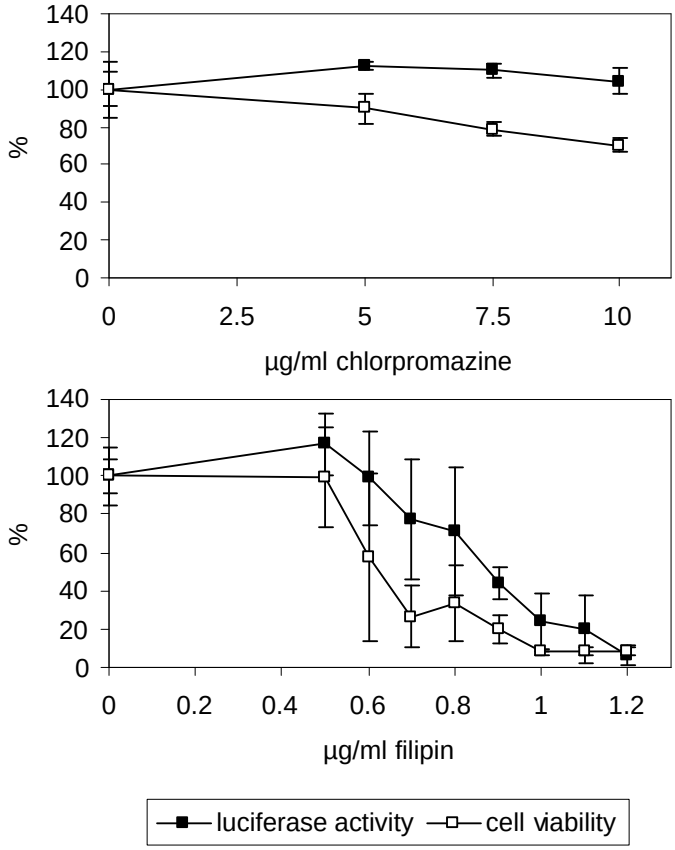

Figure 32: Effect of endocytosis inhibitors on cellular viability (HUH-7) and luciferase activity of HUH-7 cells stably expressing the luciferase gene. HUH-7 cells and HUH-7 EGFP-Luc cells were treated with chlorpromazine or filipin for 3 h and incubated with inhibitor-free medium for 22 h. Cells were then analyzed for viability (MTT assay) and luciferase activity, respectively. The level of control cells was set as 100 % and mean values +/- SD of duplicates are shown.

To test the specificity of chlorpromazine and filipin, uptake of transferrin and cholera toxin B (CTB) were analyzed in the presence of endocytosis inhibitors by fluorescence microscopy (Figure 33). As expected, chlorpromazine prevented only uptake of transferrin but not that of CTB. By contrast, filipin inhibited only endocytosis of CTB but not that of transferrin.

These results confirmed that at those concentrations used in the present transfection studies (Figure 29, Figure 30, Figure 31: 10 µg/ml chlorpromazine and 0.5 µg/ml filipin), chlorpromazine and filipin specifically and efficiently interfered with the clathrin- and the raft-dependent pathway, respectively.

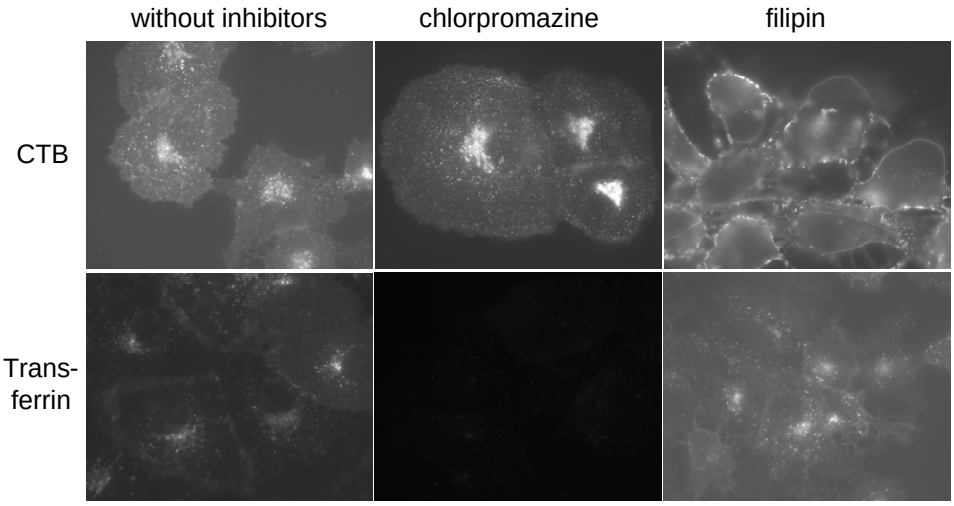

Figure 33: Effect of endocytosis inhibitors on internalization of the pathway markers transferrin and CTB. HUH-7 cells were pretreated with 10 µg/ml chlorpromazine or 0.5 µg/ml filipin and then incubated with either fluorescent CTB (Alexa Fluor® 488) or fluorescent transferrin (Alexa Fluor® 647) to highlight the level of uptake via lipid raft-mediated or clathrin-dependent endocytosis, respectively. Cells were then visualized by epifluorescence microscopy.

3.5.5 Pathways mediating successful gene delivery vary between cell types

To evaluate whether the clathrin-dependent pathway was also the most relevant in other cell lines, transfection experiments were performed also in HeLa cells. Since, however, these cells do not overexpress the EGFR (35,000-65,000 EGFRs/cell (122)) only the unmodified polyplexes were tested.

HeLa human cervical carcinoma cells were preincubated with either 7.5 µg/ml chlorpromazine or 1 µg/ml filipin. At these concentrations, cell viability was not affected (MTT assay, data not shown). Transfection with different PEI polyplex formulations revealed that in this cell line, blockage of the raft-mediated pathway was more derogatory to gene delivery than inhibition of the clathrin-dependent pathway (Figure 34). Accordingly, treatment with filipin caused a strong reduction in gene transfer (by 41-98 %), whereas chlorpromazine only moderately decreased (by 0-67 %) transfection efficiency.

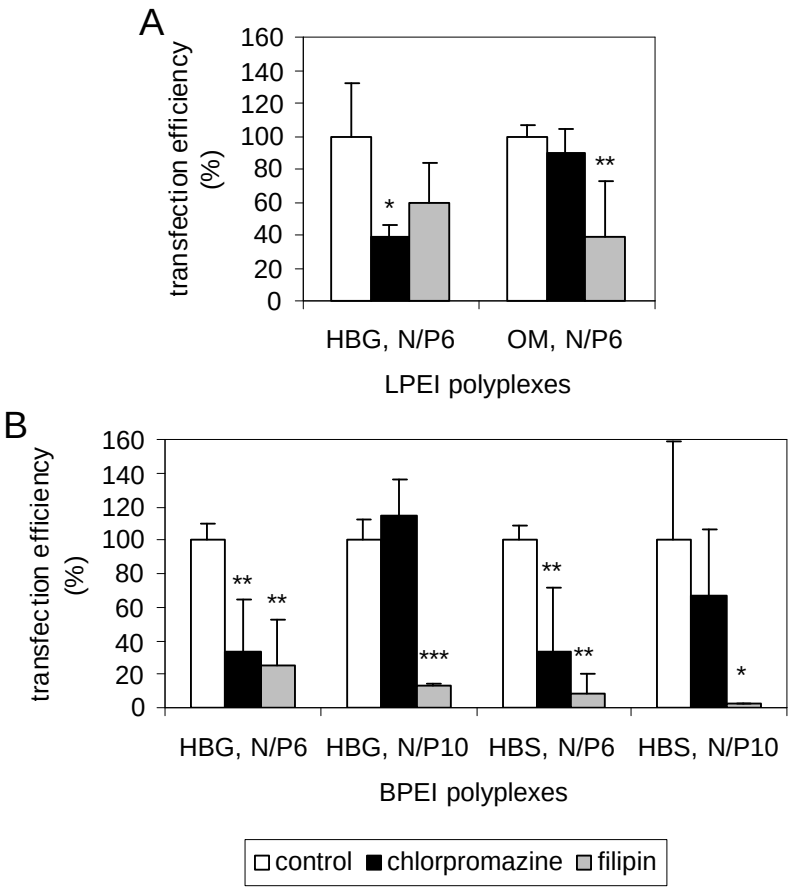

*Figure 34: Transfection efficiency of PEI polyplexes in the presence of endocytosis inhibitors. HeLa cells were pretreated with 7.5 µg/ml chlorpromazine or 1 µg/ml filipin, transfected with LPEI- (A) or BPEI- (B) based polyplexes and luciferase reporter gene expression was determined 24 h after transfection. Data were corrected by protein content and luciferase activity of control cells without inhibitor treatment was set as 100 %. Mean values + SD of triplicates are shown. ***p < 0.001; **p < 0.01; *p < 0.05, compared to control cells without inhibitor treatment (ANOVA, Duncan).*

As opposed to the results obtained in HUH-7 cells, these findings suggested that intracellular processing of PEI polyplexes in HeLa cells differed from that in HUH-7 cells.

3.5.6 Pathways mediating successful gene delivery depend on the polyplex formulation applied

Chlorpromazine and filipin essentially interfere with vital processes in the cell. Inhibition of clathrin-dependent endocytosis will, for example, impair many receptor-mediated processes and filipin might – at elevated concentrations – affect all the processes confined to lipid rafts and eventually destroy membrane integrity.

To rule out artifacts due to inhibitor-induced toxicity, cell viability was assayed in parallel to reporter gene expression at increasing concentrations of inhibitors (Figure 35). Since PEI-based gene delivery vectors cause significant cellular toxicity (16), viability measurements were performed in the presence of the corresponding polyplex formulation. In general, a narrow window of specific inhibitory function and unspecific toxicity was observed.

Transfection by BPEI polyplexes could be prevented by both inhibitors in HUH-7 (Figure 35B) and HeLa cells (Figure 35D). In contrast, transfection by LPEI polyplexes in HUH-7 cells could be inhibited only with chlorpromazine but not with filipin (Figure 35A). In HeLa cells, however, transfection by LPEI polyplexes was affected by both inhibitors (Figure 35C). These results imply that cellular polyplex processing depends not only on the cell type but also on the polyplex formulation applied.

In summary, uptake of small polyplexes into HUH-7 cells was inhibited by interference with both clathrin- and caveolae/raft-dependent endocytosis. Notably, neither PEGylation nor incorporation of EGF showed an effect on the mode of polyplex internalization. In HUH-7 cells, transfection was predominantly inhibited by chlorpromazine treatment, indicating that the two pathways differed in their ability to mediate efficient transfection. However, the role of each pathway in gene delivery depended on both, cell type and polyplex formulation applied.

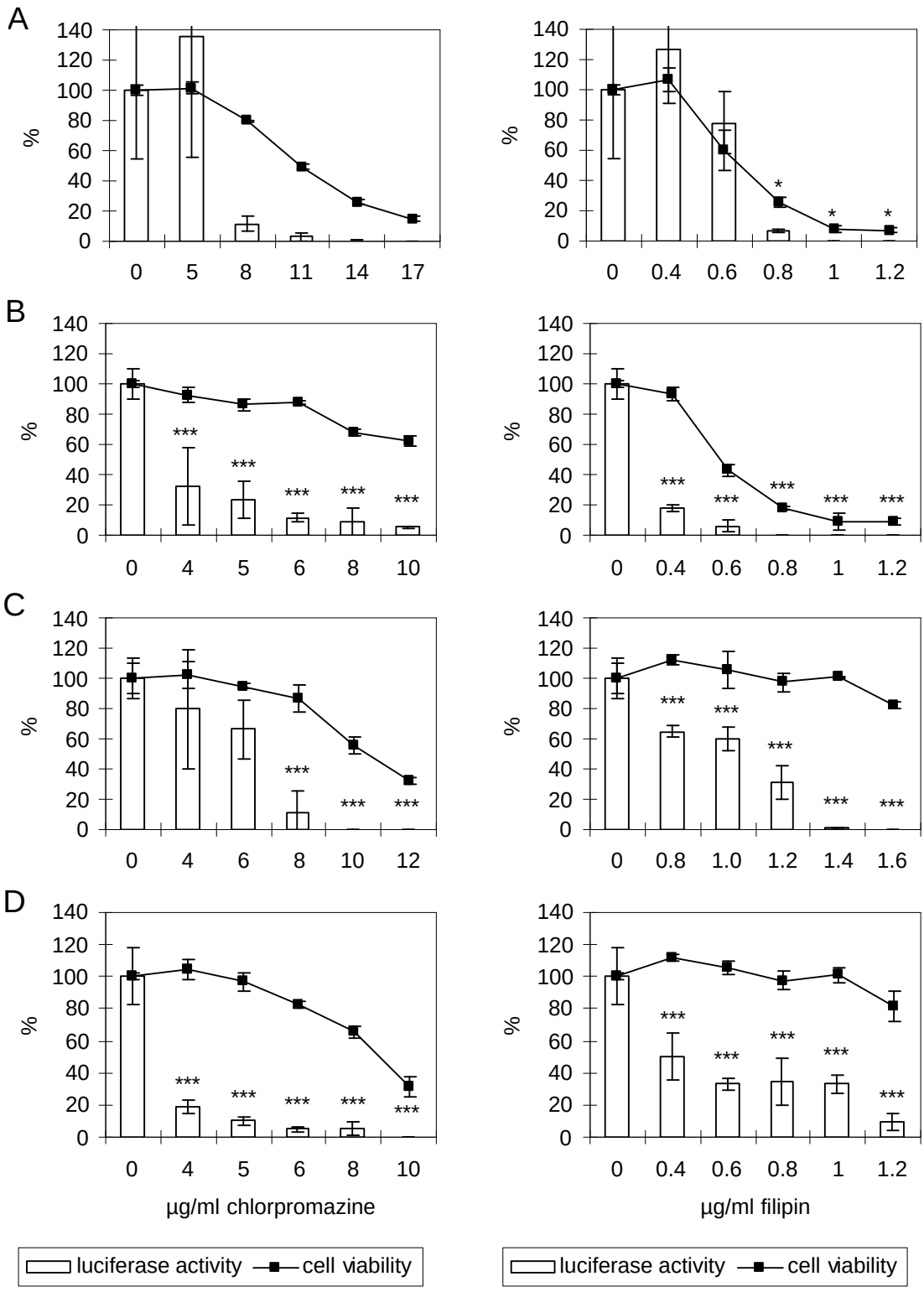

*Figure 35: Transfection efficiency of PEI polyplexes and cellular viability in the presence of endocytosis inhibitors. HUH-7 (A, B) and HeLa (C, D) cells were pretreated with chlorpromazine or filipin and transfected with LPEI (HBG, N/P 6) (A, C) or BPEI (HBS, N/P 10) (B, D) polyplexes. 24 h after transfection, luciferase activity and cellular viability were determined. Data of transfected control cells without inhibitor treatment were set as 100 %. Mean values +/- SD of triplicates are shown. Transfection efficiency data were analyzed for statistical significance. ***p < 0.001; **p < 0.01; *p < 0.05, compared to control cells without inhibitor treatment (ANOVA, Duncan).*

3.6 Characterization of dynamic interactions of polyplexes with the cytoskeleton

To enable further analysis of the mechanisms that account for cell type- and polyplex type-related variations of the transfection process, high resolution live cell imaging techniques can be employed. Thus, dynamic interactions between the polyplexes and different parts of the cell can be visualized that help to further characterize the processes involved.

It was recently proposed that the actin cytoskeleton is involved in the cellular uptake of PEI polyplexes (43), whereas microtubules were implicated in intracellular particle transport (67). Therefore, to unravel the role of actin and tubulin filaments in the process of EGFR-targeted transfection, gene-modified HUH-7 cell lines stably expressing EGFP-actin or -tubulin chimera were generated. These single cell clones were isolated from a cell culture containing both transduced and wild-type cells and were characterized by flow cytometry to comprise a single population with all cells positive for EGFP (data not shown). In transfection experiments it was ensured that in these recombinant cells, EGFR-targeting still improved PEI-based gene delivery (data not shown).

Furthermore, polyplexes were formed containing Cy3- or Cy5-labeled DNA. To minimize the risk that the Cy-dyes affect the cell-biological behavior of these complexes, a transfection experiment was performed. It revealed that gene transfer efficiency of labeled polyplexes was not changed compared to unlabeled particles (data not shown).

In order to unravel the dynamics of the processes involved, newly developed single particle tracing techniques were employed (6) which allowed simultaneous fluorescence imaging of labeled polyplexes and intracellular filaments in living cells. These measurements were carried out in the group of Prof. Bräuchle (Department for Physical Chemistry, LMU, Munich) as part of a collaboration project (SFB 486 “Nanoman”). The results with LPEI polyplexes are described in detail in the thesis of Ralf Bausinger and in (123). The measurements with EGF(-) and mEGF(+) complexes were performed by Karla de Bruin and Dr. Nadia Ruthardt. The obtained results are discussed in the discussion part of this thesis (see 4.3).

4 Discussion

PEI is one of the most efficient nonviral gene delivery vectors both *in vitro* and *in vivo*. However, cellular specificity is necessary to deliver the gene of interest into the desired cell or tissue. Unmodified PEI polyplexes are not able to distinguish between target and non-target tissue but rather stick to any cell membrane they reach. Therefore, systemic administration of PEI polyplexes into the tail vein of a test animal is always associated with high gene expression in the lung (22) and considerable systemic toxicity (124). To prevent non-specific trapping, PEI polymers have been grafted with polyethylene glycol (PEG) which has been shown to reduce cytotoxicity and significantly prolong circulation time (24). However, gene delivery with PEGylated polyplexes turned out to be less efficient. To introduce cell specificity and to restore the transfection efficiency of shielded polyplexes, receptor-mediated endocytic pathways are being exploited for nonviral gene delivery. For this purpose, targeting molecules have been incorporated into PEI polyplexes.

The EGFR is a tempting target for gene delivery since it is overexpressed in a wide variety of human tumors, including HCC. Recently, cryoconservable PEG-shielded and EGFR-targeted polyplexes were engineered for tumor-directed gene delivery (37). They were formed by complexing DNA with a mixture of LPEI, PEG(20 kDa)-PEI22 and a conjugate where mEGF is linked to BPEI via a heterobifunctional 3.4 kDa PEG spacer. *In vitro*, these EGFR-targeted polyplexes significantly enhanced gene transfer efficiency into human EGFR-overexpressing HCC cells compared to non-targeted, PEG-shielded polyplexes (37). They were also able to target subcutaneous tumors after tail vein injection into HCC xenograft bearing mice (37). Notably, no acute toxicity was observed in any of these animals. Further improvement of EGFR-targeted nucleic acid transfer has been achieved recently by incorporation of endosomolytic melittin into PEG-shielded, EGFR-targeted PEI polyplexes: This strategy enabled successful elimination of brain cancer (glioblastoma) after delivery of double-stranded RNA (polyinosine-cytosine [poly IC]) which induced rapid apoptosis in the target cells both *in vitro* and *in vivo* (125).

These findings suggest that EGFR-targeted gene delivery is a promising approach for the treatment of patients with EGFR-overexpressing tumors. However, until now the process of EGFR-specific gene delivery has not been characterized in detail.

4.1 Transfection efficiency of EGFR-targeted polyplexes

Strategies towards the development of nonviral vectors for tissue-targeted delivery of therapeutic genes require the engineering of stable polyplexes that are storable without significant changes in size, charge or transfection efficiency. Without glucose, however, large aggregates are formed after the freezing/thawing procedure (37;126;127). To avoid this, a 5 % glucose buffer was used that allowed freezing and storage of polyplexes at - 80 °C (Table 2). The glucose obviously served as a cryoprotectant and was therefore important to avoid aggregation during the freezing/thawing procedure (119).

Hence, polyplexes met the following requirements for systemic EGFR-targeted gene delivery: (i) Particle size remained small after thawing (approximately 150 nm). This is relevant not only for *in vivo* applications (17) but also for the intracellular mechanisms of targeted gene delivery since, for example, receptor-mediated endocytosis requires small particle sizes (17;103). (ii) The PEG-shield reduced the polyplex surface charge (approximately + 2.5 mV) preventing unspecific interactions with both blood components and non-target tissue (24). (iii) The EGF linked to the distal end of a 3.4 kDa PEG chain guaranteed maximum accessibility to its receptor (126).

Gene transfer studies using a luciferase marker gene construct showed that mEGF(+) polyplexes mediated enhanced reporter gene expression towards EGFR-expressing cells (HUH-7, Renca-EGFR) as compared to polyplexes without EGF (Figure 4). This is in good agreement with previous studies using similar polyplexes and other cell lines (36;37).

As expected, the percentage of transfected cells increased when EGFR-targeted polyplexes were applied compared to non-targeted complexes (Figure 8). When using EGFR-free Renca-LacZ cells, however, no significant difference between

targeted and non-targeted gene delivery was found (Figure 10), indicating direct involvement of the EGFR in gene delivery with mEGF(+) polyplexes.

Addition of free EGF as competing ligand before transfection resulted in a decrease in transfection efficiency of mEGF(+) complexes to nearly the levels of non-targeted gene delivery (Figure 5, Figure 9). In contrast, transfection efficiency of EGF-free polyplexes tended to increase in the presence of free EGF. Since rather large amounts of EGF were used to interfere with EGFR-dependent processes, this effect is probably due to the mitogenic activity of the free growth factor favoring nuclear polyplex entry during nuclear disassembly (71;81). However, despite this high concentration of free EGF, transfection efficiency of EGF(-) complexes did not reach that of mEGF(+) complexes, indicating that the mitogenic activity of complex-bound EGF, if at all involved, is not the major reason for enhanced transfection efficiency of mEGF(+) polyplexes.

These experiments were performed with polyplexes generated with a PEG-PEI conjugate coupled to murine EGF. Human EGF contains two lysines in the peptide chain which hampers specific chemical coupling via its N-terminal amino group. Notably, N-terminal PEGylation does not hinder binding of EGF to its receptor because the N-terminal residue is located far from the receptor-binding site (113;114). However, the biological activity of EGF is significantly reduced when PEGylation occurs at the ε-amino groups of Lys 28 and Lys 48 (113;114). Therefore, to selectively PEGylate the N-terminal amino group of huEGF, the protein was modified at a slightly acidic pH (pH 6). This enables selective deprotonation of the N-terminal amino group since α-amino groups are known to be less basic than ε-amino groups (114). Gene transfer efficiency of huEGF(+) polyplexes was similar to that of the corresponding mEGF(+) complexes (Figure 6, Figure 7), indicating that mEGF is able to substitute huEGF in the design of EGFR-targeted gene delivery vehicles. It further proved that the huEGF-PEG-PEI conjugate contained a biologically active EGFR ligand, indicating that the protein was selectively coupled via its α-amino group.

4.2 Cellular uptake kinetics of EGFR-targeted polyplexes

Incorporation of receptor-binding ligands into PEI complexes enhances cell binding and cellular internalization. Under physiological conditions, activated EGFR complexes are internalized and elevated intracellular EGFR levels can already be detected less than one minute after stimulation (115). It was therefore expected that uptake of EGF(+) polyplexes proceeds much faster than that of non-targeted complexes. Indeed, with a similar polyplex formulation it had been shown previously that in EGFR-expressing KB cells, EGFR-targeted PEI polyplexes showed enhanced cellular uptake properties (103). A similar finding was reported with transferrin receptor-targeted polyplexes in K562 cells (103).

In all these cellular binding studies, labeled DNA was used to stain the polyplexes. Labeled PEI – although widely used – would have caused artifacts since PEI polyplex formulations usually contain an excess of PEI that is not complexed to DNA (16). Improved cellular binding of EGF(+) polyplexes was demonstrated by transfection of HUH-7 cells on ice when endocytosis was inhibited. Incubating cells at 37 °C for 30 min to 4 h with EGF(+) polyplexes resulted in strong cellular association, which was two- to three-fold higher as compared to EGF(-) polyplexes (Figure 11). The difference in cellular association was already pronounced after only 30 min of incubation, indicating a fast interaction of EGFR-targeted polyplexes with the cell surface of EGFR-expressing cells. This was probably due to the high affinity interaction between complex-bound EGF and the EGFR localized in the plasma membrane.

EGFR specificity was confirmed by transfection of EGFR-free Renca-LacZ cells which showed no relevant differences in total cellular association between targeted and non-targeted polyplexes (Figure 13). The small differences in cellular binding at early time points were probably attributed to small differences in the biophysical properties of these polyplexes or the presence of low levels of wild-type murine EGFR on Renca-LacZ cells. Furthermore, binding of EGF(+) polyplexes to HUH-7 or Renca-EGFR cells was reduced to levels of EGF(-) polyplexes in the presence of excess free EGF over polyplex-bound EGF (Figure 12), again pointing out the specificity of interaction. In contrast, addition of albumin as control did not influence

cell association. Similarly, it has been reported previously that cellular uptake of transferrin receptor-targeted PEI polyplexes can be significantly reduced in the presence of excess free transferrin (103).

Fluorescence microscopy of HUH-7 cells transfected with Cy3-labeled polyplexes revealed that the increased cell binding was also associated with clustering of EGF(+) polyplexes (Figure 15). EGF(-) polyplexes appeared as a faint punctual pattern on the cells, whereas EGF(+) polyplexes were observed as large (micrometer) aggregates associated with the cells. Both, EGF(+) and EGF(-) polyplexes had a similar particle size prior to transfection, indicating that the clustering observed was due to the interaction of polyplex-bound EGF with the EGFR. Clustering of EGFRs after binding of EGF(+) polyplexes could account for this phenomenon of polyplex aggregation since such clustering has been described for this receptor family upon ligand binding (128). In addition to the accelerated cellular binding of EGF(+) polyplexes, the observed aggregation may be an important mechanism to enhance transfection efficiency. Polyplex aggregation obviously required specific ligand-receptor interaction and might be another feature contributing to the enhanced transfection efficiency of EGF(+) polyplexes. Consistent with this hypothesis, we observed that in incubations of EGF(+) polyplexes with (EGFR-positive) Renca-EGFR cells or (EGFR-negative) Renca-LacZ cells, only Renca-EGFR cells mediated clustering of polyplexes (Figure 15).

Quantification of internalized complexes revealed that already within 30 min, the majority of cells had taken up a significant amount of EGF(+) polyplexes (approximately 81 %) (Figure 16A, Figure 17A) whereas cellular entry of EGF(-) polyplexes was very slow and only detectable after approximately 2 h (approximately 62 % Cy5-positive cells) (Figure 16B, Figure 17A). Similarly, LPEI polyplexes (HBG, N/P 6) were taken up by the cells to a significant extent only after 2 h (approximately 77 % Cy5-positive cells) (Figure 16C, Figure 17A) – despite their favorable cellular binding properties (Figure 16C).

The results in Figure 16 and Figure 17 thus revealed characteristic differences between the three formulations. 30 min after transfection, total cellular association levels (regarding both Cy5 fluorescence intensity and percentage of Cy5-positive

cells) showed the following ranking: EGF(+) > LPEI >> EGF(-), whereas internalization levels were observed as follows: EGF(+) >> LPEI > EGF(-). This demonstrated that cellular uptake of the two non-targeted formulations occurred very slowly – in contrast to that of the targeted formulation. All three polyplexes had a similar particle size (approximately 100-150 nm), indicating that this property did not account for the variations observed. However, they showed different particle surface charges: LPEI polyplexes display a net positive surface potential (approximately + 20-30 mV) facilitating binding to the negatively charged cell membrane (Figure 16C), whereas EGF(-) complexes are nearly neutrally charged (approximately + 2.5 mV) causing low cellular association (Figure 16B). Despite these differences, uptake kinetics were slow in both cases. In contrast, EGF(+) complexes showed cellular binding characteristics similar to that of LPEI (Figure 16A, C), however, internalization was evident already within 30 min (Figure 16A, Figure 17A, B). This proves that EGFR-targeted complexes, once attached to the cell, are taken up indeed very fast. This finding fits well into the lines of evidence that receptor-mediated endocytosis is a fast process (85;115). Under physiological conditions, elevated intracellular EGFR levels have already been detected less than one minute after stimulation (115). Accordingly, uptake of EGF-containing polyplexes was found to proceed also within a few minutes (Figure 16A, Figure 17A, B). In contrast, LPEI polyplexes with similar cellular association characteristics showed slow uptake behavior similar to slow-binding EGF(-) complexes (Figure 16C, Figure 17A, B), indicating that unspecific uptake through adsorptive endocytosis is less efficient and requires extended periods of time to reach the same degree of internalization. Similar results have been previously reported in a study where cellular uptake kinetics of transferrin receptor- and CD3 receptor-targeted complexes had been related to that of non-targeted PEI polyplexes (103).

Interestingly, cellular uptake velocity (i. e. increase in Cy5 fluorescence intensity over time) of EGF(+) complexes was not constant over the 4 h period as observed with the non-targeted formulations (Figure 17B). The slope of the curve during the first 30 min was 10-times higher than that of the rest of the curve. Notably, two pathways of EGFR internalization exist: a saturable route via clathrin-coated pits and a constitutive route via clathrin-independent endocytosis which is 5- to 10-times slower

(86;87;129). Since uptake velocity of EGF(+) polyplexes dropped down very early in transfection, one might speculate that this was due to an EGF-induced downregulation of the inducible pathway leaving the slow constitutive pathway intact.

Fast cellular polyplex uptake suggests that the onset of reporter gene expression is also accelerated. A time course experiment confirmed this assumption. Already 4 h after transfection with luciferase-encoding EGF(+) polyplexes, luciferase activity could be detected (Figure 18). This result strongly suggests that accelerated polyplex uptake is an important mechanism for enhanced transfection efficiency of EGFR-targeted PEI polyplexes.

All these cellular binding and uptake kinetics data imply that EGFR-targeted polyplexes bind to the EGFR and are internalized by the cells via receptor-mediated endocytosis. The interactions of polyplexes with HUH-7 cells were therefore studied by single particle ultrasensitive fluorescence microscopy experiments by our collaboration partners in the the group of Prof. Bräuchle (Physical Chemistry, LMU). Since involvement of the cytoskeleton in PEI-based gene delivery had been proposed recently (43;67), HUH-7 cells stably expressing EGFP-actin or EGFP-tubulin chimera were generated for these experiments.

4.3 Dynamic interactions of polyplexes with the cell

Details on single particle fluorescence microscopy experiments using LPEI polyplexes can be found in (123) and in the thesis of Ralf Bausinger (in preparation). Experiments using mEGF(+) and EGF(-) polyplexes were performed by Karla de Bruin and Dr. Nadia Ruthardt.

First observations of time-lapse and stream recordings revealed typically three different motion kinetics for particles interacting with the cells: immobility, diffusion, and directed motion.

For a typical mEGF(+) polyplex, after docking onto the plasma membrane, a first phase of immobility was observed. Slow movement of the particle during this phase can be attributed to movement of the plasma membrane generated by the underlying cortical actin network. This was also supported by the correlated movement of several particles in close proximity. After a certain time – entering the second phase

– the particle started to move independently of the underlying plasma membrane movement. In this phase, diffusion was observed and could be distinguished from the immobility phase by increased step length distribution. Whether or not the particle had been internalized at this time point remained unclear. The third phase was defined by occurrence of directed motion. In this case, the step length increased further and particles showed highly directed motion for several frames interrupted by phases of diffusion. These phases of directed motion were typical of the transport by motor proteins. The straight trajectories indeed suggested transport along microtubules. However, further studies are required to determine whether this transport takes place along these microtubule filaments.

Movies with EGF(+) polyplexes in HUH7 cells expressing actin-GFP also revealed particle movement by actin tails which might indicate presence of the particle in an endosomal vesicle. By comparing the values of the diffusion coefficient D and the velocity v during the different phases of a statistically significant number of trajectories, the motion characteristics will be determined in greater detail. This should allow identification of the motor proteins and cytoskeletal elements involved and eventually the prediction whether the particle is inside or outside the cell.

In contrast to the tight binding of EGF(+) polyplexes to the plasma membrane, several EGF(-) particles did not exhibit the immediate immobility after touching the plasma membrane. Instead, particles diffused back into the medium. For EGF(-) particles, immobility combined with movement generated by plasma membrane dynamics as well as diffusion was also observed. However, it remained unclear whether the early diffusive motion of EGF(-) particles occured along or bound to the plasma membrane or even within the cytosol after internalization.

Analysis of the movies with EGF(+) and EGF(-) particles revealed a difference regarding the onset of directed motion. When defining directed motion as an indication for motion along microtubules in the cytosol and therefore for successful internalization, the time by which more than 50 % of EGF(-) particles were internalized seemed to be longer than in the case of EGF(+) polyplexes.

For quantitative data in a statistically significant range, quantitative movie analysis of the particle trajectories in detail is necessary. As this work is in progress, more measurements will be conducted to obtain adequate movies for analysis.

These results are in good agreement with the flow cytometry data since they imply that cellular uptake of EGFR-targeted polyplexes proceeds faster than that of non-targeted polyplexes. A further indication for involvement of the EGFR in cellular binding of EGF(+) polyplexes was the immediate immobility and the tight binding of the particles to the plasma membrane despite the particle´s low surface charge. Several EGF(-) complexes obviously did not exhibit the immediate immobility after touching the plasma membrane. Instead, particles easily detached from the membrane and diffused back into the medium which is due to their low surface charge impairing adsorptive electrostatic interaction with the negatively charged plasma membrane. This is in line with the slow cellular association of EGF(-) polyplexes as observed by flow cytometry (see Figure 11, Figure 16). Similarly, the slow internalization of PEG-shielded complexes (see Figure 17B) was supported by the observation that the time by which more than 50 % of EGF(-) particles were internalized seemed to be longer than in the case of EGF(+) polyplexes.

Additional measurements are being conducted to further characterize the processes involved in EGFR-targeted and non-targeted gene delivery. Correlation of the particles´ movements with cellular components like the actin and tubulin network will be of particular value to further understand the sequence of events leading to transfection. Similar experiments with LPEI polyplexes already delivered insight into the role of the cytoskeleton in PEI-mediated gene delivery (published in (123)).

In these experiments, LPEI polyplexes (HBG, N/P 6, approximately 100 nm in size) were found attached to the cell surface within 10 min after transfection. The largest fraction of observed polyplexes was found organized in filamentous arrays along the actin fibers (Figure 36A) and showed strongly reduced diffusion coefficients. In a number of cases, active transport with or along actin filaments was observed. This movement implied that actin filaments were involved in the cellular entry of membrane-bound LPEI polyplexes.

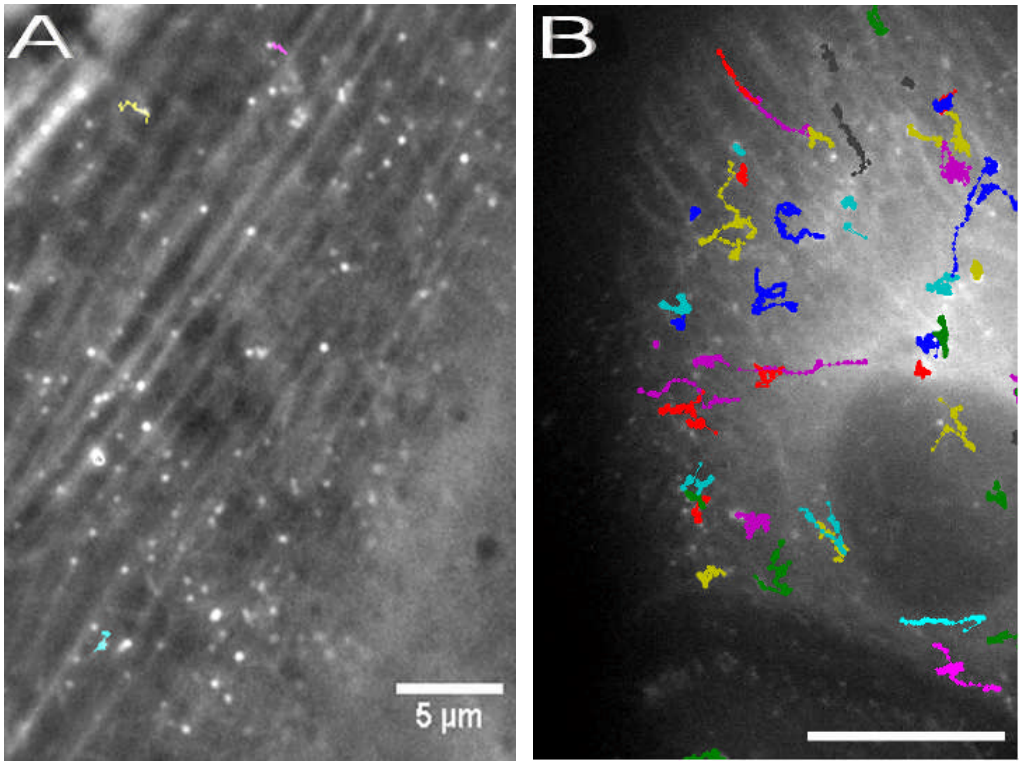

Figure 36: Interaction of LPEI polyplexes (HBG, N/P 6) with cytoskeletal filaments in HUH-7 cells. (A) Interaction of polyplexes with actin structures during the early stage of transfection. Cy3-labeled polyplexes and EGFP-actin filaments were simultaneously imaged by fluorescence microscopy. (B) Active transport of polyplexes along microtubules. Cy3-labeled polyplexes and EGFP-labeled microtubules were simultaneously imaged by fluorescence microscopy (scale bar: 5 µm). (in collaboration with Ralf Bausinger, published in (123))

Polyplex observation at a later stage of transfection revealed a distinctly different motion behavior. Its hallmarks were long range directed motion with increased velocities. Experimental data showed that the polyplex movement occured along tracks which were given by the microtubules (Figure 36B).

It is an intriguing question, in what form the polyplexes are undergoing this fast transport. Coincubation of LPEI polyplexes and the fluid phase marker dextran-Alexa Fluor® 647 revealed that all the fast moving polyplexes were found inside vesicles. Transport of vesicles along microtubules is known to be mediated by molecular motor proteins such as kinesins or dyneins. Accordingly, the maximum velocity of the polyplex movement (v_{max} = 0.65 µm•s^{-1}) was found to compare well with those reported for kinesin and dynein (67;130). Notably, polyplexes were found to change the direction of motion very fast, suggesting that both kinesin (moves towards the [+] end of the microtubule) and dynein (moves towards the [-] end of the microtubule) were involved.

4.4 EGFR activation by EGFR-targeted polyplexes

To further characterize the cellular mechanisms of EGFR-targeted gene delivery, direct involvement of the EGFR had to be proven. The observation that both reporter gene expression and cellular polyplex association could be inhibited by addition of free competing ligand (Figure 5, Figure 7, Figure 9, Figure 12) had already suggested that the EGFR is involved in the cellular uptake of EGF(+) polyplexes. This was further supported by the finding that upon EGFR-targeted transfection, EGFR-free Renca-LacZ cells showed neither enhanced cellular polyplex association (Figure 13) nor improved reporter gene expression (Figure 10).

Western blot analysis revealed that binding of mEGF(+) polyplexes to the EGFR also entails receptor activation. This is of relevance since EGFR activity controls a wide variety of biological responses. Shortly after transfection with EGF(+) polyplexes, EGFR and Akt were converted into their activated form by phosphorylation (Figure 20). This verified that EGF(+) polyplexes bind to the receptor and implied that the fast uptake of mEGF(+) polyplexes is mediated by the EGFR. In the cell line tested, elevated phospho-Erk levels were already detectable under control conditions – in contrast to EGFR and Akt. Since Erk is known to activate the transcription of genes involved in cell growth and proliferation (131), it has been implicated in tumor cell proliferation and seems to be constitutively activated in HUH-7 hepatoma cells. mEGF(+) polyplexes then induced a decrease in phospho-Erk levels below the level of untreated control cells. This was surprising since it is widely agreed that EGFR activity mediates activation of the Ras- Raf- Erk signaling pathway (131). Inactivation of phospho-Erk is associated with the activity of MAPK phosphatases (MKPs, also called “dual specificity phosphatases” (DSPs)) which dephosphorylate MAPKs (Erk, p38, JNK) and thus control duration and extent of MAPK activity (132). These enzymes show substrate specificity for all three MAPK but to a varying extent. As part of a negative feedback mechanism they are activated by the substrates themselves (132;133). Here, MKPs were probably induced by the strong EGFR activation in order to balance Erk activity. This can explain why phospho-Erk levels decreased after stimulation with both EGF(+) complexes and free mEGF.

Activation of EGFR and its downstream signaling pathways is of high relevance for therapeutic applications because EGFR activity controls cell proliferation and has been implicated in the pathogenesis of many solid tumors. Akt (= protein kinase B) – also called “survival kinase” – has been shown to promote cell survival. Thus, EGF(+) polyplex binding to EGFR-expressing cells might induce cell proliferation or even prevent cell death. Consequently, activation of these signaling pathways by EGFR-targeted PEI polyplexes may not be desirable in the treatment of tumors. However, considering the transfection process of PEI polyplexes, this conclusion has to be re-evaluated since EGFR-targeted gene delivery was shown to be more efficient in dividing cells (Figure 22). Notably, the first pulse of EGFR signaling is known to induce exit from quiescence into G_1 phase and appears to render cells responsive to subsequent mitogenic stimulus (83). Therefore, stimulation of the EGFR might indeed be of advantage in order to enhance transfection efficiency. Furthermore, gene therapy of tumors aims at eliminating the malignant cells. Initiation of cellular proliferation in dying cells will therefore be of less relevance. Notably, successful elimination of EGFR-overexpressing tumors by systemic EGFR-targeted nucleic acid delivery has already been reported (125). Similarly, if gene therapy has to be combined with chemotherapy, EGFR activation seems to be desirable since chemotherapy only attacks cells that are in the process of cell division. Cells that are at rest are much less vulnerable to chemotherapeutic damage. Induction of cell cycle progression in response to EGFR activation might therefore be useful in the chemotherapeutic treatment of cancer. Nevertheless, this concept has to prove successful in the clinical setting since EGFR overactivity was also found to be associated with resistance to cytotoxic drugs and radiotherapy (121).

It has to be considered that both EGFR activation and signaling are processes strongly dependent on the ligand concentration (86;87;134). Here, a polyplex concentration of 6 µg DNA per ml was chosen which corresponds to a mEGF concentration of approximately 120 ng/ml. Compared to the physiological range of huEGF levels (1-2 ng/ml huEGF in serum; 10-100 ng/ml huEGF in several other biological fluids) (87), this concentration is indeed very high which accounts for the noticeable activation of EGFR signaling by both EGF(+) polyplexes and free mEGF (Figure 20). However, the polyplex concentration that can be reached in a human

being will probably be clearly below the one used here *in vitro*. The pharmacological relevance of this finding will therefore only be assessable in the clinical setting. Furthermore, reduction of the content of biologically active EGF in this polyplex formulation can be achieved by removal of free EGF-PEG-PEI conjugate through removal of free PEI by a method which has been reported recently (16). This will help to further improve the safety profile of this very promising strategy.

Since overexpression of EGFR correlates with increased metastasis, decreased survival and a poor prognosis, agents targeting these receptors and their downstream signaling pathways (e. g. Erk) are now being evaluated in the clinic. Cetuximab (Erbitux®), for example, is an IgG_1 monoclonal antibody and has been approved for the treatment of advanced metastatic colorectal cancer. It operates by locking onto the external domains of the EGFR of cancer cells which prevents normal EGF from stimulating cell growth (135).

Accordingly, EGFR-binding antibodies (like cetuximab) can be used alternatively to target gene delivery vectors to EGFR-overexpressing cells while preventing EGF-induced receptor activation and downregulation. However, EGFR autophosphorylation is known to be essential for internalization via the rapid clathrin-dependent route which is induced by ligand occupancy (129;136). Since cetuximab does not induce EGFR activation, such vectors should only be internalized through the constitutive clathrin-independent pathway which is 5- to 10-times slower (129;136). Nevertheless, this concept will be of interest because EGFR activation and downregulation would be avoided. In this respect, application of EGF(+) polyplexes might emerge as a “double-edged sword”.

4.5 Cell cycle dependency of EGFR-targeted gene delivery

Recently it was reported that the EGFR after stimulation with EGF is able to translocate to the nucleus and modify sequence specific gene expression (92;137). This nuclear localization was observed in different cell lines and tissues including many human cancers and was found to be associated with the highly proliferating status of these cells (137). Interestingly, cyclin D1 – a cell cycle regulator essential for G_1 progression – was identified as one of the targets of nuclear EGFR (92).

Since nuclear entry of nonviral vectors is known to be a major bottleneck to efficient transfection, the possibility was considered that EGF mediates enhanced nuclear accumulation of the polyplexes. For polyplex-mediated gene delivery, the major path to nuclear entry seems to be via nuclear disassembly during mitosis (71). If, however, EGF has a significant effect on nuclear import, this cell cycle dependency should be less pronounced when using EGFR-targeted polyplexes.

Therefore, to determine whether EGFR-targeted polyplexes are able to efficiently transfect postmitotic cells, the number of dividing cells was reduced by a single thymidine block (Figure 21). Transfection in the presence of thymidine revealed that reporter gene expression of LPEI (HBS ½, N/P 6), EGF(-) and EGF(+) polyplexes decreased to a similar extent (Figure 22), indicating that EGFR-targeted complexes are not more efficient in transfecting postmitotic cells than non-targeted polyplexes.

Notably, in transfection experiments using elutriated HeLa cells, similar polyplexes (LPEI, OptiMEM, N/P 6) had already been shown to display moderate cell cycle dependency: cells that were allowed to undergo mitosis during transfection yielded up to 11-fold higher transfection efficiencies than cells that did not divide (72). Admittedly, centrifugal elutriation allows a better separation of cell fractions than a thymidine block. In the present study, up to 5 % were constantly cycling through G_2/M phase (Figure 21) and might have undergone cell division during the transfection process. Notably, three further undesired side effects probably led to artifacts: thymidine causes cellular toxicity, but it might also affect transgene expression on the level of protein synthesis and/or the transfection process itself. To estimate the consequences of the first two effects, HUH-7 EGFP-Luc cells were cultured in the presence of thymidine for the time of the complete experiment (34 h) and analyzed for luciferase activity. In these cells, luciferase activity was found to be 62.3 % (+/-2.3 %) of untreated control cells (data not shown). This control experiment, however, provided only a rough estimation of the relevance of these undesired thymidine effects and did not detect possible interference with the transfection process (beyond reduction of mitosis). Therefore, the data in Figure 22 can only be regarded as a rough indication for the role of mitosis in EGFR-targeted gene delivery.

To further evaluate the impact of mitosis on EGFR-targeted gene delivery, cells were synchronized and transfected 4 h after thymidine release. Analysis of cell cycle progression revealed that the cells underwent mitotic cell division between 12 h and 20 h after thymidine removal (Figure 23). 12 h after transfection (i. e. 16 h after thymidine release), transgene expression could be detected regardless whether non-targeted (LPEI, HBS ½; EGF(-)) or targeted polyplexes were used (Figure 24). This indicates that breakdown of the nuclear membrane is an important process during EGFR-targeted gene delivery. This was further supported by the observation that all polyplexes mediated a very similar progression in expression of both EGFP and the luciferase reporter gene (Figure 24C, D). The data therefore imply that mitosis is as important in EGFR-targeted gene delivery as it is in non-targeted transfection. This means that complex-bound EGF is not able to mediate efficient nuclear accumulation of EGFR-targeted polyplexes.

To obtain further evidence for the cell cycle dependency of EGFR-targeted gene delivery, cell cycle, reporter gene expression and total cellular association were monitored in parallel. Thus, no chemical drug had to be added that caused artifacts. This revealed that 6 h posttransfection, the fraction of diploid cells contained three-fold more EGFP-expressing cells than the fraction of tetraploid cells (Figure 25, Table 4). Since the fraction of diploid cells was expected to be enriched in cells that had passed mitosis during the 6 h incubation with polyplexes, it was concluded that this fraction was more susceptible to nuclear polyplex import. No difference between EGFR-targeted (EGF(+)) and non-targeted polyplexes (LPEI, HBS ½; EGF(-)) was evident, indicating that – in line with Figure 22 – mitosis is as important in EGFR-targeted gene delivery as it is in non-targeted gene delivery.

Although there is some historical evidence that GFP expression may be toxic to mammalian cells (138) and lead to a delay in cell cycle progression at G_1 phase, it is now generally assumed that low to moderate expression of GFP is minimally perturbing to the host cell (118;139;140). Since in the present study (Figure 25, Table 3, Table 4, Table 5), transfection levels were low – due to the short incubation time – it can be assumed that EGFP did not affect cell cycle progression.

The cell cycle dependency observed in this study indicates that EGF is not able to mediate efficient nuclear polyplex translocation. This process is either not available for EGFRs bound to EGF(+) polyplexes or it is possible but just not efficient enough to enhance transfection efficiency. It is difficult to explain why EGFRs are not able to (efficiently) translocate PEI polyplexes to the nucleus since the route(s) by which the EGFR moves into the nucleus have not been clearly elucidated yet (137). The process might show only a low capacity; or vesicles containing PEI polyplexes are processed by the cell in a different way than those which contain physiological *EGF/EGFR complexes*. This could be due to the PEI polyplexes affecting vesicular pH (see 1.3.2.2, (141)), vesicle size or internalization pathway. Moreover, other conditions might have to match. Since the EGF concentration present has been shown to affect the pathway of internalization (86;87), it is conceivable that it also affects nuclear translocation of the cargo. A further possible reason might be that coexistent signals are required for this process of EGFR-mediated nuclear translocation.

The advantage of this cell cycle dependency is the fact that in adults, most of the body´s cells are not dividing. These cells spend most of their time in a resting state and only divide if damage repair is necessary. Tumor growth, however, is very fast. Transfecting only dividing cells can therefore be regarded as a kind of passive tumor targeting. Admittedly, not all tumor cells are constantly dividing but some cancer cells might be resting. These cells will be less susceptible to gene therapy treatment by EGFR-targeted PEI polyplexes. Though, this in turn depends on the fact whether at those concentrations reached *in vivo*, polyplex-bound EGF is able to induce cell proliferation (see 4.4).

To enable efficient gene delivery also in non-dividing cells, further components can be incorporated into the vector. For example, signal-mediated active transport mechanisms have been exploited for trafficking vectors to the nucleus. Covalent coupling of a single NLS peptide to a CMV-Luciferase gene led to an up to 1000-fold enhancement in transfection efficiency presumably attributed to improved nuclear translocation by the nuclear import machinery (73). In this way, it will be possible to generate an artificial virus-like vector carrying domains for both cell-specific/enhanced uptake and improved nuclear polyplex/transgene accumulation.

4.6 Mode of cellular polyplex uptake

Despite various studies investigating the mechanisms of uptake and intracellular trafficking (41-43;45;46;51;123), current understanding of the processes involved in cellular uptake of PEI polyplexes is still limited. Following previous findings that HSPGs are involved in the cellular uptake of PEI polyplexes (45;56), it was recently proposed that syndecan-mediated polyplex binding triggers actin-driven internalization via a mechanism related to macropinocytosis (43). In addition, recent studies reported on the close relation between particle size and internalization pathway (41;51) where either caveolae, lipid rafts, clathrin-coated pits or membrane ruffles were involved. Regarding these relations, however, reports remain controversial. Since mEGF(+) complexes had been shown to directly bind to the EGFR (Figure 19, Figure 20) it was assumed that EGF affects these modes of uptake and thus the way of intracellular polyplex processing.

Colocalization experiments of the pathway markers transferrin and CTB with small LPEI, EGF(-) and EGF(+) polyplexes revealed involvement of both clathrin- and raft-dependent endocytosis in the cellular uptake of small polyplexes (Figure 26). Most remarkably, neither a change in particle surface potential by PEGylation nor incorporation of EGF as a ligand had an impact on the route of cellular polyplex entry. This result was surprising since the various polyplex formulations were expected to be processed by the cells in different ways which in turn was suggested by their different biophysical properties, their diverse molecular composition and, most remarkably, by their different binding and uptake kinetics (as illustrated by Figure 16, Figure 17).

Since all three polyplex formulations were of similar size (LPEI: approximately 100 nm; EGF(-), mEGF(+): approximately 140 nm) (Table 2, Figure 27), it was concluded that cellular polyplex processing mainly depends on the particle size. Notably, close relation between particle size and internalization pathway had been proposed recently (41;51). This size dependency probably accounts for the similar results with different polyplex formulations (Figure 26, Figure 28) and further suggests that both pathways are utilized by the polyplexes because of a coexistence of small and medium-sized particles during transfection (Figure 26, Figure 28). The

PEGylated polyplexes formed in HBG (EGF(-), EGF(+)) had an initial size of approximately 100-200 nm and were therefore in the size range for uptake via both clathrin- and caveolae/raft-mediated endocytosis (41;51). LPEI polyplexes had an initial size of approximately 100 nm. In transfection medium, however, salt-induced aggregation of unshielded PEI polyplexes occurs (18) which is known to result in a mixture of differently sized particles (17). To test the aggregation behavior under transfection conditions, HUH-7 cells were incubated with Cy3-labeled polyplexes and visualized for 2 h by fluorescence microscopy (data not shown). Due to very fast cellular binding, particles grew only slightly in size (approximately up to 300 nm). Assuming different pathways for differently sized particles (41;51), this mixture of small and medium-sized polyplexes (17) (ranging from approximately 70 to 300 nm) probably accounts for the observation that both clathrin- and raft-dependent endocytosis mediate cellular uptake of these polyplex formulations (Figure 26, Figure 28).

In contrast, large polyplexes (LPEI, EGF(-)) were taken up by the cells via a third, clathrin- and raft-independent pathway (Figure 28). This was concluded since uptake of aggregated polyplexes was affected neither by chlorpromazine nor by filipin. Accordingly, endocytic and non-endocytic processes could be involved. One possible internalization pathway for aggregated LPEI and EGF(-) polyplexes is macropinocytosis which has been proposed to mediate uptake of large complexes (> 200 nm) (51). Interstingly, this pathway has also been implicated in polyplex uptake by a human hepatoma cell line (46). It is further known that the high charge density of unshielded PEI polyplexes is capable of inducing local membrane damage, especially when large aggregates interact with the plasma membrane (55). In the case of PEG-shielded EGF(-) complexes, this mechanism will be less relevant because of their nearly neutral surface charge.

Figure 28 thus supports the hypothesis that the capacity of internalization pathways is mainly limited by the particle size and not by other particle properties like surface charge or molecular composition. Nevertheless, regarding the small polyplexes, the similar results with the three different polyplex formulations can also be mere chance: PEI polyplexes with a size of 80-200 nm (LPEI, EGF(-), EGF(+)) are small enough for both, caveolae/raft-mediated and clathrin-dependent endocytosis (51). These

pathways happen to be the same as those involved in the physiological internalization process of *EGF/EGFR complexes*. It therefore remains elusive whether particle size is indeed the all-dominant factor defining the cellular internalization route of PEI polyplexes. Uptake studies with differently sized polyplexes of defined diameter and varying composition will be necessary to address this question.

4.7 Pathways mediating successful transfection

Since pathways obviously differ in their way to deliver transgenes (42;46;51;52), pathways were determined that mediate successful gene transfer of the various polyplex formulations. Previously, it was reported that lipoplex-mediated transfection occurs through the clathrin-dependent pathway of endocytosis (42;52). However, less is known about the relative contribution of each pathway to gene transfer efficiency mediated by PEI polyplexes. Rejman and coworkers recently addressed this issue and proposed that only the caveolae/raft-mediated pathway leads to efficient transfection of BPEI polyplexes (42).

To test whether this route is also the most relevant in EGFR-targeted gene delivery, transfection experiments were performed in the presence of specific endocytosis inhibitors. They revealed that in HUH-7 cells, clathrin-dependent endocytosis predominantly mediates transfection by EGFR-targeted as well as PEG-shielded and unmodified PEI polyplexes (Figure 29, Figure 30, Figure 31). This result was surprising since – although the various polyplex formulations had been found to be taken up via the same pathways (see Figure 26, Figure 28) – they were at least expected to be processed by the cells in different ways. Small polyplexes can be taken up into small vesicles, whereas aggregated polyplexes are either confined to large vesicles or might exploit non-endocytic pathways for efficient cellular entry (as discussed in 4.6) (51;55). Furthermore, large polyplexes are expected to exert a stronger proton sponge effect than small polyplexes, due to a higher PEI content (17;142). PEG-shielded complexes are known to display weak cellular binding properties (Figure 11, Figure 16) and probably have reduced ability to force endosomal rupture (143). In contrast, EGFR-targeted polyplexes are expected to enter the cells via EGFR-related pathways, namely clathrin- and caveolae/raft-

dependent endocytosis (86;87). Aggregated EGFR-targeted polyplexes, on the other hand, will show strong cellular association due to EGFR binding but can not be internalized via EGFR-related pathways since clathrin- and caveolae-derived vesicles are limited regarding their size. This had been observed, for example, with large transferrin receptor-targeted PEI polyplexes which displayed improved cellular binding characteristics but only sparse internalization, probably because they were too large for transferrin-mediated clathrin-dependent endocytosis (103).

Figure 29, Figure 30 and Figure 31 thus revealed that in PEI-mediated transfection of HUH-7 cells, the clathrin-dependent pathway has a much better ability to efficiently deliver the transgene than the raft-dependent route. Although only 30 % of small PEI (LPEI, EGF(-), EGF(+)) polyplexes were taken up by HUH-7 cells via clathrin-dependent endocytosis (Figure 26), these 30 % of particles predominantly mediated successful transfection (Figure 29). It can therefore be concluded that the polyplexes taken up via these two pathways are processed by the cells in different ways. This is indeed conceivable since each endocytic pathway serves different tasks and therefore bears its own characteristics which favor or impair intracellular polyplex trafficking.

Considering the biophysical properties of PEI (e. g. their buffering capacity), the differences in vesicular pH between the clathrin- and the raft-dependent pathways probably play an important role in PEI-mediated gene delivery and might account for these differences. Caveolar vesicles and caveosomes have a neutral pH (49). In contrast, clathrin-coated vesicles – after loosing their clathrin coat – become acidified leading to the formation of early (pH ~ 6) and late endosomes (pH ~ 5) which ultimately fuse with lysosomes (pH ~ 4.5) (47). Although controversial data exist whether PEI polyplexes can be found in lysosomes (55;144;145) it is widely agreed that the strong endosomal buffering capacity of PEI can lead to enhanced endosomal escape (19;44;60). Consequently, blockage of endosomal buffering with bafilomycin resulted in a substantial decrease in reporter gene expression (60), indicating that successful gene expression of PEI polyplexes occurs through vesicles that acidify. It is therefore conceivable that in HUH-7 cells, uptake of PEI polyplexes via clathrin-dependent endocytosis favors efficient transfection (Figure 29, Figure 30, Figure 31).

Transfection data of large PEI polyplexes (Figure 30) further suggest that pathways can also favor successful gene delivery without being directly involved in cellular polyplex uptake. Aggregated polyplexes (LPEI, EGF(-)) were taken up by the cells via clathrin- and raft-independent pathways (Figure 28), whereas transfection was strongly affected by chlorpromazine (Figure 30). This implies that routes might be involved in the transfection process that do not mediate uptake of these polyplexes and further suggests that in the transfection process of aggregated PEI polyplexes, the clathrin-dependent pathway plays an important role at a later stage of transfection. It is, for example, conceivable that crosstalk or traveling between the internalization pathway and the clathrin-dependent route exist which might then trigger polyplex escape into the cytosol. In this way, clathrin-mediated endocytosis might favor efficient transfection without being directly involved in cellular polyplex uptake. Furthermore, aggregated PEI polyplexes are very heterogeneous in size with small particles of 100 nm and aggregates in the micrometer range both being present in the same solution (17). The possible conclusion that the moderate effect of inhibitors on the transgene expression of aggregated polyplexes (Figure 30) is partially due to interference with the fraction of small-sized polyplexes, however, is not plausible. The reason is that this theory - where the fraction of small particles predominantly mediates gene transfer by aggregated polyplexes – contrasts with the finding that in general, transfection by aggregated polyplexes is much more efficient than that by small complexes (17;18).

Interestingly, different results had been reported recently regarding the importance of the clathrin-dependent pathway in PEI-mediated gene delivery. They suggested that only caveolae/raft-mediated uptake contributes to efficient transfection by PEI polyplexes in HeLa cells (42). It can therefore be concluded that cell-specific differences in intracellular polyplex trafficking exist. Transfection experiments in HeLa cells verified this conclusion since here – opposed to the data with HUH-7 cells – the raft-mediated pathway was more relevant (Figure 34). Notably, similar experiments – performed by our collaboration partners Roosmarjin Vandenbroucke and Dr. Niek Sanders (Ghent University) – revealed that COS-7 (african green monkey kidney) cells show a pattern similar to HUH-7 cells since gene transfer is predominantly mediated by the clathrin-dependent pathway. Taken together, these findings suggest

that HeLa cells process PEI polyplexes in a different way than HUH-7 and COS-7 cells. However, since nearly all cells are specialized for certain functions which require different actions within the cell, it is indeed conceivable that different cell lines differ in their way to process the same material.

Since working concentrations of the inhibitors were very close to toxicity, cellular viability and reporter gene expression were assayed in parallel at increasing concentrations of inhibitors (Figure 35). As PEI-based gene delivery vectors cause significant cellular toxicity (16), viability measurements were performed in the presence of the corresponding polyplex formulation. In general, a narrow window of specific inhibitor function and unspecific toxicity was observed, emphasizing that a high level of caution had to be exercised to distinguish between specific and unspecific effects.

The results revealed that cellular polyplex processing depends on both, the cell line and the polyplex formulation applied (Figure 35). Most remarkably, LPEI-mediated transfection in HUH-7 cells was not susceptible to filipin, whereas internalization had been shown to occur via both pathways (Figure 26, Figure 28). Filipin acts by sequestering cholesterol within a complex in the plasma membrane and thus inhibits uptake via both caveolae and lipid rafts (54). HUH-7 and other hepatoma cell lines are known to be caveolin-1-deficient (146;147), the lipid raft internalization pathway, however, still exists (148). Apparently, LPEI polyplexes could not efficiently transfect HUH-7 cells via this route (Figure 35A). Since, however, BPEI successfully transfected HUH-7 cells via both pathways (Figure 35B), differences between LPEI and BPEI have to account for this effect.

Previously, it was proposed that the higher buffering capacity of branched PEI versus linear PEI accounts for the fact that LPEI polyplexes can be found in – on average – more acidic vesicles than BPEI polyplexes (149). According to the proton sponge hypothesis, efficient vesicular buffering favors polyplex release into the cytosol. It was therefore suggested that BPEI polyplexes escape early into the cytoplasm while preventing sorting of the vesicles towards more acidic compartments (149). Consequently when compared to LPEI complexes, BPEI polyplexes might be released more easily from vesicles with a nearly neutral pH characteristic of the

caveolae/raft-mediated pathway. This possibly made BPEI-mediated transfection more susceptible to the inhibitor filipin.

Moreover, BPEI and LPEI polyplexes differ in their DNA binding activity. Binding of DNA to BPEI is stronger than to LPEI (Julia Klöckner, unpublished observations) impairing BPEI polyplex disassembly and thus reducing the amount of free plasmid accessible to the transcription machinery. Due to this effect, BPEI polyplexes in HUH-7 cells need both pathways for efficient transfection as the deletion of one pathway probably reduces the intracellular available amount of transgene below the minimum amount necessary for successful transfection. In contrast, LPEI polyplexes seem to efficiently transfect cells even at reduced intracellular amounts of transgene, since DNA is released more easily from the polyplexes making more DNA available for transcription.

A further reason for the interference of filipin with BPEI polyplex- but not with LPEI polyplex-mediated transfection in HUH-7 cells might rely on the different N/P ratios of these formulations. Successful transfection by BPEI polyplexes with an N/P of 10 obviously does not require immediate vesicle acidification, whereas transfection by LPEI polyplexes with an N/P of 6 does. Due to the high amount of PEI in these BPEI polyplexes, the complexes probably have enhanced capability of disrupting the membrane of vesicles with a neutral pH. This leads to the conclusion that not only the type of PEI but also the amount of polycation in PEI polyplexes might influence the route leading to successful transfection.

In HeLa cells, however, also transfection by LPEI polyplexes was affected by filipin (Figure 35C). Most likely, cell type-related variations in intracellular vesicle processing account for this effect.

Furthermore, the possibility has to be considered that the clathrin- and caveolae/raft-dependent pathways interact at some point after internalization so that both pathways are required for successful gene delivery. Although traveling between caveosomes and endosomes has not been evaluated yet, some kind of interaction is likely. Notably, colocalization of Alexa Fluor® 647 transferrin and Alexa Fluor® 488 CTB was found in both HUH-7 (data not shown) and HeLa cells (Karla de Bruin, unpublished observations) already after approximately 1 h.

5 Summary

Recently, PEG-shielded and EGFR-targeted polyplexes were designed for tumor-directed gene transfer. In this thesis, the cellular mechanisms of EGFR-targeted gene delivery were evaluated to obtain a detailed understanding of the processes involved which is a key aspect for further improving the design of the vector.

EGFR-targeted PEGylated PEI polyplexes significantly enhanced transfection efficiency into EGFR-expressing cell lines as compared to EGF-free PEGylated complexes. Enhanced gene transfer efficiency was accompanied by a significant increase in the number of transfected cells. No targeting effect, however, was evident in cells devoid of EGFR or when the receptor was occupied by competing free ligand, indicating that enhanced EGFR-targeted gene delivery is primarily mediated via a ligand/receptor interaction. In addition to the established targeting system containing murine EGF, also a polyplex formulation was generated containing human EGF. Similar transfection efficiencies and targeting properties compared to mEGF(+) polyplexes were obtained.

Increased cellular binding and accelerated uptake of EGFR-targeted polyplexes into EGFR-expressing cells was identified as a substantial mechanism for improved gene transfer efficiency. In line with this result, reporter gene expression upon EGFR-targeted transfection was detectable much earlier than upon non-targeted gene transfer. Cellular binding of EGFR-targeted polyplexes was further associated by clustering of polyplexes into micrometer-sized particles, resembling typical receptor clustering upon ligand binding.

In contrast to non-targeted polyplexes, EGFR-targeted polyplexes triggered EGFR activation and initiation of the downstream signaling transducer Akt. Notably, EGFR signaling is known to induce cell cycle progression and cell proliferation. Since nuclear membrane breakdown during mitosis is known to facilitate nuclear polyplex entry, the putative mitogenic effect of EGFR-targeted polyplexes is therefore another feature possibly contributing to their enhanced transfection efficiency. Investigations

however demonstrated that the EGF ligand was not capable of mediating enhanced nuclear polyplex accumulation.

To further elucidate the process of EGFR-targeted gene delivery, the pathways involved in cellular polyplex uptake were determined. Internalization of EGFR-targeted polyplexes occurred via at least two endocytic pathways: 30 % entered the cells via clathrin-dependent and 70 % via raft-dependent endocytosis. Despite structural and biophysical differences of the polyplexes applied (LPEI, EGF(-) and EGF(+)), this uptake pattern did not vary between the formulations, provided that the particles were of similar size (approximately 80-200 nm). In contrast, internalization of aggregated PEI polyplexes (LPEI, EGF(-)) proceeded via clathrin- and raft-independent pathways, supporting the hypothesis that particle size is an important factor determining the route of cellular polyplex entry.

In our model, successful transfection of the three polyplex formulations (LPEI, EGF(-) and mEGF(+)) was predominantly mediated by the clathrin-dependent pathway, emphasizing the relevance of vesicular acidification in intracellular trafficking of PEI-based gene delivery systems. Nevertheless, depending on the cell type and the polyplex formulation applied, also the caveolae/raft-dependent pathway was able to mediate successful transfection. This was observed – in particular – when polyplexes with a high N/P ratio (e. g. 10) were used. This indicates that different routes of endocytosis can contribute to efficient transfection by PEI-based gene delivery vectors.

6 Appendix

6.1 Abbreviations

AS-ON	antisense oligonucleotides
ATP	adenosine triphosphate
bp	base pairs
BPEI	branched PEI of 25 kDa
BSA	bovine serum albumine
CLSM	confocal laser scanning microscope
CMV	cytomegalovirus
CN	negative control
CTB	cholera toxin subunit B
Da	Dalton
DAPI	4,6-diamidino-2-phenylindole
DMEM	Dulbecco´s Modified Eagle´s Medium
DMSO	dimethyl sulfoxide
DNA	deoxyribonucleic acid
DSP	dual specificity phosphatase
DTT	dithiothreitol
EDTA	ethylenediaminetetraacetic acid
EGF	epidermal growth factor
EGF(-) complexes	EGF-free complexes
EGF(+) complexes	EGFR-targeted complexes
EGFP	enhanced green fluorescent protein

EGF-PEG-PEI25	EGF covalently linked to BPEI via a heterobifunctional 3.4 kDa PEG spacer
EGFR	epidermal growth factor receptor
EGTA	ethyleneglycol-bis-(aminoethylether)-tetraacetic acid
EPR	enhanced permeability and retention effect
Erk	extracellular-signal-regulated kinase
FBS	fetal bovine serum
HBG	HEPES-buffered glucose
HBS ½	HEPES-buffered glucose and HEPES-buffered saline 1/1 (v/v)
HBS	HEPES-buffered saline
HCC	hepatocellular carcinoma
HEPES	N-(2-hydroxyethyl)piperazine-N´-(2-ethanesulfonic acid)
HSPG	heparan sulphate proteoclycan
huEGF	human EGF
huEGF(+) complexes	EGFR-targeted complexes containing huEGF
JNK	jun N-terminal kinase
kb	kilo bases
K_d	dissociation constant
kDa	kilo Dalton
LB medium	Luria Bertani medium
LPEI	linear PEI of 22 kDa
LPEI polyplexes	LPEI/DNA complexes, N/P 6
LSM	(confocal) laser scanning microscope
Lys	lysine
MAPK	mitogen-activated kinase

mEGF	murine EGF
mEGF(+) complexes	EGFR-targeted complexes containing mEGF
MKP	MAPK phosphatase
MTT	methylthiazol tetrazolium salt
MW	molecular weight
n. d.	not detectable
NHS-PEG-MAL	α-Maleimide-ω-N-hydroxysuccinimide ester-polyethylene glycol
NLS	nuclear localization signal
NPC	nuclear pore complex
N/P ratio	molar ratio of PEI nitrogen to DNA phosphate
OM	OptiMEM
PBMC	peripheral blood mononuclear cells
PBS	phosphate-buffered saline
pCMVLuc	plasmid encoding luciferase under control of the CMV promoter/enhancer
PEG	polyethylene glycol
pEGFP	plasmid encoding EGFP
PEG-PEI22	PEG of 20 kDa covalently attached to LPEI of 22 kDa
PEI	polyethylenimine
PFA	paraformaldehyde
PI	propidium iodide
PI3-kinase	phosphatidylinositol 3-kinase
PLL	polylysine
PVDF	polyvinylidene fluoride
RFU	relative fluorescence units

RLU	relative light units
RNA	ribonucleic acid
RTK	receptor tyrosine kinases
SAPK	stress-activated protein kinases
SCID	severe combined immunodeficiency syndrome
SD	standard deviation
SPDP	succinimidyl 3-(2-pyridyldithio)propionate
siRNA	small interfering RNA
TNBS	trinitrobenzenesulfonic acid
Tris	2-amino-2-(hydroxymethyl)propane-1,3-diol
v	volume
v_{max}	maximum velocity
w	weight

6.2 Publications

6.2.1 Original papers

Boeckle, S., von Gersdorff, K., van der Piepen, S., Culmsee, C., Wagner, E., and Ogris, M. (2004), Purification of polyethylenimine polyplexes highlights the role of free polycations in gene transfer, J. Gene Med. 6, 1102-1111

von Gersdorff, K., Ogris, M., and Wagner, E. (2005), Cryoconserved Shielded and EGF Receptor Targeted DNA Polyplexes: Cellular Mechanisms, EJPB 60, 279-285

Bausinger*, R., von Gersdorff*, K., Ogris, M., Wagner, E., Braeckmans, K., Bräuchle, C., and Zumbusch, A. (2006), The Transport of Nanosized Gene Carriers Unravelled by Live Cell Imaging, Angew. Chem., 118, 1568-1602 (* equally contributed)

Huth, S., Hoffmann, F., von Gersdorff, K., Laner, A:, Reinhardt, D., Rosenecker, J., and Rudolph, C., Cytosolic RNA Induces Disassmebly of Polyamine Gene Vectors as a Precondition for Nuclear Import of Plasmid DNA and Gene Expression, submitted

von Gersdorff, K., Sanders, N. N., Vandenbroucke, R., De Smedt, S. C., Wagner, E., and Ogris, M., The internalization route resulting in successful gene expression depends on both cell line and polyethylenimine polyplex type, submitted

6.2.2 Book chapters

Ogris, M., von Gersdorff, K., van der Piepen, S., Brunner, S., and Wagner, E. (2004), Non-viral gene delivery systems – delivery techniques and therapeutic concepts for cancer, Chapter 7 in "Advanced Biomaterials for Medical Applications", D. W. Thomas (Ed), Kluwer Academic Publishers, p. 79-92

6.2.3 Oral presentations

von Gersdorff, K., Boeckle, S., and Wagner, E. (2004), Development of an intelligent artificial virus for gene delivery, SFB 486 “Nanoman” meeting, Schloß Ringberg, Tegernsee, Germany

Bausinger, R., von Gersdorff, K., Ogris, M., Bräuchle, C., Wagner, E., and Zumbusch, A. (2005), Single particle fluorescence microscopy enlights active and diffusive transport processes of nanoparticles in living cells, Spring Meeting of the German Physical Society, Berlin, Germany

Bausinger, R., Ruthardt, N., de Bruin, K., von Gersdorff, K., Ogris, M., Wagner, E., Zumbusch, A., and Bräuchle, C. (2006), Fluorescence Microscopy reveals the mechanistic details of nano-sized gene carrier transport in living cells, Spring Meeting of the German Physical Society, Dresden, Germany

6.2.4 Poster presentations

Boeckle, S., von Gersdorff, K., Wagner, E., Ogris, M. (2003), Strategies to overcome cellular barriers to nonviral gene transfer: Towards artificial viruses, Controlled Release Society, German Chapter Annual Meeting, Munich, Germany

Pelisek, J., von Gersdorff, K., Wagner, E., Culmsee, C. (2006), Efficiency of polyethylenimine-based siRNA vectors in transiently versus stably transfected cells, 47. Frühjahrstagung der Deutschen Gesellschaft für Experimentelle und Klinische Pharmakologie und Toxikologie (DGPT), Mainz, Germany

Boeckle, S., von Gersdorff, K., Ogris, M., Wagner, E. (2003), Purification of DNA/polyethylenimine complexes by size exclusion chromatography, 11th Annual Congress of the European Society of Gene Therapy, Edinburgh, Scotland

7 References

1. Hughes, M. D., Hussain, M., Nawaz, Q., Sayyed, P., and Akhtar, S. (2001), The cellular delivery of antisense oligonucleotides and ribozymes, Drug Discov. Today 6, 303-315

2. Scanlon, K. J., Jiao, L., Funato, T., Wang, W., Tone, T., Rossi, J. J., and Kashani-Sabet, M. (1991), Ribozyme-mediated cleavage of c-fos mRNA reduces gene expression of DNA synthesis enzymes and metallothionein, Proc. Natl. Acad. Sci. USA 88, 10591-10595

3. Shuey, D. J., McCallus, D. E., and Giordano, T. (2002), RNAi: gene-silencing in therapeutic intervention, Drug Discov. Today 7, 1040-1046

4. The Journal of Gene Medicine web site: www.wiley.co.uk/genmed/clinical

5. Sodeik, B. (2000), Mechanisms of viral transport in the cytoplasm, Trends Microbiol. 8, 465-472

6. Seisenberger, G., Ried, M. U., Endress, T., Buning, H., Hallek, M., and Brauchle, C. (2001), Real-time single-molecule imaging of the infection pathway of an adeno-associated virus, Science 294, 1929-1932

7. Mulligan, R. C. (1993), The basic science of gene therapy, Science 260, 926-932

8. Hacein-Bey-Abina, S., Von Kalle, C., Schmidt, M., McCormack, M. P., Wulffraat, N., Leboulch, P., Lim, A., Osborne, C. S., Pawliuk, R., Morillon, E., Sorensen, R., Forster, A., Fraser, P., Cohen, J. I., de Saint, B. G., Alexander, I., Wintergerst, U., Frebourg, T., Aurias, A., Stoppa-Lyonnet, D., Romana, S., Radford-Weiss, I., Gross, F., Valensi, F., Delabesse, E., Macintyre, E., Sigaux, F., Soulier, J., Leiva, L. E., Wissler, M., Prinz, C., Rabbitts, T. H., Le Deist, F., Fischer, A., and Cavazzana-Calvo, M. (2003), LMO2-associated clonal T cell proliferation in two patients after gene therapy for SCID-X1, Science 302, 415-419

9. Check, E. (2002), A tragic setback, Nature 420, 116-118

10. Raper, S. E., Chirmule, N., Lee, F. S., Wivel, N. A., Bagg, A., Gao, G. P., Wilson, J. M., and Batshaw, M. L. (2003), Fatal systemic inflammatory response syndrome in a ornithine transcarbamylase deficient patient following adenoviral gene transfer, Mol. Genet. Metab. 80, 148-158

11. Wagner, E., Culmsee, C., and Boeckle, S. (2005), Targeting of Polyplexes: Towards Synthetic Virus Vector Systems. In Nonviral Vectors for Gene Therapy, Second Edition (Advances in Genetics, Volumes 53 and 54), Huang, L., Hung, M. C., and Wagner, E., editors. Elsevier Academic Press

12. De Smedt, S. C., Demeester, J., and Hennink, W. E. (2000), Cationic polymer based gene delivery systems, Pharm. Res. 17, 113-126

13. Zuber, G., Dauty, E., Nothisen, M., Belguise, P., and Behr, J. P. (2001), Towards synthetic viruses, Adv. Drug Deliv. Rev. 52, 245-253

14. Boussif, O., Lezoualc'h, F., Zanta, M. A., Mergny, M. D., Scherman, D., Demeneix, B., and Behr, J. P. (1995), A versatile vector for gene and oligonucleotide transfer into cells in culture and in vivo: polyethylenimine, Proc. Natl. Acad. Sci. USA 92, 7297-7301

15. Chollet, P., Favrot, M. C., Hurbin, A., and Coll, J. L. (2002), Side-effects of a systemic injection of linear polyethylenimine-DNA complexes, J. Gene Med. 4, 84-91

16. Boeckle, S., von Gersdorff, K., van der Piepen, S., Culmsee, C., Wagner, E., and Ogris, M. (2004), Purification of polyethylenimine polyplexes highlights the role of free polycations in gene transfer, J. Gene Med. 6, 1102-1111

17. Ogris, M., Steinlein, P., Kursa, M., Mechtler, K., Kircheis, R., and Wagner, E. (1998), The size of DNA/transferrin-PEI complexes is an important factor for gene expression in cultured cells, Gene Ther. 5, 1425-1433

18. Wightman, L., Kircheis, R., Rossler, V., Carotta, S., Ruzicka, R., Kursa, M., and Wagner, E. (2001), Different behavior of branched and linear polyethylenimine for gene delivery in vitro and in vivo, J. Gene Med. 3, 362-372

19. Demeneix, B. A. and Behr, J. P. (1996) The proton spronge: A trick the viruses didn´t exploit. In Artificial Self-Assembling Systems for Gene Delivery, Felgner, P. L., Heller, M. J., Lehn, P., Behr, J. P., and Szoka, F. C., editors. American Chemical Society

20. Wagner, E. (2004), Strategies to improve DNA polyplexes for in vivo gene transfer: will "artificial viruses" be the answer?, Pharm. Res. 21, 8-14

21. Demeneix, B., Hassani, Z., and Behr, J. P. (2004), Towards multifunctional synthetic vectors, Curr. Gene Ther. 4, 445-455

22. Goula, D., Benoist, D., Mantero, S., Merlo, G., Levi, G., and Demeneix, B. A. (1998), Polyethylenimine-based intravenous delivery of transgenes to mouse lung, Gene Ther. 5, 1291-1295

23. Chollet, P., Favrot, M. C., Hurbin, A., and Coll, J. L. (2002), Side-effects of a systemic injection of linear polyethylenimine-DNA complexes, J. Gene Med. 4, 84-91

24. Ogris, M., Brunner, S., Schuller, S., Kircheis, R., and Wagner, E. (1999), PEGylated DNA/transferrin-PEI complexes: reduced interaction with blood components, extended circulation in blood and potential for systemic gene delivery, Gene Ther. 6, 595-605

25. Erbacher, P., Bettinger, T., Belguise-Valladier, P., Zou, S., Coll, J. L., Behr, J. P., and Remy, J. S. (1999), Transfection and physical properties of various saccharide, poly(ethylene glycol), and antibody-derivatized polyethylenimines (PEI), J. Gene Med. 1, 210-222

26. Oupicky, D., Ogris, M., Howard, K. A., Dash, P. R., Ulbrich, K., and Seymour, L. W. (2002), Importance of lateral and steric stabilization of polyelectrolyte gene delivery vectors for extended systemic circulation, Mol. Ther. 5, 463-472

27. Maeda, H. (2001), The enhanced permeability and retention (EPR) effect in tumor vasculature: the key role of tumor-selective macromolecular drug targeting, Adv. Enzyme Regul. 41, 189-207

28. Merdan, T., Kopecek, J., and Kissel, T. (2002), Prospects for cationic polymers in gene and oligonucleotide therapy against cancer, Adv. Drug Deliv. Rev. 54, 715-758

29. Schaffer, D. V. and Lauffenburger, D. A. (2000), Targeted synthetic gene delivery vectors, Curr. Opin. Mol. Ther. 2, 155-161

30. Zanta, M. A., Boussif, O., Adib, A., and Behr, J. P. (1997), In vitro gene delivery to hepatocytes with galactosylated polyethylenimine, Bioconjug. Chem. 8 (6), 839-844

31. Bettinger, T., Remy, J. S., and Erbacher, P. (1999), Size reduction of galactosylated PEI/DNA complexes improves lectin-mediated gene transfer into hepatocytes, Bioconjug. Chem. 10, 558-61

32. Morimoto, K., Nishikawa, M., Kawakami, S., Nakano, T., Hattori, Y., Fumoto, S., Yamashita, F., and Hashida, M. (2003), Molecular weight-dependent gene transfection activity of unmodified and galactosylated polyethyleneimine on hepatoma cells and mouse liver, Mol. Ther. 7, 254-261

33. Diebold, S. S., Kursa, M., Wagner, E., Cotten, M., and Zenke, M. (1999), Mannose polyethylenimine conjugates for targeted DNA delivery into dendritic cells, J. Biol. Chem. 274, 19087-19094

34. Guo, W. and Lee, R. J. (1999), Receptor-Targeted Gene Delivery Via Folate-Conjugated Polyethylenimine, AAPS Pharmsci 1, Article 19

35. Kircheis, R., Kichler, A., Wallner, G., Kursa, M., Ogris, M., Felzmann, T., Buchberger, M., and Wagner, E. (1997), Coupling of cell-binding ligands to polyethylenimine for targeted gene delivery, Gene Ther. 4, 409-418

36. Blessing, T., Kursa, M., Holzhauser, R., Kircheis, R., and Wagner, E. (2001), Different strategies for formation of pegylated EGF-conjugated PEI/DNA complexes for targeted gene delivery, Bioconjug. Chem. 12, 529-537

37. Wolschek, M. F., Thallinger, C., Kursa, M., Rossler, V., Allen, M., Lichtenberger, C., Kircheis, R., Lucas, T., Willheim, M., Reinisch, W., Gangl, A., Wagner, E., and Jansen, B. (2002), Specific systemic nonviral gene delivery to human hepatocellular carcinoma xenografts in SCID mice, Hepatology 36, 1106-1114

38. Lee, H., Kim, T. H., and Park, T. G. (2002), A receptor-mediated gene delivery system using streptavidin and biotin-derivatized, pegylated epidermal growth factor, J. Control. Release 83, 109-119

39. O'Neill, M. M., Kennedy, C. A., Barton, R. W., and Tatake, R. J. (2001), Receptor-mediated gene delivery to human peripheral blood mononuclear cells using anti-CD3 antibody coupled to polyethylenimine, Gene Ther. 8, 362-368

40. Buschle, M., Cotten, M., Kirlappos, H., Mechtler, K., Schaffner, G., Zauner, W., Birnstiel, M. L., and Wagner, E. (1995), Receptor-mediated gene transfer into human T lymphocytes via binding of DNA/CD3 antibody particles to the CD3 T cell receptor complex, Hum. Gene Ther. 6, 753-761

41. Rejman, J., Oberle, V., Zuhorn, I. S., and Hoekstra, D. (2004), Size-dependent internalization of particles via the pathways of clathrin- and caveolae-mediated endocytosis, Biochem. J. 377, 159-169

42. Rejman, J., Bragonzi, A., and Conese, M. (2005), Role of clathrin- and caveolae-mediated endocytosis in gene transfer mediated by lipo- and polyplexes, Mol. Ther. 12, 468-474

43. Kopatz, I., Remy, J. S., and Behr, J. P. (2004), A model for non-viral gene delivery: through syndecan adhesion molecules and powered by actin, J. Gene Med. 6, 769-776

44. Sonawane, N. D., Szoka, F. C., Jr., and Verkman, A. S. (2003), Chloride Accumulation and Swelling in Endosomes Enhances DNA Transfer by Polyamine-DNA Polyplexes, J. Biol. Chem. 278, 44826-44831

45. Mislick, K. A. and Baldeschwieler, J. D. (1996), Evidence for the role of proteoglycans in cation-mediated gene transfer, Proc. Natl. Acad. Sci. USA 93, 12349-12354

46. Goncalves, C., Mennesson, E., Fuchs, R., Gorvel, J. P., Midoux, P., and Pichon, C. (2004), Macropinocytosis of polyplexes and recycling of plasmid via the clathrin-dependent pathway impair the transfection efficiency of human hepatocarcinoma cells, Mol. Ther. 10, 373-385

47. Brodsky, F. M., Chen, C. Y., Knuehl, C., Towler, M. C., and Wakeham, D. E. (2001), Biological basket weaving: formation and function of clathrin-coated vesicles, Annu. Rev. Cell Dev. Biol. 17, 517-568

48. Rothberg, K. G., Heuser, J. E., Donzell, W. C., Ying, Y. S., Glenney, J. R., and Anderson, R. G. (1992), Caveolin, a protein component of caveolae membrane coats, Cell 68, 673-682

49. Pelkmans, L. and Helenius, A. (2002), Endocytosis via caveolae, Traffic 3, 311-320

50. Grimmer, S., van Deurs, B., and Sandvig, K. (2002), Membrane ruffling and macropinocytosis in A431 cells require cholesterol, J. Cell Sci. 115, 2953-2962

51. Grosse, S., Aron, Y., Thevenot, G., Francois, D., Monsigny, M., and Fajac, I. (2005), Potocytosis and cellular exit of complexes as cellular pathways for gene delivery by polycations, J. Gene Med. 7, 1275-1286

52. Zuhorn, I. S., Kalicharan, R., and Hoekstra, D. (2002), Lipoplex-mediated transfection of mammalian cells occurs through the cholesterol-dependent clathrin-mediated pathway of endocytosis, J. Biol. Chem. 277, 18021-18028

53. Wang, L. H., Rothberg, K. G., and Anderson, R. G. (1993), Mis-assembly of clathrin lattices on endosomes reveals a regulatory switch for coated pit formation, J. Cell Biol. 123, 1107-1117

54. Orlandi, P. A. and Fishman, P. H. (1998), Filipin-dependent inhibition of cholera toxin: evidence for toxin internalization and activation through caveolae-like domains, J. Cell Biol. 141, 905-915

55. Bieber, T., Meissner, W., Kostin, S., Niemann, A., and Elsasser, H. P. (2002), Intracellular route and transcriptional competence of polyethylenimine-DNA complexes, J. Control. Release 82, 441-454

56. Ruponen, M., Ronkko, S., Honkakoski, P., Pelkonen, J., Tammi, M., and Urtti, A. (2001), Extracellular glycosaminoglycans modify cellular trafficking of lipoplexes and polyplexes, J. Biol. Chem. 276, 33875-33880

57. Mounkes, L. C., Zhong, W., Cipres-Palacin, G., Heath, T. D., and Debs, R. J. (1998), Proteoglycans mediate cationic liposome-DNA complex-based gene delivery in vitro and in vivo, J. Biol. Chem. 273, 26164-26170

58. Zabner J, Fasbender AJ, Moninger T, Poellinger KA, and Welsh MJ (1995), Cellular and molecular barriers to gene transfer by a cationic lipid, J. Biol. Chem. 270, 18997-19007

59. Labat, M., Steffan, A. M., Brisson, C., Perron, H., Feugeas, O., Furstenberger, P., Oberling, F., Brambilla, E., and Behr, J. P. (1996), An electron microscopy study into the mechanism of gene transfer with lipopolyamines, Gene Ther. 3, 1010-1017

60. Kichler, A., Leborgne, C., Coeytaux, E., and Danos, O. (2001), Polyethylenimine-mediated gene delivery: a mechanistic study, J. Gene Med. 3, 135-144

61. Thomas, M. and Klibanov, A. M. (2002), Enhancing polyethylenimine's delivery of plasmid DNA into mammalian cells, Proc. Natl. Acad. Sci. USA 99, 14640-14645

62. Merdan, T., Kunath, K., Fischer, D., Kopecek, J., and Kissel, T. (2002), Intracellular processing of poly(ethylene imine)/ribozyme complexes can be observed in living cells by using confocal laser scanning microscopy and inhibitor experiments, Pharm. Res. 19, 140-146

63. Godbey, W. T., Wu, K. K., and Mikos, A. G. (2001), Poly(ethylenimine)-mediated gene delivery affects endothelial cell function and viability, Biomaterials 22, 471-80

64. Baker, A., Saltik, M., Lehrmann, H., Killisch, I., Mautner, V., Lamm, G., Christofori, G., and Cotten, M. (1997), Polyethylenimine (PEI) is a simple, inexpensive and effective reagent for condensing and linking plasmid DNA to adenovirus for gene delivery, Gene Ther. 4, 773-82

65. Ogris, M., Carlisle, R. C., Bettinger, T., and Seymour, L. W. (2001), Melittin enables efficient vesicular escape and enhanced nuclear access of nonviral gene delivery vectors, J. Biol. Chem. 276, 47550-47555

66. Lukacs, G. L., Haggie, P., Seksek, O., Lechardeur, D., Freedman, N., and Verkman, A. S. (2000), Size-dependent DNA mobility in cytoplasm and nucleus, J. Biol. Chem. 275, 1625-1629

67. Suh, J., Wirtz, D., and Hanes, J. (2003), Efficient active transport of gene nanocarriers to the cell nucleus, Proc. Natl. Acad. Sci. USA 100, 3878-3882

68. Capecchi, M. R. (1980), High efficiency transformation by direct microinjection of DNA into cultured mammalian cells, Cell 22, 479-488

69. Pollard, H., Remy, J. S., Loussouarn, G., Demolombe, S., Behr, J. P., and Escande, D. (1998), Polyethylenimine but not cationic lipids promotes transgene delivery to the nucleus in mammalian cells, J. Biol. Chem. 273, 7507-7511

70. Liu, G., Li, D., Pasumarthy, M. K., Kowalczyk, T. H., Gedeon, C. R., Hyatt, S. L., Payne, J. M., Miller, T. J., Brunovskis, P., Fink, T. L., Muhammad, O., Moen, R. C., Hanson, R. W., and Cooper, M. J. (2003), Nanoparticles of compacted DNA transfect postmitotic cells, J. Biol. Chem. 278, 32578-32586

71. Brunner, S., Sauer, T., Carotta, S., Cotten, M., Saltik, M., and Wagner, E. (2000), Cell cycle dependence of gene transfer by lipoplex, polyplex and recombinant adenovirus, Gene Ther. 7, 401-407

72. Brunner, S., Furtbauer, E., Sauer, T., Kursa, M., and Wagner, E. (2002), Overcoming the nuclear barrier: cell cycle independent nonviral gene transfer with linear polyethylenimine or electroporation, Mol. Ther. 5, 80-86

73. Zanta, M. A., Belguise, V. P., and Behr, J. P. (1999), Gene delivery: A single nuclear localization signal peptide is sufficient to carry DNA to the cell nucleus, Proc. Natl. Acad. Sci. USA 96, 91-96

74. Kwok, T. T. and Sutherland, R. M. (1991), Differences in EGF related radiosensitisation of human squamous carcinoma cells with high and low numbers of EGF receptors, Br. J. Cancer 64, 251-254

75. Schlessinger, J. (2000), Cell signaling by receptor tyrosine kinases, Cell 103, 211-225

76. Mineo, C., Gill, G. N., and Anderson, R. G. (1999), Regulated migration of epidermal growth factor receptor from caveolae, J. Biol. Chem. 274, 30636-30643

77. Roepstorff, K., Thomsen, P., Sandvig, K., and van Deurs, B. (2002), Sequestration of epidermal growth factor receptors in non-caveolar lipid rafts inhibits ligand binding, J. Biol. Chem. 277, 18954-18960

78. Schlessinger, J. (2002), Ligand-induced, receptor-mediated dimerization and activation of EGF receptor, Cell 110, 669-672

79. Wilde, A., Beattie, E. C., Lem, L., Riethof, D. A., Liu, S. H., Mobley, W. C., Soriano, P., and Brodsky, F. M. (1999), EGF receptor signaling stimulates SRC kinase phosphorylation of clathrin, influencing clathrin redistribution and EGF uptake, Cell 96, 677-687

80. Katzmann, D. J., Odorizzi, G., and Emr, S. D. (2002), Receptor downregulation and multivesicular-body sorting, Nat. Rev. Mol. Cell Biol. 3, 893-905

81. Yarden, Y. and Sliwkowski, M. X. (2001), Untangling the ErbB signalling network, Nat. Rev. Mol. Cell Biol. 2, 127-137

82. Hackel, P. O., Zwick, E., Prenzel, N., and Ullrich, A. (1999), Epidermal growth factor receptors: critical mediators of multiple receptor pathways, Curr. Opin. Cell Biol. 11, 184-189

83. Pennock, S. and Wang, Z. (2003), Stimulation of cell proliferation by endosomal epidermal growth factor receptor as revealed through two distinct phases of signaling, Mol. Cell Biol. 23, 5803-5815

84. Vieira, A. V., Lamaze, C., and Schmid, S. L. (1996), Control of EGF receptor signaling by clathrin-mediated endocytosis, Science 274, 2086-2089

85. McPherson, P. S., Kay, B. K., and Hussain, N. K. (2001), Signaling on the endocytic pathway, Traffic 2, 375-384

86. Aguilar, R. C. and Wendland, B. (2005), Endocytosis of membrane receptors: two pathways are better than one, Proc. Natl. Acad. Sci. USA 102, 2679-2680

87. Sigismund, S., Woelk, T., Puri, C., Maspero, E., Tacchetti, C., Transidico, P., Di Fiore, P. P., and Polo, S. (2005), Clathrin-independent endocytosis of ubiquitinated cargos, Proc. Natl. Acad. Sci. USA 102, 2760-2765

88. Tervahauta, A., Syrjanen, S., and Syrjanen, K. (1994), Epidermal growth factor receptor, c-erbB-2 proto-oncogene and estrogen receptor expression in human papillomavirus lesions of the uterine cervix, Int. J. Gynecol. Pathol. 13, 234-240

89. Kamio, T., Shigematsu, K., Sou, H., Kawai, K., and Tsuchiyama, H. (1990), Immunohistochemical expression of epidermal growth factor receptors in human adrenocortical carcinoma, Hum. Pathol. 21, 277-282

90. Gusterson, B., Cowley, G., McIlhinney, J., Ozanne, B., Fisher, C., and Reeves, B. (1985), Evidence for increased epidermal growth factor receptors in human sarcomas, Int. J. Cancer 36, 689-693

91. Lipponen, P. and Eskelinen, M. (1994), Expression of epidermal growth factor receptor in bladder cancer as related to established prognostic factors, oncoprotein (c-erbB-2, p53) expression and long-term prognosis, Br. J. Cancer 69, 1120-1125

92. Lin, S. Y., Makino, K., Xia, W., Matin, A., Wen, Y., Kwong, K. Y., Bourguignon, L., and Hung, M. C. (2001), Nuclear localization of EGF receptor and its potential new role as a transcription factor, Nat. Cell Biol. 3, 802-808

93. Carlin, C. R., Simon, D., Mattison, J., and Knowles, B. B. (1988), Expression and biosynthetic variation of the epidermal growth factor receptor in human hepatocellular carcinoma-derived cell lines, Mol. Cell Biol. 8, 25-34

94. Schlessinger, J. (1986), Allosteric regulation of the epidermal growth factor receptor kinase, J. Cell Biol. 103, 2067-2072

95. Chen, J., Gamou, S., Takayanagi, A., and Shimizu, N. (1994), A novel gene delivery system using EGF receptor-mediated endocytosis, FEBS Lett. 338, 167-169

96. Shimizu, N., Chen, J., Gamou, S., and Takayanagi, A. (1996), Immunogene approach toward cancer therapy using erythrocyte growth factor receptor-mediated gene delivery, Cancer Gene Ther. 3, 113-120

97. Fominaya, J., Uherek, C., and Wels, W. (1998), A chimeric fusion protein containing transforming growth factor-alpha mediates gene transfer via binding to the EGF receptor, Gene Ther. 5, 521-530

98. Frederiksen, K. S., Abrahamsen, N., Cristiano, R. J., Damstrup, L., and Poulsen, H. S. (2000), Gene delivery by an epidermal growth factor/DNA polyplex to small cell lung cancer cell lines expressing low levels of epidermal growth factor receptor, Cancer Gene Ther. 7, 262-268

99. Xu, B., Wiehle, S., Roth, J. A., and Cristiano, R. J. (1998), The contribution of poly-L-lysine, epidermal growth factor and streptavidin to EGF/PLL/DNA polyplex formation, Gene Ther. 5, 1235-1243

100. Lee, T. K., Han, J. S., Fan, S. T., Liang, Z. D., Tian, P. K., Gu, J. R., and Ng, I. O. (2001), Gene delivery using a receptor-mediated gene transfer system targeted to hepatocellular carcinoma cells, Int. J. Cancer 93, 393-400

101. Liu, X., Tian, P., Yu, Y., Yao, M., Cao, X., and Gu, J. (2002), Enhanced antitumor effect of EGF R-targeted p21WAF-1 and GM-CSF gene transfer in the established murine hepatoma by peritumoral injection, Cancer Gene Ther. 9, 100-108

102. Liu, X., Tian, P. K., Ju, D. W., Zhang, M. H., Yao, M., Cao, X. T., and Gu, J. R. (2003), Systemic genetic transfer of p21WAF-1 and GM-CSF utilizing of a novel oligopeptide-based EGF receptor targeting polyplex, Cancer Gene Ther. 10, 529-539

103. Ogris, M., Steinlein, P., Carotta, S., Brunner, S., and Wagner, E. (2001), DNA/polyethylenimine transfection particles: Influence of ligands, polymer size, and PEGylation on internalization and gene expression, AAPS PharmSci 3, E21

104. Carlsson, J., Drevin, H., and Axen, R. (1978), Protein thiolation and reversible protein-protein conjugation. N-Succinimidyl 3-(2-pyridyldithio)propionate, a new heterobifunctional reagent, Biochem. J. 173, 723-737

105. Riddles, P. W., Blakeley, R. L., and Zerner, B. (1979), Ellman's reagent: 5,5'-dithiobis(2-nitrobenzoic acid)--a reexamination, Anal. Biochem. 94, 75-81

106. Snyder, S. L. and Sobocinski, P. Z. (1975), An improved 2,4,6-trinitrobenzenesulfonic acid method for the determination of amines, Anal. Biochem. 64, 284-8

107. Kursa, M., Walker, G. F., Roessler, V., Ogris, M., Roedl, W., Kircheis, R., and Wagner, E. (2003), Novel Shielded Transferrin-Polyethylene Glycol-Polyethylenimine/DNA Complexes for Systemic Tumor-Targeted Gene Transfer, Bioconjug. Chem. 14, 222-231

108. Plank, C., Zatloukal, K., Cotten, M., Mechtler, K., and Wagner, E. (1992), Gene transfer into hepatocytes using asialoglycoprotein receptor mediated endocytosis of DNA complexed with an artificial tetra-antennary galactose ligand, Bioconjug. Chem. 3, 533-539

109. Kircheis, R., Wightman, L., Schreiber, A., Robitza, B., Rossler, V., Kursa, M., and Wagner, E. (2001), Polyethylenimine/DNA complexes shielded by transferrin target gene expression to tumors after systemic application, Gene Ther. 8, 28-40

110. Stein, G. S. and Borun, T. W. (1972), The synthesis of acidic chromosomal proteins during the cell cycle of HeLa S-3 cells. I. The accelerated accumulation of acidic residual nuclear protein before the initiation of DNA replication, J. Cell Biol. 52, 292-307

111. Ogris, M., Wagner, E., and Steinlein, P. (2000), A versatile assay to study cellular uptake of gene transfer complexes by flow cytometry, Biochim. Biophys. Acta 1474, 237-243

112. Lemmon, M. A., Bu, Z., Ladbury, J. E., Zhou, M., Pinchasi, D., Lax, I., Engelman, D. M., and Schlessinger, J. (1997), Two EGF molecules contribute additively to stabilization of the EGFR dimer, Embo J. 16, 281-294

113. Bach, M., Holig, P., Schlosser, E., Volkel, T., Graser, A., Muller, R., and Kontermann, R. E. (2003), Isolation from phage display libraries of lysine-deficient human epidermal growth factor variants for directional conjugation as targeting ligands, Protein Eng. 16, 1107-1113

114. Lee, H., Jang, I. H., Ryu, S. H., and Park, T. G. (2003), N-terminal site-specific mono-PEGylation of epidermal growth factor, Pharm. Res. 20, 818-825

115. Hanover, J. A., Beguinot, L., Willingham, M. C., and Pastan, I. H. (1985), Transit of receptors for epidermal growth factor and transferrin through clathrin-coated pits. Analysis of the kinetics of receptor entry, J. Biol. Chem. 260, 15938-45

116. Yarden, Y. (2001), The EGFR family and its ligands in human cancer. signalling mechanisms and therapeutic opportunities, Eur. J. Cancer 37 Suppl. 4, S3-S8

117. Kalejta, R. F., Brideau, A. D., Banfield, B. W., and Beavis, A. J. (1999), An integral membrane green fluorescent protein marker, Us9-GFP, is quantitatively retained in cells during propidium iodide-based cell cycle analysis by flow cytometry, Exp. Cell Res. 248, 322-8

118. Chu, Y. W., Wang, R., Schmid, I., and Sakamoto, K. M. (1999), Analysis with flow cytometry of green fluorescent protein expression in leukemic cells, Cytometry 36, 333-9

119. Talsma, H., Cherng, J. Y., Lehrmann, H., Kursa, M., Ogris, M., Hennink, W. E., Cotten, M., and Wagner, E. (1997), Stabilization of gene delivery systems by freeze-drying, Int. J. Pharm. 157, 233-238

120. Silva, D., Cortez, C. M., and Louro, S. R. (2004), Quenching of the intrinsic fluorescence of bovine serum albumin by chlorpromazine and hemin, Braz. J. Med. Biol. Res. 37, 963-968

121. Romanini, D., Avalle, G., Farruggia, B., Nerli, B., and Pico, G. (1998), Spectroscopy features of the binding of polyene antibiotics to human serum albumin, Chem. Biol. Interact. 115, 247-260

122. Berkers, J. A., van Bergen en Henegouwen PM, and Boonstra, J. (1991), Three classes of epidermal growth factor receptors on HeLa cells, J. Biol. Chem. 266, 922-927

123. Bausinger, R., von Gersdorff, K., Ogris, M., Wagner, E., Braeckmans, K., Bräuchle, C., and Zumbusch, A. (2006), The Transport of Nanosized Gene Carriers Unraveled by Live-Cell Imaging, Angew. Chem. 118, 1598-1602

124. Chollet, P., Favrot, M. C., Hurbin, A., and Coll, J. L. (2002), Side-effects of a systemic injection of linear polyethylenimine-DNA complexes, J. Gene Med. 4, 84-91

125. Shir, A., Ogris, M., Wagner, E., and Levitzki, A. (2005), EGF Receptor Targeted Synthetic Double-Stranded RNA Eliminates Glioblastoma, Breast Cancer and Adenocarcinoma Tumors in Mice, PLoS Medicine, in press

126. Ogris, M., Walker, G., Blessing, T., Kircheis, R., Wolschek, M., and Wagner, E. (2003), Tumor-targeted gene therapy: strategies for the preparation of ligand-polyethylene glycol-polyethylenimine/DNA complexes, J. Control. Release 91, 173-181

127. Cherng, J. Y., vd, W. P., Talsma, H., Crommelin, D. J., and Hennink, W. E. (1999), Stabilization of polymer-based gene delivery systems, Int. J. Pharm. 183, 25-28

128. Goldman, J. P., Gullick, W. J., Bray, D., and Johnson, C. G. (2002), Individual-based simulation of the clustering behaviour of epidermal growth factor receptors, Proceedings of the 2002 ACM symposium on Applied computing 127-131

129. Lund, K. A., Opresko, L. K., Starbuck, C., Walsh, B. J., and Wiley, H. S. (1990), Quantitative analysis of the endocytic system involved in hormone-induced receptor internalization, J. Biol. Chem. 265, 15713-15723

130. King, S. J. and Schroer, T. A. (2000), Dynactin increases the processivity of the cytoplasmic dynein motor, Nat. Cell Biol. 2, 20-24

131. Kolch, W. (2000), Meaningful relationships: the regulation of the Ras/Raf/MEK/ERK pathway by protein interactions, Biochem. J. 351 Pt 2, 289-305

132. Camps, M., Nichols, A., Gillieron, C., Antonsson, B., Muda, M., Chabert, C., Boschert, U., and Arkinstall, S. (1998), Catalytic activation of the phosphatase MKP-3 by ERK2 mitogen-activated protein kinase, Science 280, 1262-1265

133. Zhao, Y. and Zhang, Z. Y. (2001), The mechanism of dephosphorylation of extracellular signal-regulated kinase 2 by mitogen-activated protein kinase phosphatase 3, J. Biol. Chem. 276, 32382-32391

134. Guthridge, M. A., Powell, J. A., Barry, E. F., Stomski, F. C., McClure, B. J., Ramshaw, H., Felquer, F. A., Dottore, M., Thomas, D. T., To, B., Begley, C. G., and Lopez, A. F. (2006), Growth factor pleiotropy is controlled by a receptor Tyr/Ser motif that acts as a binary switch, Embo J. 25, 479-485

135. www.drugdevelopment-technology.com

136. Sorkin, A. (1998), Endocytosis and intracellular sorting of receptor tyrosine kinases, Frontiers in Bioscience 3, 729-738

137. Wells, A. and Marti, U. (2002), Signalling shortcuts: cell-surface receptors in the nucleus?, Nat. Rev. Mol. Cell Biol. 3, 697-702

138. Liu, H. S., Jan, M. S., Chou, C. K., Chen, P. H., and Ke, N. J. (1999), Is green fluorescent protein toxic to the living cells?, Biochem. Biophys. Res. Commun. 260, 712-717

139. Trifan, O. C., Smith, R. M., Thompson, B. D., and Hla, T. (1999), Overexpression of cyclooxygenase-2 induces cell cycle arrest. Evidence for a prostaglandin-independent mechanism, J. Biol. Chem. 274, 34141-34147

140. Thomas, N., Kenrick, M., Giesler, T., Kiser, G., Tinkler, H., and Stubbs, S. (2005), Characterization and gene expression profiling of a stable cell line expressing a cell cycle GFP sensor, Cell Cycle 4, 191-195

141. Akinc, A., Thomas, M., Klibanov, A. M., and Langer, R. (2005), Exploring polyethylenimine-mediated DNA transfection and the proton sponge hypothesis, J. Gene Med. 7, 657-663

142. Fischer, D., Bieber, T., Li, Y., Elsasser, H. P., and Kissel, T. (1999), A novel non-viral vector for DNA delivery based on low molecular weight, branched polyethylenimine: effect of molecular weight on transfection efficiency and cytotoxicity, Pharm. Res. 16, 1273-1279

143. Walker, G. F., Fella, C., Pelisek, J., Fahrmeir, J., Boeckle, S., Ogris, M., and Wagner, E. (2005), Toward synthetic viruses: endosomal pH-triggered deshielding of targeted polyplexes greatly enhances gene transfer in vitro and in vivo, Mol. Ther. 11, 418-425

144. Klemm, A. R., Young, D., and Lloyd, J. B. (1998), Effects of polyethyleneimine on endocytosis and lysosome stability, Biochem. Pharmacol. 56, 41-46

145. Godbey, W. T., Barry, M. A., Saggau, P., Wu, K. K., and Mikos, A. G. (2000), Poly(ethylenimine)-mediated transfection: A new paradigm for gene delivery, J. Biomed. Mater. Res. 51, 321-328

146. Fujimoto, T., Kogo, H., Nomura, R., and Une, T. (2000), Isoforms of caveolin-1 and caveolar structure, J. Cell Sci. 113 Pt 19, 3509-3517

147. Damm, E. M., Pelkmans, L., Kartenbeck, J., Mezzacasa, A., Kurzchalia, T., and Helenius, A. (2005), Clathrin- and caveolin-1-independent endocytosis: entry of simian virus 40 into cells devoid of caveolae, J. Cell Biol. 168, 477-488

148. Vainio, S., Heino, S., Mansson, J. E., Fredman, P., Kuismanen, E., Vaarala, O., and Ikonen, E. (2002), Dynamic association of human insulin receptor with lipid rafts in cells lacking caveolae, EMBO Rep. 3, 95-100

149. Akinc, A. and Langer, R. (2002), Measuring the pH environment of DNA delivered using nonviral vectors: implications for lysosomal trafficking, Biotechnol. Bioeng. 78, 503-508

8 Acknowledgments

This work was funded by Deutsche Forschungsgemeinschaft, SFB 486 “Nanoman”.

Foremost, I would like to thank Prof. Dr. Ernst Wagner for giving me the opportunity to perform this work in his laboratories. His constant guiding and support were very helpful and essential for the success of this thesis.

I am also very grateful to Dr. Manfred Ogris for continuous advice, intensive discussions and for patiently answering all my questions. Many thanks also to Dr. Carsten Culmsee for the careful review of many manuscripts.

I am also very grateful to the group of Prof. Dr. Christoph Bräuchle. Ralf Bausinger, Karla de Bruin and Dr. Nadia Ruthardt performed the single particle tracing experiments and constantly provided us with interesting new data.

Furthermore, I would like to thank Dr. Niek Sanders and Roosmarjin Vandenbroucke from the group of Prof. Dr. Stefaan De Smedt. Thanks to Niek for teaching me how to handle the inhibitors and to Roosmarjin for performing the COS-7 experiments.

A big thank you to all my colleagues in the lab. Special thanks to Stefan Landshamer for performing the western blot analysis and to Wolfgang Rödl for excellent technical support in lab and office and for carrying out the synthesis of the conjugates. Many thanks also to Olga Brück for assistance in completing the `Reference Manager´ database.

I would also like to thank my parents for giving me financial as well as moral support. And last but not least, I am very grateful to Alexander Adam: thank you very much for your support, your patience and continuous encouragement.

9 Curriculum vitae

Personal Data

Name:	Katharina Veronika Maria Freiin von Gersdorff
Date of birth:	20.12.1976
Place of birth:	Frankfurt/Main
Marital status:	unmarried
Citizenship:	German

Education

08/2002-present	PhD thesis at the Department of Pharmaceutical Biology/Biotechnology, Ludwig-Maximilians-University, Munich, Germany, supervisor: Prof. Dr. Ernst Wagner
02/2006	Licensure as a pharmacist
11/2001-04/2002	Internship at the Department of Pharmaceutical Biology, Ludwig-Maximilians-University, Munich, Germany, supervisor: Prof. Dr. Angelika Vollmar
05/2001-10/2002	Internship at Kurfürstenapotheke, Munich, Germany
10/1996-04/2001	Studies of pharmacy, Ruprecht-Karls-University, Heidelberg, Germany
06/1996	Abitur
09/1987-06/1996	Secondary school, Kaiserin-Friedrich-Gymnasium, Bad Homburg v. d. Höhe, Germany
09/1993-08/1994	The Leys, Cambridge, Great Britain